立项编号： cstc2021jcyj-msxmX0100

重庆市自然科学基金面上项目
结题自评估报告

项目名称	基于 AIEgen 的甲基汞在浮游动物体内的富集水平与分布规律
承担单位	西南大学
项目负责人	何滔
通讯地址	重庆市北碚区天生路 1 号
联系电话	15023177126
起止年限	2021-10-01 至 2024-1-15

西南大学

二 O 二四年一月

1. 项目概述

1.1 立项依据

1.1.1 国内外研究现状

（一） 甲基汞（MeHg）在水域生态系统内的迁移转化备受关注

汞是一种广泛分布的有毒元素和污染物，因其对世界环境和人类健康均有各种不利影响，在科学界引起极大关注。汞元素以多种形式存在，可与氯、碳和氧等其他元素结合形成有毒化合物。在水生系统中，汞尽管是以低浓度的形式自然存在，但它仍被认为是一种具有危害性和普遍性的重金属污染物，在危害物质清单中排在砷和铅之后的第三位。其中，汞离子(Hg^{2+})很容易通过皮肤、呼吸道和肠道组织等进入机体，对神经系统和内分泌系统造成损害。进入水体后，Hg^{2+} 还可被许多水生微生物转化为甲基汞(MeHg)，存在于众多水生生物体内。水生生物中 MeHg 的浓度因物种和生境的不同而不同，污染地区水生生物体内的甲基汞含量一般较高。作为最易富集的汞元素形态，MeHg 通过水生食物链上各类水生生物之间的营养转移和生物放大作用，从而最终影响到人体的发育和各项功能，人体接触到的汞元素的主要形式就是甲基汞。

甲基汞（MeHg）在水生生物中的生物积累是非同寻常的，其接触范围比其他形式的汞元素也更为普遍，这也正是汞污染的最大问题之一。近年来，关于甲基汞在水生生态系统中的研究仍以定量测定为主。Jiang 等总结了近年来水生生物中甲基汞摄入含量的研究进展，发现不同水生生物体内甲基汞的含量趋势为：肉食性鱼类 > 杂食性鱼类 > 滤食性鱼类 > 底栖类生物 > 草食性鱼类 > 浮游植物 > 浮游动物；在不同器官中甲基汞的含量趋势则为背肌肉 > 肚肌肉 > 肝脏 > 心脏 > 其他器官组织。Razavi 等采用冷蒸气-原子荧光光谱法测定了甲基汞在水生固着生物、水生无脊椎动物以及鱼类这一食物链上的浓度特征，他们认为大型水生无脊椎动物体内甲基汞的含量可作为预测鱼体汞含量的相关依据。Poste 等研究了陆地有机质对甲基汞在浮游动物体内富集含量的影响，结果表明有机质含量的上升会导致水体以及浮游动物体内甲基汞富集量的增加，并会间接导致食物链上层生物汞富集量的增多。

然而，甲基汞在水生食物链上的吸收、积累和转化等转移机制尚未完全摸清，特别是在各类小型水生生物之间（比如藻类、枝角类、桡足类等），而它们却是

甲基汞在水生系统中转移积累的关键位点。此外，用传统方法检测 MeHg 的含量需要专业精密的仪器，比如冷蒸气-原子荧光光谱法、电感耦合等离子质谱仪（ICP-MS）等，而监测 MeHg 在生物体内的分布则需要更加复杂精密的同步辐射 X 荧光仪（S-XRF），实验操作都不便利，且无法进行活体观察。故而开发一种新的技术方法来检测和量化水生生物体内的汞元素含量，便于更直观地了解甲基汞在水生生物体内的富集和转移过程，显得尤其必要。

（二） 聚集诱导荧光物（AIEgen）——一种特异性的新型荧光探针

传统的荧光物质一般在稀溶液中具有较高的发光效率，但在浓溶液或聚集态时由于分子间相互作用增加了非辐射能的损耗，表现为发光效率降低甚至不发光，这种现象被称作“浓度猝灭”效应或“聚集导致荧光猝灭(aggregation-caused quenching, ACQ)”，见图 1。然而在实际应用中，荧光物质多以薄膜或聚集态形式存在，其 ACQ 效应在一定程度上降低了体系的灵敏度，进而限制了其在光电、传感和生物等领域的应用。

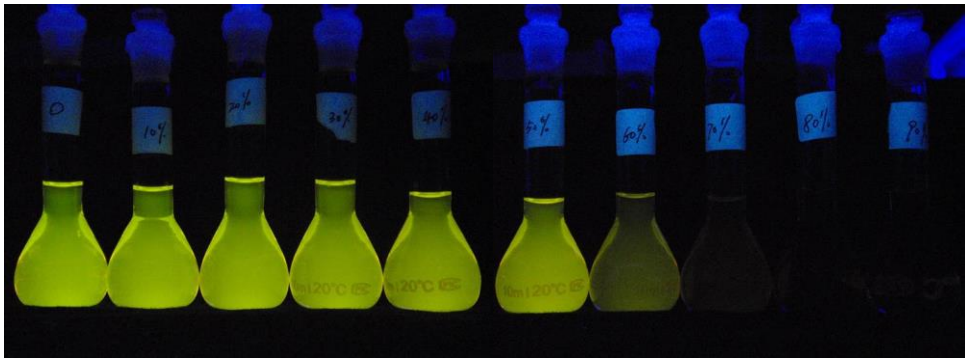

图 1 高浓度引起的荧光淬灭

聚集诱导发光(Aggregation-induced emission, AIE)是指一种光物理效应，即荧光团的发光效应是由聚集体形成而激活的，与荧光淬灭（ACQ）的性质刚好相反，即在聚集状态下发出的荧光反而比溶液状态下更强（图 2），解决了荧光探针在应用中效率降低的难题，在生物检测中可作为一种更有效的标记方法。这一研究成果也因此曾荣获 2017 年国家自然科学一等奖。

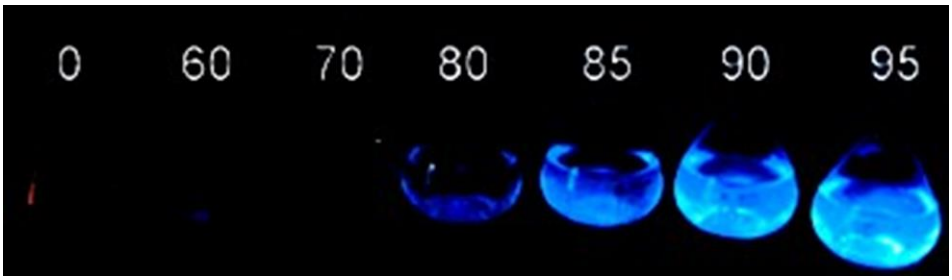

图 2 聚集诱导荧光物浓度增高亮度越强

聚集诱导荧光物（Aggregation-induced emission fluorogen，AIEgen），在生物分子检测、细胞成像、细胞分子追踪等方面具有广泛实用性。而聚集诱导发光的特性使得在微小生物中通过荧光定量和原位成像监测痕量物质成为了可能。最近，本项目团队已开发出特异性的 AIEgen 荧光探针，这种特异性 AIEgen：TPE-RNS 在紫外线的激发下可呈现蓝色荧光，然而在与汞离子(Hg^{2+})发生反应后其化学结构会发生变化，转变成 TPE-RNO 的形式，并在紫外线的激发下呈现红色荧光（图 3）。

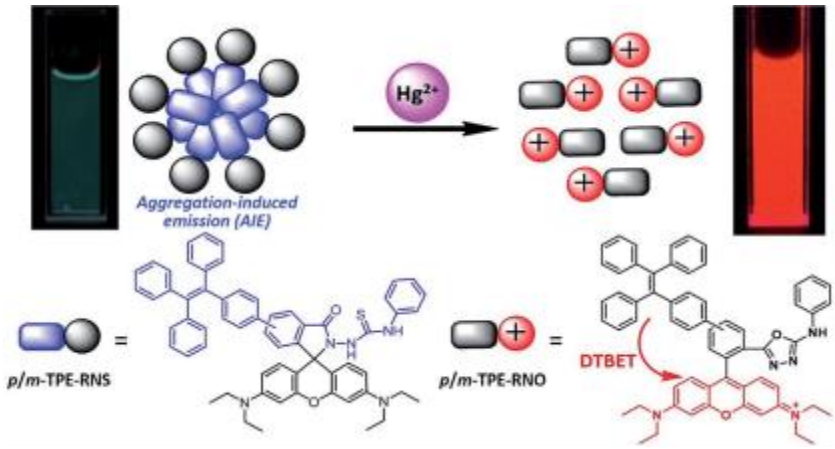

图 3 特异性 AIEgen (TPE-RNS)与汞离子（Hg^{2+}）的反应机理

本项目研究团队已利用这一显色变色原理建立了一种新的检测方法，可用于定量和示踪溶液中的汞离子(Hg^{2+})，而这一新的检测方法已被应用于检测 Hg^{2+}在微藻中的生物蓄积和代谢释放，以及 Hg^{2+}在小型水生无脊椎动物(轮虫和水蚤)中的代谢水平以及动态位点分布，在定量测定及定性分析两个方面均有显著效果，尤其是随着代谢进程 Hg^{2+}在生物活体内的示踪定位。

项目申请人的前期研究还发现，特异性 AIEgen (TPE-RNS)不仅可以与汞离

子（Hg^{2+}）发生显色反应，TPE-RNS 与氯化甲基汞（MeHgCl）亦可发生类似的显色反应（见图 4）。在可见光下，TPE-RNS 与 MeHgCl 发生反应之后，由无色转变成红色；在紫外线下，TPE-RNS 在与 MeHgCl 反应后，由淡蓝色变为橘红色。故而推测，特异性 AIEgen (TPE-RNS)亦可用于定量和示踪溶液中的甲基汞（MeHg）。然而，特异性 AIEgen (TPE-RNS)与氯化甲基汞（MeHgCl）的化学反应机理、以及与汞离子（Hg^{2+}）显色反应的异同等还需要继续研究。

A1　　A2　　B1　　B2

图 4 特异性 AIEgen (TPE-RNS)与氯化甲基汞（MeHgCl）的显色反应

可见光：A1：TPE-RNS；A2：TPE-RNS + MeHgCl

紫外线：B1：TPE-RNS；B2：TPE-RNS + MeHgCl

（三）隆线蚤 （*Daphnia carinata*）——一种适宜生态毒理研究的实验动物

浮游动物是初级生产者（藻类等）与捕食者（鱼虾贝类等）之间的重要营养环节，是连接能量通量的桥梁。水蚤是一种小型的甲壳动物，属于节肢动物门、甲壳纲、枝角亚目，又称鱼虫，是各种淡水水域中最常见的浮游动物。由于水蚤的生命周期相对较短，可通过无性繁殖产生大量后代，而且其对多种水生污染物敏感，可作为一种毒性指示生物，故而经常用于生理学、生态学、毒理学等方面的科学研究。隆线蚤（溞）（学名：*Daphnia carinata*），见图 5，隶属于蚤科蚤属，是最常见的水蚤之一，其分布广，采集方便，易于实验室培养，在生态、毒理等试验中常常被用作研究对象，是小型淡水无脊椎动物的典型代表之一。

图 5 隆线蚤

1.1.2 研究意义

在水生系统中，汞元素多以甲基汞的形式进行生物富集，并在水生生物之间转移，最终对人类产生危害，故而研究甲基汞的代谢水平以及分布规律具有相当的实际意义。目前关于甲基汞在水生生物群落中的研究，主要以测量甲基汞在浮游植物、浮游动物和鱼类中的相关浓度、转化效率、富集率等定量测定为主，然而这些研究没有提供关于甲基汞在水生生物体内摄入和输出的动力学信息，即未能阐明甲基汞在整个生物代谢过程中吸收释放量的变化过程，更未能展示甲基汞在水生生物体内的靶器官位点以及在靶器官之间的代谢分布变化，而这些是解释和预测甲基汞在水生食物链中转移机制的重要参数。另外，有实验证据表明饵料在鱼类接触甲基汞方面占主导地位，但在浮游动物物种方面还未见相关报道，故而甲基汞在浮游动物中的积累主要是直接来源于水中的吸收，还是间接来自饵料的摄入基本尚不清楚。

本研究拟以浮游动物的代表种之一：隆线蚤（*Dahphia carinata*）为研究对象，基于一种新型聚集诱导荧光物（AIEgen），建立定量测定甲基汞（MeHg）浓度的新方法，进而测定 MeHg 在隆线蚤体内吸收及释放的变化规律；以荧光示踪的方式，检测 MeHg 在隆线蚤体内的代谢位点以及分布变化；并通过浸泡和投喂两种实验手段，对比分析甲基汞在隆线蚤体内的积累水平，判定 MeHg 积累的主要方式（水中吸收或是饵料摄入）。在理论上，本项目可为研究甲基汞在浮游动物体内的代谢水平及分布提供重要的理论参考，为今后研究甲基汞在水生生物群落之

间的富集转移打下良好的实验基础；在实践上，通过新型聚集诱导荧光物（AIEgen），以期在水域生态系统中建立以 AIEgen 为基础的检测 MeHg 污染程度的新技术。

1.2 研究内容与目标

1.2.1 研究目标

1）在阐明甲基汞（MeHg）与聚集诱导荧光物 AIEgen（TPE-RNS）的化学反机理的基础上，建立定量测定 MeHg 浓度的 AIEgen 显色法，并分析鉴定此法与 ICP-MS 测定结果的吻合度。

2) 在 MeHg 以不同方式（浸泡、投喂）感染隆线蚤后，比较 MeHg 在其体内的富集释放水平及分布位点的异同，分析隆线蚤在水生环境中所富集 MeHg 的主要来源，以及 MeHg 在隆线蚤体内的代谢水平及分布规律；

3) 在前期汞离子（Hg^{2+}）处理隆线蚤的研究结果基础上，对比分析有机汞（MeHg）与无机汞（Hg^{2+}）在隆线蚤体内的代谢水平及分布规律的异同。

1.2.2 研究内容

1）弄清甲基汞（MeHg）与聚集诱导荧光物 AIEgen（TPE-RNS）的化学反应体系，确定两者的化学反应方程式，分析鉴定 AIEgen（TPE-RNS）反应后的结构变化，并与汞离子（Hg^{2+}）+TPE-RNS 的反应式（图 3）做比较分析；以系列浓度梯度的 MeHg 与 AIEgen 发生反应，利用荧光光谱仪，测定两个显色波峰光强度的比值（I_{585}/I_{480}，图 6），建立 MeHg 浓度与光强比值（I_{585}/I_{480}）的最佳标准曲线；

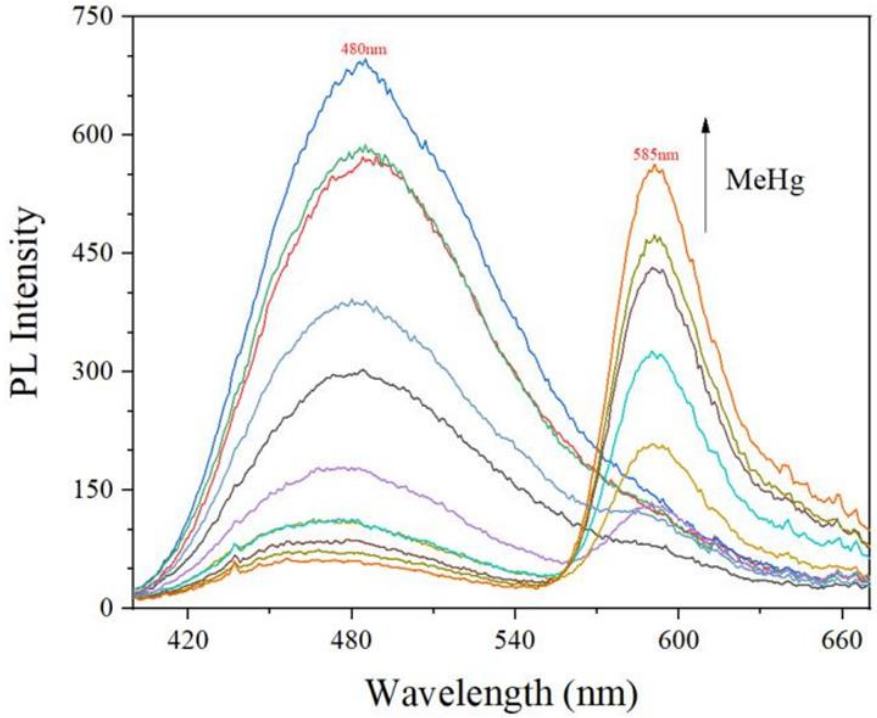

图 6 不同浓度下 AIEgen 与 MeHg 的反应图谱。AIEgen 的显色波峰为 480 nm，与 MeHg 反应后的显色波峰为 585 nm。

2）以 MeHg 溶液直接浸泡隆线蚤，按照一定的时间间隔连续取样，通过标准曲线定量检测隆线蚤对 MeHg 的吸收及释放量的变化规律，并与电感耦合等离子质谱仪（ICP-MS）测定的 MeHg 含量结果做比较，分析 AIEgen 测定法的准确度；并以荧光示踪（活体染色&组织染色）的方式检测 MeHg 在隆线蚤体内的富集靶器官，以及富集位点的转移变化规律；

3）先以 MeHg 毒化微藻，并测定微藻体内 MeHg 的含量及蓄积位点；再以毒化的微藻投喂隆线蚤，定量测定一段时间内隆线蚤体内 MeHg 含量的变化规律（与 ICP-MS 测定结果做比较分析），并监测 MeHg 在其体内代谢分布位点的变化（活体染色&组织染色）；

4）对比分析浸泡与投喂两组处理方式之下，MeHg 在隆线蚤体内代谢水平及分布规律的异同，并结合隆线蚤两组处理下的不同死亡率以及外部形态变化，分析 MeHg 致死隆线蚤的主要机制，并与项目组前期有关 Hg^{2+}的研究结果做比较分析。

1.2.3 技术方案

1）显色原理的鉴定：以系列浓度梯度(0, 0.1, 0.2, 0.3, 0.4, 0.5, 0.6, 0.7, 0.8, 0.9, 1.0 μM)的氯化甲基汞（MeHgCl）分别与不同浓度的 AIEgen（0, 0.1, 0.2, 0.3, 0.4, 0.5, 0.6, 0.7, 0.8, 0.9, 1.0μM）反应（MeHgCl 与 AIEgen 均以乙腈作为溶剂），通过荧光光谱仪测定光强度，判定 MeHg 与 AIEgen 的反应比例，并通过核磁共振仪和质谱仪鉴定反应生成物的结构式，分析出化学反应式；

2）标准曲线的建立：设置 MeHgCl 的浓度梯度(0, 0.1, 0.2, 0.3, 0.4, 0.5, 0.6, 0.7, 0.8, 0.9, 1.0 μM)，分别与 AIEgen（1.0 μM）反应，在荧光光谱仪下分别读取 AIEgen 原始波峰 (480nm) 与反应后波峰（585nm）的光强度，并计算光强度比值 I_{585}/I_{480}，而后通过统计软件 SPSS19.0 拟合 MeHg 浓度与光强比值（I_{585}/I_{480}）的标准曲线，并选取 R 值最大的作为最佳标准曲线；

3）隆线蚤及藻液的培养：选取纤细裸藻（*Euglena gracilis*）作为实验藻液，将 30g 面粉、25 g 米粉和 5g 奶粉混入 1L 的双蒸水中，高压灭菌 5 min 后，在 4℃下保存备用，用以裸藻的培养。隆线蚤的培养以投喂裸藻藻液和酵母溶液为主，以 3g 干酵母溶于 60ml 蒸馏水中制备成酵母溶液，并在 4℃下保存备用。

4）浸泡组的检测：

① MeHg 的吸收

参照蚤类对汞的毒性耐受能力[32]，设置了低（0.1μM）、中（0.5μM）、高（1.0μM）三组浓度的 MeHgCl 溶液浸泡处理隆线蚤，每隔 10min 连续取水样与隆线蚤样品至 60min，此后每隔 30min 取水样与隆线蚤至 240min 备用。在解剖镜下观察各个时期隆线蚤的形态变化，并计算其死亡率。

在所取水样与 AIEgen 发生显色反应后，通过荧光光谱仪测定两个波峰的光强度，并计算光强比值，运用上述标准曲线计算隆线蚤对 MeHg 吸收量的变化；另以电感耦合等离子质谱仪（ICP-MS）测定水样中的 MeHg 含量，并与 AIEgen 显色法的测定结果作比较分析。

在所取隆线蚤样品中加入 AIEgen，反应一段时间之后，在活体状态下以激光共聚焦荧光显微镜直接观测 MeHg 在隆线蚤体内的分布位点及变化；另取部分隆线蚤样品，先以冷冻切片机进行组织切片，置于载玻片之上后，再以 AIEgen 溶液进行染色，随后在激光共聚焦荧光显微镜下进行组织学观察。

② MeHg 的释放

以低（0.1μM）、中（0.5μM）、高（1.0μM） 三种浓度的 MeHgCl 溶液浸泡处理隆线蚤 30min，取水样检测并计算出隆线蚤对 MeHg 的吸收量，随后将隆线蚤移入清水中。每隔 10min 连续取水样以及隆线蚤至 60min，此后每隔 30min 取水样与隆线蚤至 240min 备用。在解剖镜下观察各个时期隆线蚤的形态变化，并计算相应时期的死亡率。

按照上述①所示方法，通过荧光光谱仪与激光共聚焦荧光显微镜，检测 MeHg 释放量的变化（与 ICP-MS 测定结果做比较）以及在隆线蚤体内的分布变化（活体染色&组织染色）。

5）投喂组的检测：

① 藻液的毒化与投喂

以低（0.1μM）、中（0.5μM）、高（1.0μM）三组浓度的 MeHgCl 溶液浸泡处理纤细裸藻（*Euglena gracilis*）30min，藻液以 4500 r/min 的转速离心 1min 后备用。通过荧光光谱仪和共聚焦荧光显微镜，测定裸藻体内 MeHg 的含量（与 ICP-MS 测定结果相比较）以及分布位置。而后以毒化后的藻液投喂隆线蚤。

② MeHg 的检测

每隔 10min 连续取水样与隆线蚤至 60min，此后每隔 30min 取水样与隆线蚤至 240min 备用。在解剖镜下观察各个时期隆线蚤的形态变化，并计算相应时期的死亡率。按照上述 4)①所示方法，通过荧光光谱仪与激光共聚焦荧光显微镜，检测投喂毒化的藻液后 MeHg 在隆线蚤体内的含量（与 ICP-MS 测定结果相比较）及分布位点变化（活体染色&组织染色）。

6）对比分析

对比浸泡组与投喂组实验结果的异同（隆线蚤的外部形态变化、死亡率、MeHg 富集量、MeHg 分布位点），分析隆线蚤在水域环境中富集 MeHg 的主要来源、MeHg 对隆线蚤的致死机理等；并对比前期以 Hg^{2+} 处理隆线蚤的实验结果，分析有机汞与无机汞在浮游动物体内代谢机制的异同。

1.2.4 技术路线

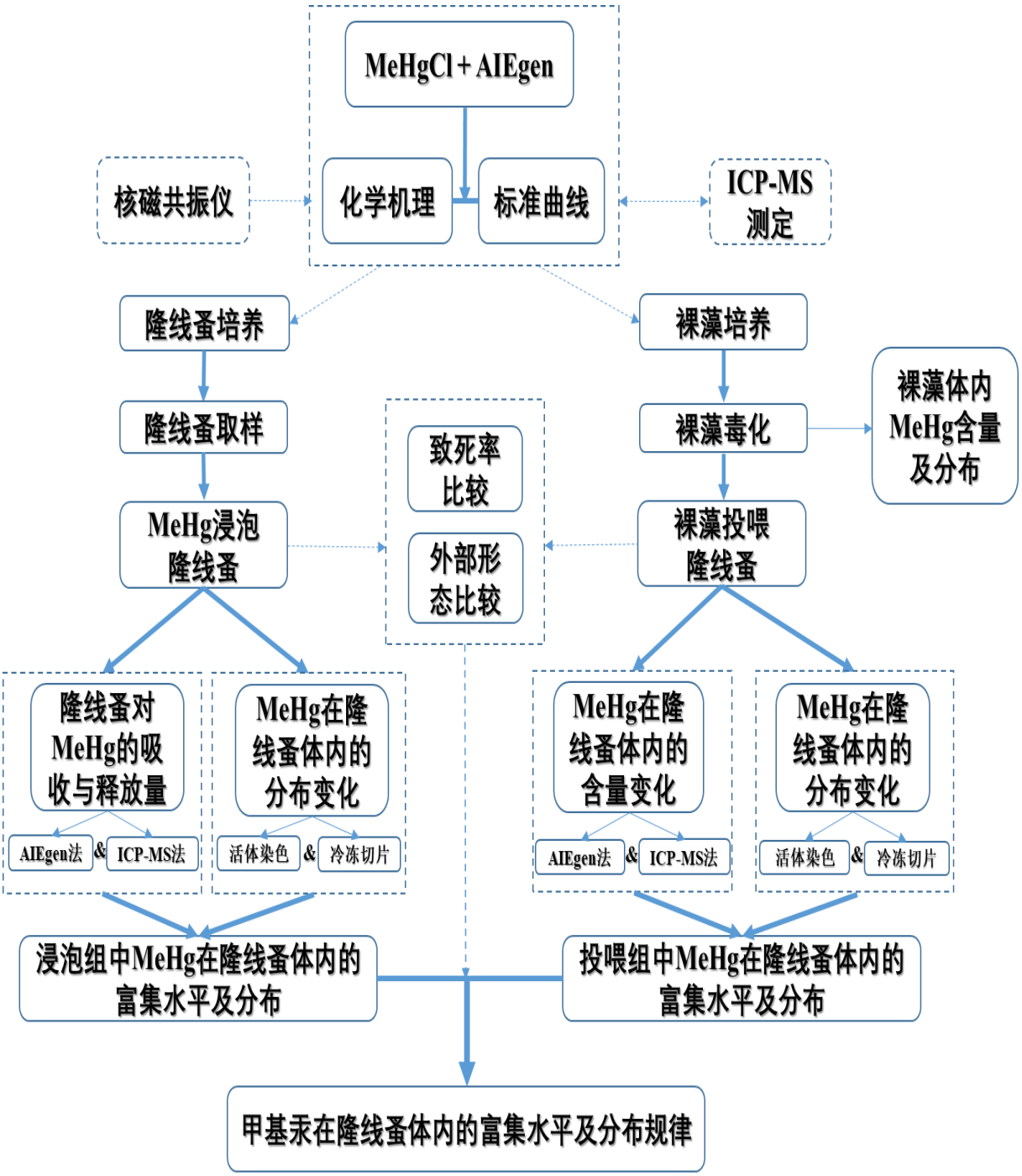
MeHgCl+AIEgen
核磁共振仪
化学机理
标准曲线
ICP-MS测定
隆线蚤培养
裸藻培养
隆线蚤取样
裸藻毒化
裸藻体内MeHg含量及分布
致死率比较
MeHg浸泡隆线蚤
外部形态比较
裸藻投喂隆线蚤
隆线蚤对MeHg的吸收与释放量
MeHg在隆线蚤体内的分布变化
MeHg在隆线蚤体内的含量变化
MeHg在隆线蚤体内的分布变化
AIEgen法
&
ICP-MS法
活体染色
&
冷冻切片
AIEgen法
&
ICP-MS法
活体染色
&
冷冻切片
浸泡组中MeHg在隆线蚤体内的富集水平及分布
投喂组中MeHg在隆线蚤体内的富集水平及分布
甲基汞在隆线蚤体内的富集水平及分布规律

2. 项目研究进展与主要工作

本研究通过聚集诱导荧光探针 AIEgen 法，研究了浮游动物的代表种之一：隆线蚤对 MeHg 的富集特征，主要工作进展如下：

1）聚集诱导荧光探针 AIEgen 法检测 MeHg

建立了一种聚集诱导荧光探针 AIEgen 方法，可以特异性识别溶液或生物体内的 MeHg，在通过拟合标准曲线定量检测溶液中 MeHg 的浓度的同时，也可以通过荧光示踪的方式定性检测 MeHg 在浮游动物隆线蚤体内的积累位点和富集规律。

2）MeHg 在隆线蚤体内的富集水平

隆线蚤表现出对水体环境中 MeHg 的快速吸收现象，并且能够将 MeHg 富集在体内。以两组不同浓度的 MeHg 分别浸泡隆线蚤，在浸泡后 0-60 min 之内，2.5 μM/L 组隆线蚤体内 MeHg 的吸收量持续增加至 0.123 μM，而 5.0 μM/L 组隆线蚤体内 MeHg 的吸收量为 0.218 μM；隆线蚤对 MeHg 的释放结果表明：在 5.0 μM/L 组中，将攻毒后的隆线蚤转入纯水中 5min 后，隆线蚤向外释放了 0.061 μM 的 MeHg，而后 MeHg 的释放量变化不大。在 2.5 μM/L 组中，隆线蚤在 5 min 后释放 0.076 μM 的 MeHg，该释放量逐渐在 60 min 内稳定，随后释放的 MeHg 持续减少到 0.061 μM，直到 240 min。通过浸泡组与投喂组的比较，我们发现直接浸泡时，MeHg 的吸收量随着时间的延长而逐渐增加，直到 150 min 后 MeHg 生物积累量趋于稳定；在投喂组中，MeHg 的积累从开始计时的 10 到 30 min 持续增加，然后在 60 min 时下降，最后趋于平稳。

3）MeHg 在隆线蚤体内的富集位点

直接将隆线蚤浸泡孵育在 MeHg 溶液中，我们发现 MeHg 主要富集在隆线蚤的复眼中，随着孵育时间的不断增加，复眼处特异性结合产物的红色荧光显现的更加明显。然而，尽管这些红色荧光靠近复眼和视神经，但在眼上细胞和大脑上并没有检测到 MeHg 的富集。通过间接摄入被 MeHg 毒化的纤细裸藻，我们发现在进食毒化藻类后，隆线蚤对 MeHg 的吸收量开始趋于平稳并随着时间的推移趋于稳定，通过共聚焦倒置荧光显微镜观察发现食入后 MeHg 富集在前肠囊和肠道处，而在复眼和视神经处未出现荧光信号。

隆线蚤体内的 MeHg 大多数与机体组织相结合，难以被排泄系统通过代谢作用排出体外。通过特异性聚集诱导荧光探针 AIEgen 对 MeHg 进行可视化研究，为观察 MeHg 在浮游动物中的分布和了解 MeHg 在水生食物网中的生物积累过程提供了一种新的工具。

3. 任务书指标完成情况及成效

1) 已建立基于 AIEgen 的 MeHg 定量检测标准曲线: $CMeHg = 1.14*\ln(I_{585}/I_{480}) - 0.333$
2) 已完成浸泡组中 MeHg 在隆线蚤体内的吸收释放水平以及在体内代谢分布位点的变化检测；裸藻的毒化后建立投喂组，并完成了投喂组中隆线蚤对 MeHg 的吸收水平及代谢分布位点分析。
3) 参加国内学术会议一次（2023 年中国水产学会青年学术年会）；发表 SCI 论文 2 篇（均为中科院一区期刊）；完成结题报告

4. 项目创新点和取得的突破

1）通过新型聚集诱导荧光物 AIEgen（TPE-RNS）与 MeHg 发生特异性荧光显色反应，建立了一种新型便捷的，可定量测定甲基汞含量的方法；

2）通过 AIEgen 的特异荧光显色，可在活体条件下连续观测 MeHg 在浮游动物（隆线蚤）体内的代谢分布规律；

3）为在水域生态系统中建立以 AIEgen 为基础的、检测 MeHg 污染程度的新技术提供了理论基础。

5. 需要重点说明的内容或其他需要说明的内容

无。

立项编号： cstc2021jcyj-msxmX0100

重庆市自然科学基金面上项目研究报告

项目名称	基于 AIEgen 的甲基汞在浮游动物体内的富集水平与分布规律
承担单位	西南大学
项目负责人	何滔
通讯地址	重庆市北碚区天生路 1 号
联系电话	15023177126
起止年限	2021-10-01 至 2024-1-15

西南大学

二 O 二四年一月

一、研究目标

在水生系统中，汞元素多以甲基汞的形式进行生物富集，并在水生生物之间转移，最终对人类产生危害，故而研究甲基汞的代谢水平以及分布规律具有相当的实际意义。目前关于甲基汞在水生生物群落中的研究，主要以测量甲基汞在浮游植物、浮游动物和鱼类中的相关浓度、转化效率、富集率等定量测定为主，然而这些研究没有提供关于甲基汞在水生生物体内摄入和输出的动力学信息，即未能阐明甲基汞在整个生物代谢过程中吸收释放量的变化过程，更未能展示甲基汞在水生生物体内的靶器官位点以及在靶器官之间的代谢分布变化，而这些是解释和预测甲基汞在水生食物链中转移机制的重要参数。另外，有实验证据表明饵料在鱼类接触甲基汞方面占主导地位，但在浮游动物物种方面还未见相关报道，故而甲基汞在浮游动物中的积累主要是直接来源于水中的吸收，还是间接来自饵料的摄入基本尚不清楚。

本研究以浮游动物的代表种之一：隆线蚤（*Dahphia carinata*）为研究对象，基于一种新型聚集诱导荧光物（AIEgen），建立定量测定甲基汞（MeHg）浓度的新方法，进而测定 MeHg 在隆线蚤体内吸收及释放的变化规律；以荧光示踪的方式，检测 MeHg 在隆线蚤体内的代谢位点以及分布变化；并通过浸泡和投喂两种实验手段，对比分析甲基汞在隆线蚤体内的积累水平，判定 MeHg 积累的主要方式（水中吸收或是饵料摄入）。在理论上，本项目可为研究甲基汞在浮游动物体内的代谢水平及分布提供重要的理论参考，

为今后研究甲基汞在水生生物群落之间的富集转移打下良好的实验基础；在实践上，通过新型聚集诱导荧光物（AIEgen），以期在水域生态系统中建立以 AIEgen 为基础的检测 MeHg 污染程度的新技术。

二、研究方法

2.1 显色原理的鉴定

以系列浓度梯度(0, 0.1, 0.2, 0.3, 0.4, 0.5, 0.6, 0.7, 0.8, 0.9, 1.0 μM)的氯化甲基汞（MeHgCl）分别与不同浓度的 AIEgen（0, 0.1, 0.2, 0.3, 0.4, 0.5, 0.6, 0.7, 0.8, 0.9, 1.0μM）反应（MeHgCl 与 AIEgen 均以乙腈作为溶剂），通过荧光光谱仪测定光强度，判定 MeHg 与 AIEgen 的反应比例，并通过核磁共振仪和质谱仪鉴定反应生成物的结构式，分析出化学反应式。

2.2 标准曲线的建立

设置 MeHgCl 的浓度梯度(0, 0.1, 0.2, 0.3, 0.4, 0.5, 0.6, 0.7, 0.8, 0.9, 1.0 μM)，分别与 AIEgen（1.0 μM）反应，在荧光光谱仪下分别读取 AIEgen 原始波峰 (480nm) 与反应后波峰（585nm）的光强度，并计算光强度比值 I_{585}/I_{480}，而后通过统计软件 SPSS19.0 拟合 MeHg 浓度与光强比值（I_{585}/I_{480}）的标准曲线，并选取 R 值最大的作为最佳标准曲线。

2.3 隆线蚤及藻液的培养

选取纤细裸藻（*Euglena gracilis*）作为实验藻液，将 30g 面粉、25 g 米粉和 5g 奶粉混入 1L 的双蒸水中，高压灭菌 5 min 后，在 4℃下保存备用，用以裸藻的培养。隆线蚤的培养以投喂裸藻藻液和酵母溶液为主，以 3g 干

酵母溶于 60ml 蒸馏水中制备成酵母溶液，并在 4℃下保存备用。

2.4 浸泡组的检测

2.4.1 MeHg 的吸收

参照蚤类对汞的毒性耐受能力[32]，设置了低（0.1μM）、中（0.5μM）、高（1.0μM）三组浓度的 MeHgCl 溶液浸泡处理隆线蚤，每隔 10min 连续取水样与隆线蚤样品至 60min，此后每隔 30min 取水样与隆线蚤至 240min 备用。在解剖镜下观察各个时期隆线蚤的形态变化，并计算其死亡率。

在所取水样与 AIEgen 发生显色反应后，通过荧光光谱仪测定两个波峰的光强度，并计算光强比值，运用上述标准曲线计算隆线蚤对 MeHg 吸收量的变化；另以电感耦合等离子质谱仪（ICP-MS）测定水样中的 MeHg 含量，并与 AIEgen 显色法的测定结果作比较分析。

在所取隆线蚤样品中加入 AIEgen，反应一段时间之后，在活体状态下以激光共聚焦荧光显微镜直接观测 MeHg 在隆线蚤体内的分布位点及变化；另取部分隆线蚤样品，先以冷冻切片机进行组织切片，置于载玻片之上后，再以 AIEgen 溶液进行染色，随后在激光共聚焦荧光显微镜下进行组织学观察。

2.4.2 MeHg 的释放

以低（0.1μM）、中（0.5μM）、高（1.0μM） 三种浓度的 MeHgCl 溶液浸泡处理隆线蚤 30min，取水样检测并计算出隆线蚤对 MeHg 的吸收量，随后将隆线蚤移入清水中。每隔 10min 连续取水样以及隆线蚤至 60min，此后每隔 30min 取水样与隆线蚤至 240min 备用。在解剖镜下观察各个时期隆线

蚤的形态变化，并计算相应时期的死亡率。

按照上述所示方法，通过荧光光谱仪与激光共聚焦荧光显微镜，检测 MeHg 释放量的变化（与 ICP-MS 测定结果做比较）以及在隆线蚤体内的分布变化（活体染色&组织染色）。

2.5 投喂组的检测

2.5.1 藻液的毒化与投喂

以低（0.1μM）、中（0.5μM）、高（1.0μM）三组浓度的 MeHgCl 溶液浸泡处理纤细裸藻（*Euglena gracilis*）30min，藻液以 4500 r/min 的转速离心 1min 后备用。通过荧光光谱仪和共聚焦荧光显微镜，测定裸藻体内 MeHg 的含量（与 ICP-MS 测定结果相比较）以及分布位置。而后以毒化后的藻液投喂隆线蚤。

2.5.2 MeHg 的检测

每隔 10min 连续取水样与隆线蚤至 60min，此后每隔 30min 取水样与隆线蚤至 240min 备用。在解剖镜下观察各个时期隆线蚤的形态变化，并计算相应时期的死亡率。按照上述所示方法，通过荧光光谱仪与激光共聚焦荧光显微镜，检测投喂毒化的藻液后 MeHg 在隆线蚤体内的含量（与 ICP-MS 测定结果相比较）及分布位点变化（活体染色&组织染色）。

2.6 对比分析

对比浸泡组与投喂组实验结果的异同（隆线蚤的外部形态变化、死亡率、MeHg 富集量、MeHg 分布位点），分析隆线蚤在水域环境中富集 MeHg 的主要来源、MeHg 对隆线蚤的致死机理等；并对比前期以 Hg^{2+}处理隆线蚤的

实验结果，分析有机汞与无机汞在浮游动物体内代谢机制的异同。

三、研究结果

3.1 基于 AIEgen 的 MeHg 检测方法的建立

3.1.1 AIEgen 与 MeHg 反应体系内的纯水/乙腈比例

聚集诱导荧光探针 AIEgen 和甲基汞 MeHg 在不同的纯水含量下（体积分数 fw，由 0 至 90%）结合产物具有不同的荧光发光能力如图 3-1。由图可得，当整个 AIEgen 和 MeHg 反应体系中水份含量在 60%的时候，MeHg 和 AIEgen 特异性反应后的产物 m-TPE-RNO 在可见光与紫外线激发下产生的荧光程度均最强，特异性荧光发光效果最好。因此在之后的荧光特异性显色试验中，我们将调控 AIEgen 和 MeHg 的混合反应体系中水份的含量为 60%，即水的体积与乙腈的体积比为 3：2，以便使得特异性反应达到最佳荧光显色效果。

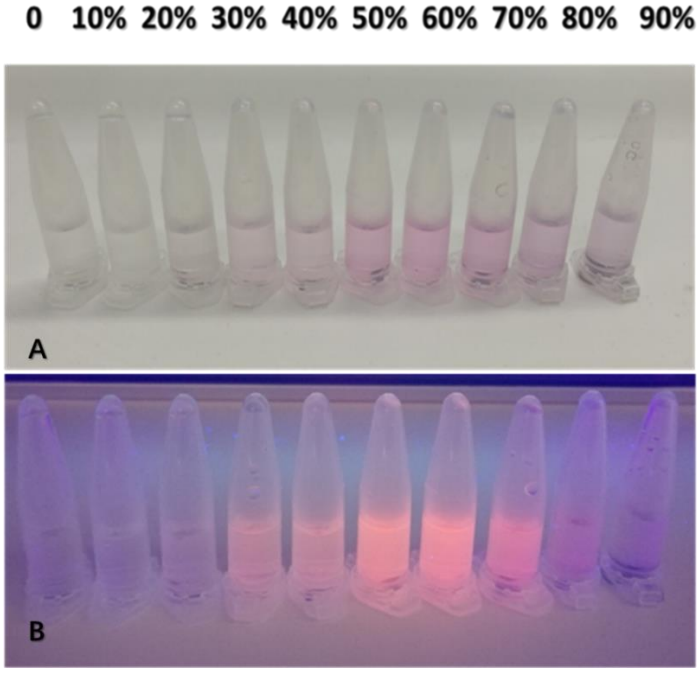

图 3-1 MeHg 和 AIEgen 混合反应体系中不同水份含量下的荧光呈现。（A）可见光下；（B）紫外线照射下。

3.1.2 AIEgen 与 MeHg 的特异性反应

在可见光和紫外光下 1 μmol L^{-1} 的聚集诱导荧光探针 m-TPE-RNS 和 1 μmol L^{-1} 的甲基汞以及其他 1 μmol L^{-1} 的有机化金属化合物相互反应，发现无论是在可见光还是在紫外光下只有 MeHg 和 AIEgen 表现出特异性荧光如图 3-2。随后在荧光分光光度计下测量 PL 强度发现只有 MeHg 和 AIEgen 特异性结合反应产出 TPE-RNO 并在 585nm 表现强 PL 值的波峰如图 3-3。

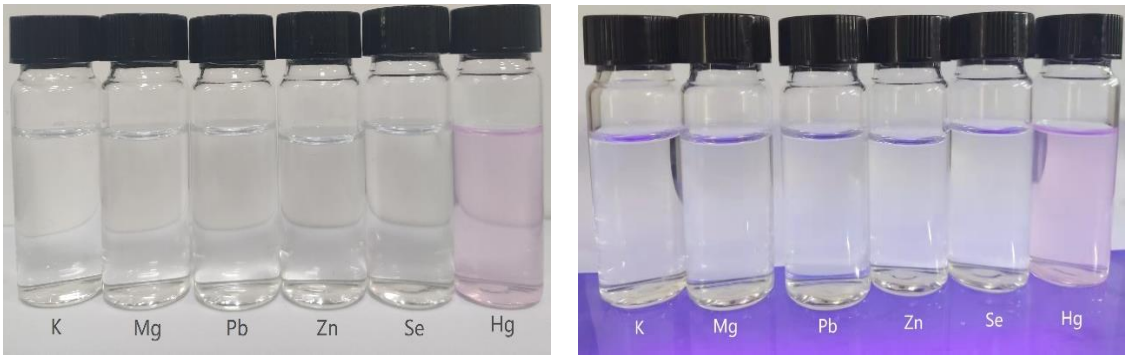

图 3-2 重金属的特异性和敏感性检测（1：可见光；2：350nm 荧光激发）

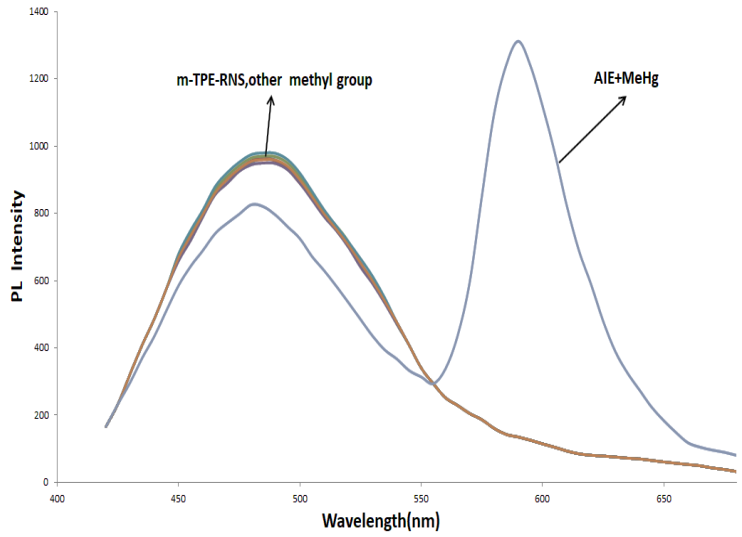

图 3-3 在 350nm 荧光激发下不同金属元素（methyl-Mg, K, Se, Zn, Pb, Hg）与 AIEgen 在乙腈纯水混合体系（水分数 60%）中的 PL 光谱

3.1.3 确定特异性反应的效应时间

控制聚集诱导荧光探针 AIEgen 和甲基汞 MeHg 的浓度均为 1 μmol L^{-1}，分别在 0 - 60 min 内通过荧光分光光度计测定荧光光照强度。结果表明：荧光光照强度的比值 $I = I_{585} / I_{480}$ 在 20 – 40min 内具有较高的稳定性，说明在整个混合体系中反应 20-40min 内，AIEgen 及其特异性反应产物发射荧光效果好如图 3-4。因此，在后续检测样品时特异性反应时间定为 30 min。

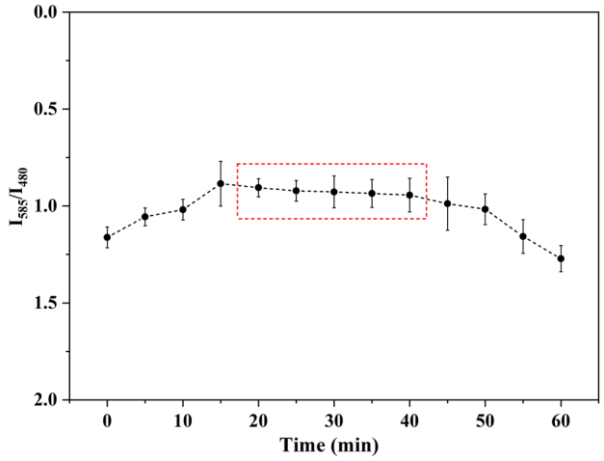

图 3-4 聚集诱导荧光探针 AIEgen 和甲基汞的反应时间

3.1.4 MeHg 定量测定的标准曲线

在不同浓度（0，1，2.5，5，7.5，10 μmol L^{-1}）的 MeHg 中加入 5.0μmol L^{-1} AIEgen 后，我们分别测量了 I_{585} 与 I_{480} 并计算了 PL 强度比，将不同浓度的 MeHg 与 m-TPE-RNS 的特异性反应荧光光谱合并得到了直观的 PL 变化光谱图如图 3-5 并建立了 PL 比(I_{585}/I_{480})与甲基汞浓度(C_{MeHg})的回归方程，如图 3-6 所示。

C_{MeHg} 与 I_{585}/I_{480} 的线性方程为:$C_{MeHg} = 1.14*\ln (I_{585}/I_{480}) - 0.333$

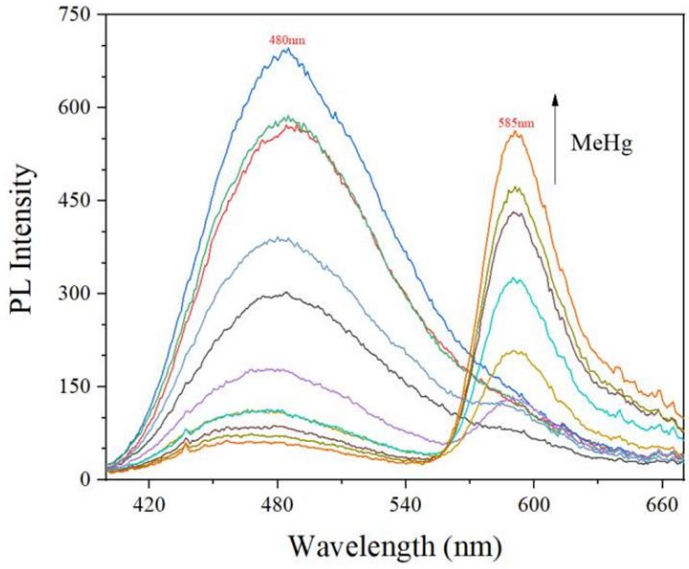

图 3-5 TPE-RNS 和 TPE-RNO 分别在 480nm 和 585nm 处显示出强烈的荧光（PL）发射峰。

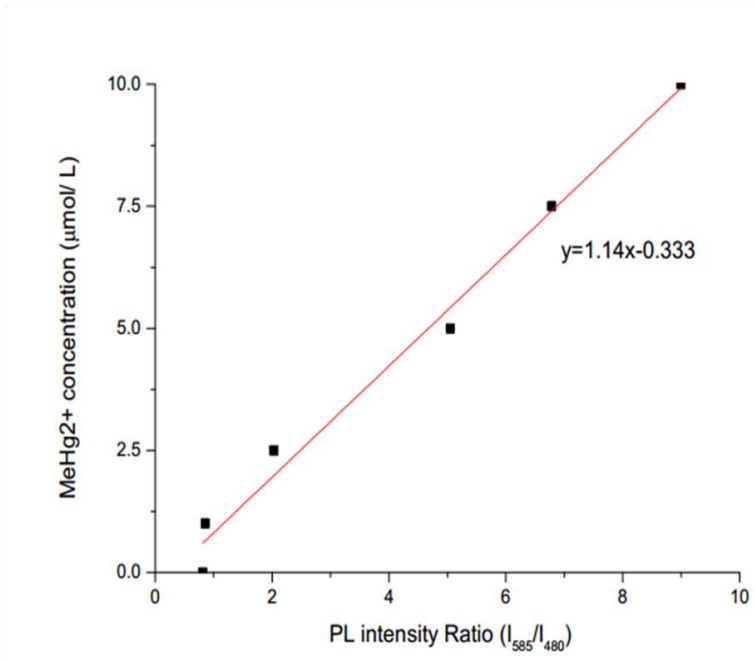

图 3-6　MeHg 浓度与 PL 强度比 I_{585}/I_{480} 的线性回归方程

3.2 MeHg 在隆线蚤体内的富集水平

3.2.1 隆线蚤对不同浓度 MeHg 吸收的定量研究

如图 3-2，我们研究了在 2.5 和 5.0 μM/L 两组不同浓度下隆线蚤对 MeHg 的生物积累趋势线，发现这两组不同浓度下 MeHg 生物积累量趋势线相似。在 MeHg 浓度为 2.5 μM/L 时，开始计时的 60 分钟之内，隆线蚤对 MeHg 的吸收从 5 分钟时的 0.08 μM 增加到 10 分钟时的 0.118 μM，而在后续的 10 分钟至 60 分钟以内，隆线蚤对 MeHg 的吸收量趋于平稳，60 分钟内最大吸收值为 0.124 μM；在 MeHg 浓度为 5 μM/L 时，隆线蚤对 MeHg 的吸收量从 10 分钟的 0.168 μM，至 20 分钟的 0.172 μM，再到 30 分钟的 0.187 μM，最后到 60 分钟的 0.218 μM。 在 0 到 60 分钟以内，隆线蚤对 MeHg 的吸收量一直不断增加。然而通过光学显微镜的观察，在这段时间内 2.5 和 5.0 μM/L 两组不同浓度下并没有隆线蚤的死亡，如图 3-3。隆线蚤的死亡发生在开始计时 60 分钟后，由图 3-2 我们可以得知 2.5 μM/L MeHg 浓度时，MeHg 的生物积累量最大为 0.142 μM，5 μM/L MeHg 浓度组，MeHg 的生物积累量发生在第 210 分钟为 0.26 μM。在 60 分钟后，隆线蚤对两组不同浓度 MeHg（2.5、5.0 μM/L）的生物积累量开始逐渐趋于平稳，其中 5 μM/L MeHg 浓度组，90 分钟的 MeHg 吸收量为 0.252 μM，120 分钟为 0.247 μM，180 分钟为 0.248 μM；2.5 μM/L MeHg 浓度组 90 分钟的 MeHg 吸收量为：0.125 μM，120 分钟吸收量为 0.129 μM，150 分钟吸收量为 0.142 μM，180 分钟 MeHg 吸收量为 0.130 μM，210 分钟 MeHg 吸收量为 0.127 μM。由图 3-3 我们可以得知无论是 MeHg 浓度为 2.5 μM/L 还是 5 μM/L，隆线蚤在 210 分钟时都全部死亡。

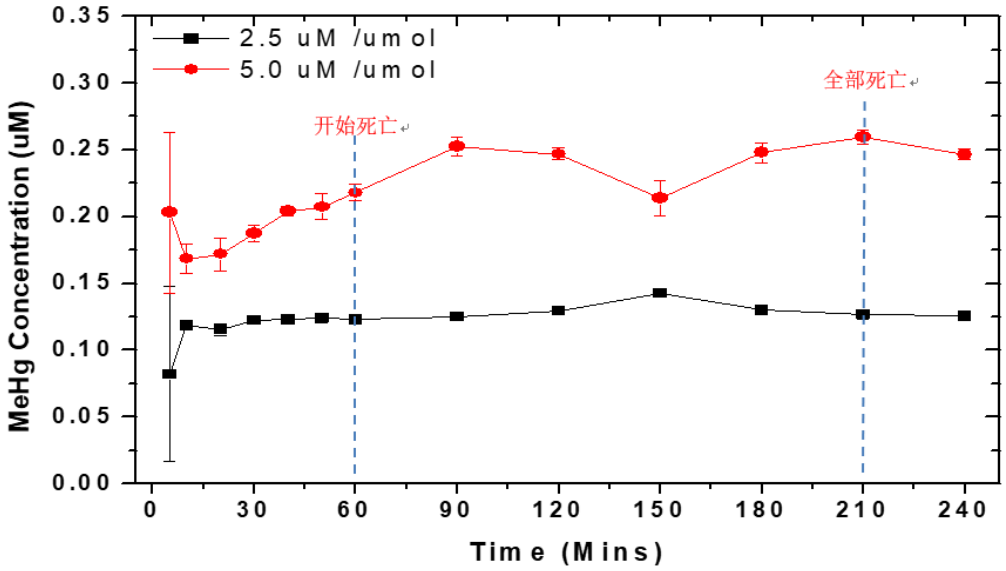

图 3-2 隆线蚤在不同时间从溶液中吸收的 MeHg 含量

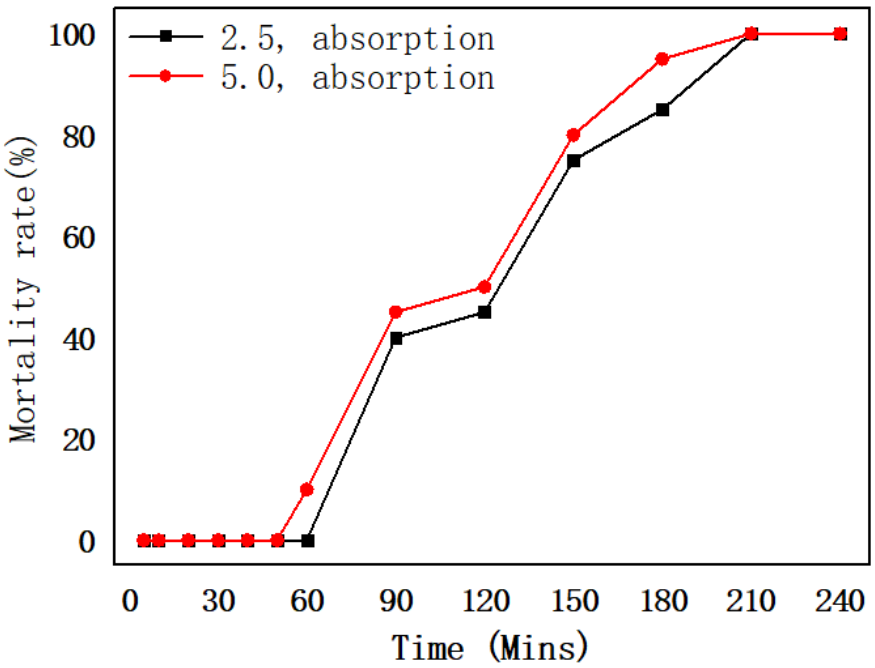

图 3-3 直接吸收不同浓度 MeHg 的隆线蚤死亡率

3.2.2 隆线蚤对不同浓度 MeHg 释放的定量研究

图 3-4 向我们展示了在不同时间段内隆线蚤向水中释放 MeHg 的情况。在 MeHg 浓度为 5.0 μM/L 组中，将被 MeHg 攻毒的隆线蚤转入纯水中 5 分钟后,隆线蚤向纯水体系内释放了 0.061 μM 的 MeHg，在 10 分钟时，检测到隆线蚤向水体释放的 MeHg 含量为 0.078 μM，在 60 分钟时，我们检测到隆线蚤向水体里释放的 MeHg 的含量为 0.058 μM，直到开始计时的 0 到 60 分钟内，纯水中 MeHg 的浓度保持相对稳定，说明这段时间隆线蚤向水中释放 MeHg 的量变化不大。60 min 后，虽然隆线蚤开始死亡(图 3-5)，但 MeHg 的释放量变化不大，由图 3-4 得知，在 90 分钟时隆线蚤向水体内释放的 MeHg 的含量为 0.056 μM，在 120 分钟时，隆线蚤向纯水体系内释放的 MeHg 的含量为 0.060 μM，150 分钟为 0.057 μM，180 分钟为 0.058 μM，210 分钟为 0.055 μM，直到实验结束 240 分钟时趋于稳定，说明进入隆线蚤体内的 MeHg 很可能与机体蛋白质相结合，形成结合性 MeHg，从而被隆线蚤富集。在 2.5 μM/L 组中，隆线蚤在 5 分钟后释放 0.076 μM 的 MeHg，在 10 分钟时，检测到隆线蚤向水体释放的 MeHg 含量为 0.079 μM，在 60 分钟时，我们检测到隆线蚤向水体里释放的 MeHg 的含量为 0.075 μM，直到开始计时的 0 到 60 分钟内，纯水中 MeHg 的浓度保持相对稳定。由图 3-4 得知，在 90 分钟时隆线蚤向水体内释放的 MeHg 的含量为 0.075 μM，在 120 分钟时，隆线蚤向纯水体系内释放的 MeHg 的含量为 0.065 μM，150 分钟为 0.065 μM，180 分钟为 0.062 μM，210 分钟为 0.068 μM，该释放量逐渐在 60 分钟内稳

定，随后释放的 MeHg 在 60 分钟以后持续减少到 0.061 μM，直到 240 分钟整个研究检测结束。

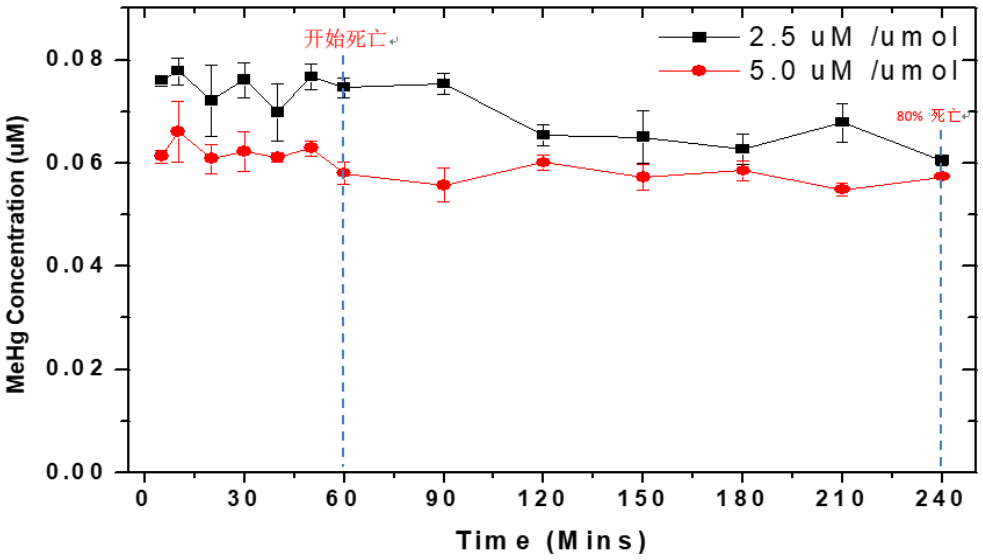

图 3-4 不同时间内隆线蚤向水中释放的 MeHg 含量

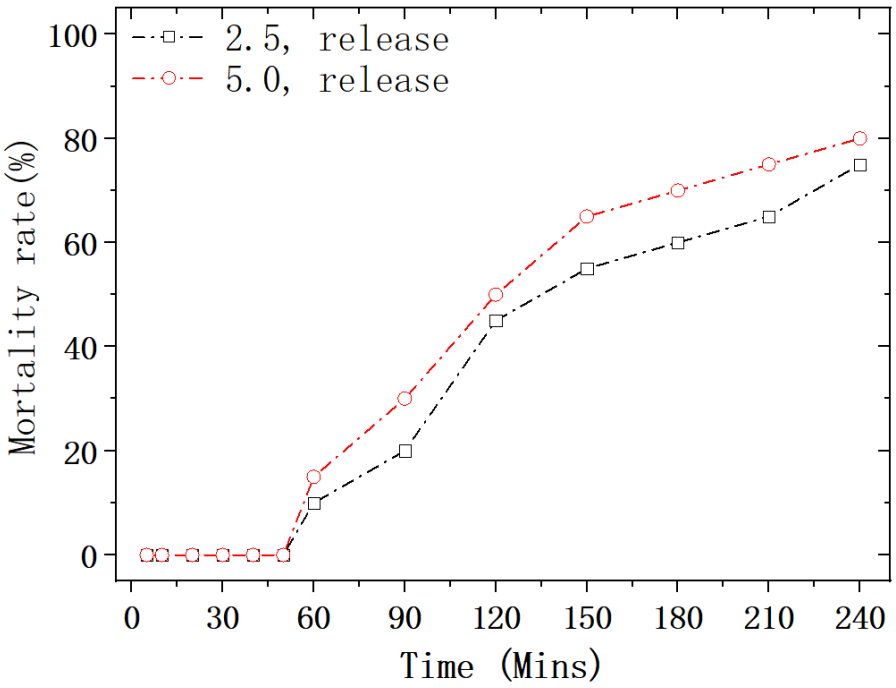

图 3-5 释放时不同浓度 MeHg 的隆线蚤死亡率

3.2.3 隆线蚤对不同方式（浸泡和投喂）MeHg 吸收的定量研究

如图 3-6 所示，隆线蚤喂食含有 MeHg 的纤细裸藻所表现出的反应与直接浸泡在 MeHg 溶液中反应有所不同。在直接浸泡吸收组中，MeHg 的吸收量随着浸泡孵育时间的延长而逐渐增加，直到 150 min 后隆线蚤对 MeHg 的生物积累量趋于平稳并随时间推移逐渐稳定。在投喂组中，隆线蚤间接进食摄入含有 MeHg 的纤细裸藻，其 MeHg 的积累从开始计时的 10 到 30 min 持续增加，然后在 60 min 时下降。在进食毒化藻类的 60 min 后，隆线蚤对 MeHg 的吸收量开始趋于平稳并随着时间的推移趋于稳定。

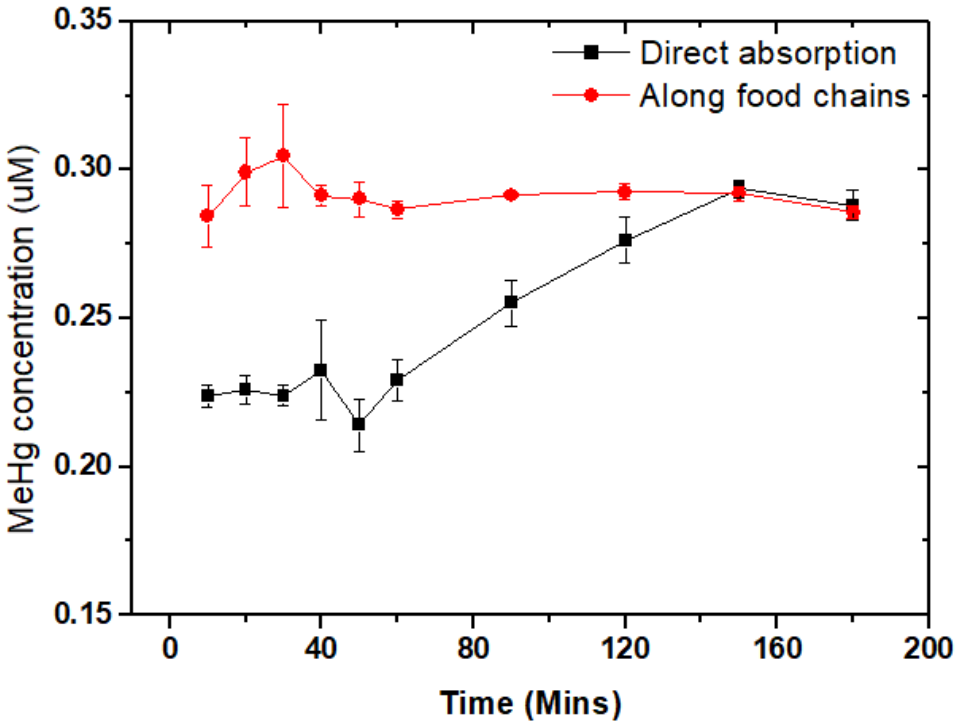

图 3-6 通过摄入被毒化的藻类和直接吸收 MeHg 的生物累积性比较

3.3 MeHg 在隆线蚤体内的富集位点：基于 AIEgen 荧光示踪

3.3.1 浸泡组—直接浸泡下 MeHg 在隆线蚤体内的富集位点

如图 3-7(a)所示，当隆线蚤在不添加 MeHg 和特异性聚集诱导荧光探针 AIEgen 时，对照组的隆线蚤没有荧光信号，这一发现与未添加 AIEgen 的 MeHg 暴露的隆线蚤相类似，如图 3-7(b)所示。浸泡在 AIEgen 中的隆线蚤在蓝色通道中显示蓝色荧光，如图 3-7 (c)所示。MeHg 在被特异性聚集诱导荧光探针 AIEgen 处理后，红色通道中显示红色荧光，如图 3-7 (d)所示。隆线蚤直接浸泡 MeHg5 分钟后，在红色通道里，复眼出现荧光信号(图 3-8(a1)、(a2))，同时随着孵育时间的不断延长，复眼表面的红色荧光显现的更加清晰，如图 3-8，说明复眼是隆线蚤吸收 MeHg 的靶位置，也说明 MeHg 首先富集在隆线蚤的复眼处，随着时间进程的进展，不断富集。同时复眼显示的红色荧光继续向该组织内部移动，如图 3-9。在处理 40 min 时，特异性聚集诱导荧光探针 AIEgen 与 MeHg 结合产生的红色荧光在视神经处微弱的发射，如图 3-9 (c)，随着孵育时间的不断增加，特异性结合产物的红色荧光发射的更加明显。然而，尽管这些红色荧光靠近复眼和视神经，但在眼上细胞和大脑上没有荧光信号(图 3-9 (c1)和 3-9 (c2))，说明 MeHg 不能通过复眼到达视神经细胞。

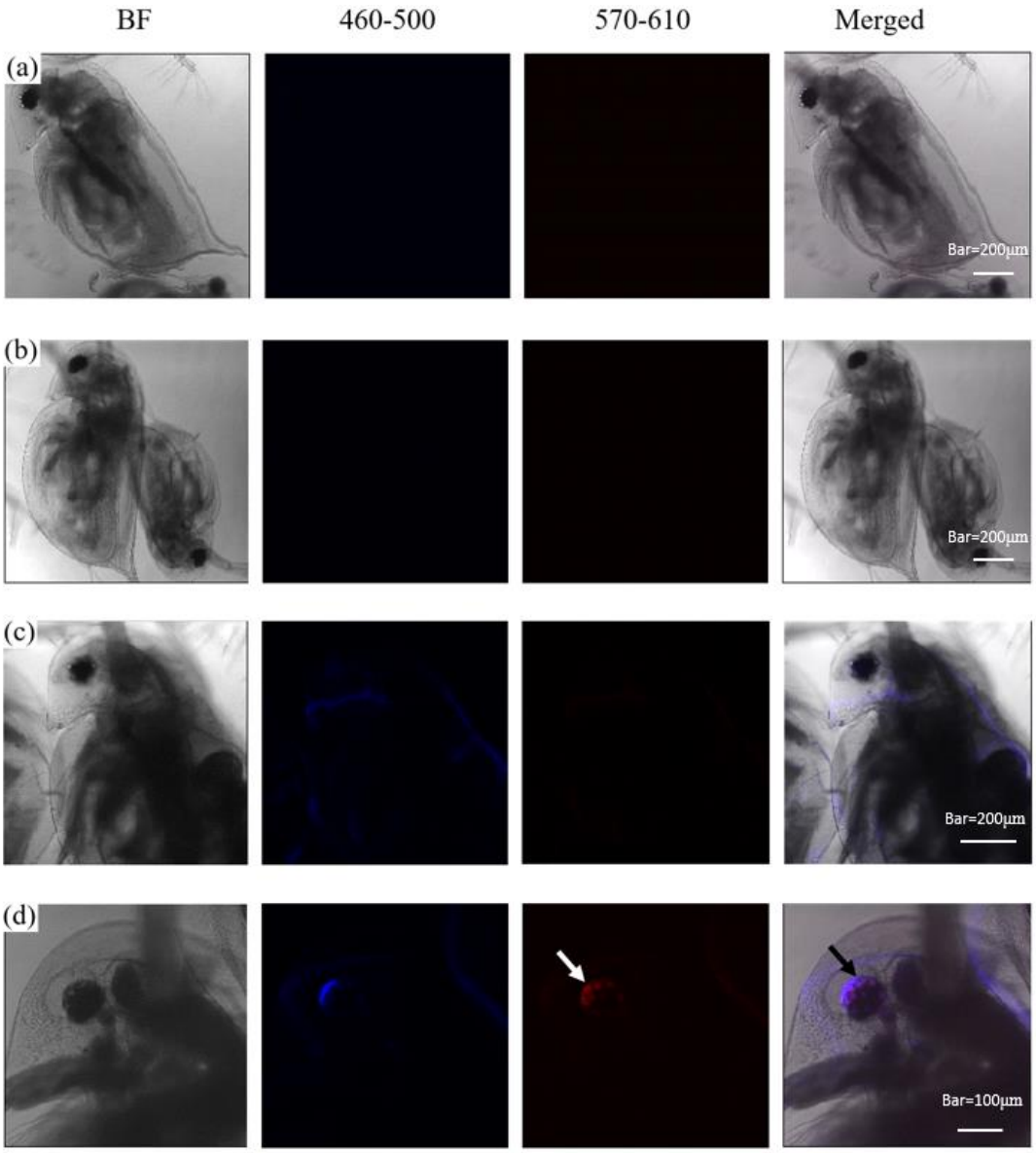

图 3-7 共聚焦显微镜下 5.0 μM MeHg 攻毒隆线蚤图像。(a)对照，无探针无 MeHg;(b)暴露于 MeHg 但未用探针 AIEgen 染色;(c)在不含 MeHg 的情况下，暴露于 1.0 μM 聚集诱导荧光探针 AIEgen 中，发出蓝色荧光;(d)暴露于 1.0 μM 聚集诱导荧光探针 AIEgen 溶液中处理的 5.0 μM MeHg，发出红色荧光(箭头)。

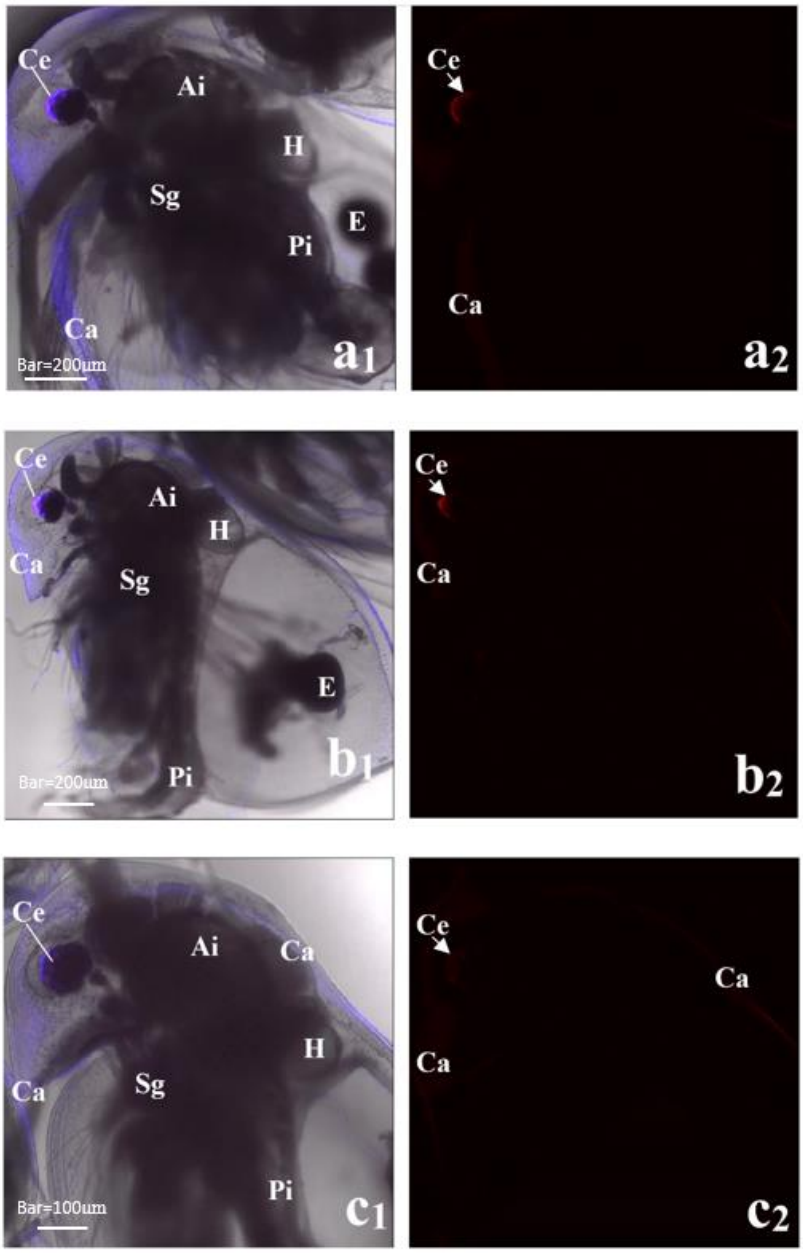

图 3-8 隆线蚤在 MeHg 溶液中孵育（a）5 分钟；（b）20 分钟；（c）60 分钟后的共聚焦荧光图像。Ai：前肠；B：脑；Ca：甲壳；Ce：复眼；E：胚胎；H：心脏；Pi：后肠；Sg：壳腺。(a1, b1, c1: 白色背景) 和 (a2, b2, c2: 黑色背景)。

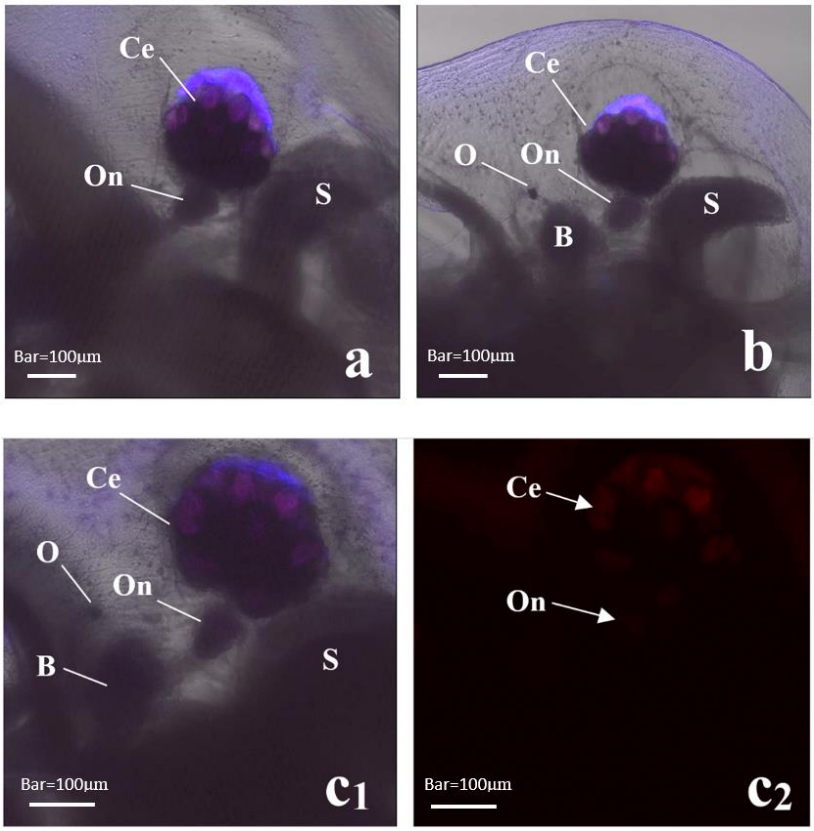

图 3-9 隆线蚤头部的荧光图像：（a）5 分钟；（b）20 分钟；（c）40 分钟后。B：大脑；Ce：复眼；O：眼球；On。视神经； S:肠囊. （c1：白色背景）和（c2：黑色背景）。

3.3.2 投喂组：摄食毒化纤细裸藻后 MeHg 在隆线蚤体内的富集位点

隆线蚤以被毒化的纤细裸藻为食后，通过共聚焦倒置荧光显微镜观察发现食入后在前肠囊和肠道处出现红色荧光，而在复眼和视神经处未出现荧光信号，如图 3-10 (b1)和(b2)所示，这一结果与直接在 MeHg 溶液中浸泡孵育的隆线蚤有显著差异，如图 3-10 (a1)和(a2)所示。说明纤细裸藻传递到隆线蚤体内的 MeHg 积累因消化作用积累在隆线蚤的消化系统内。由图 3-11 我们可以得知直接浸泡在 MeHg 的隆线蚤死亡率远高于间接投喂摄入 MeHg 的隆线蚤死亡率，直接浸泡 MeHg 的隆线蚤在 5min 时死亡率为 80%，随着时间的推移，到 120 min 时隆线蚤全部死亡。在通过使用毒化后的纤细裸藻投喂隆线蚤并

测算死亡率时我们发现，在开始摄食 60 min 以内，隆线蚤死亡率稳定在 30%，而在 60 min 至 120 min 的时间里，隆线蚤死亡率逐渐升高至 58%，最后一直稳定至 180 min 实验结束。说明隆线蚤通过消化作用将 MeHg 积累在消化系统中，并且消化系统对 MeHg 的胁迫有着一定的耐受性，然而复眼这类视觉器官直接裸露于 MeHg 中是隆线蚤死亡率高的主要原因。

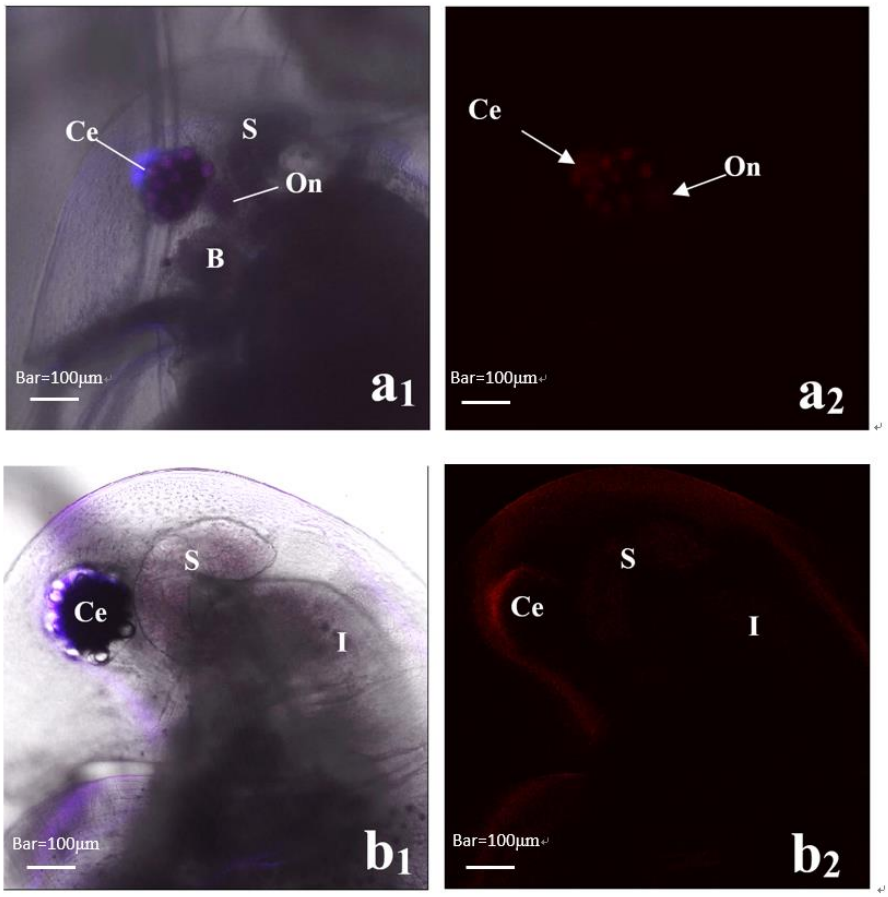

图 3-10 直接浸泡在 MeHg 中的隆线蚤（a）和用含 MeHg 的纤细裸藻喂养的隆线蚤（b）的比较共聚焦荧光图像。B：大脑；Ce：复眼； I：肠道；On: 视神经； S：肠囊 （a1，b1：白色背景）和（a2，b2：黑色背景）。

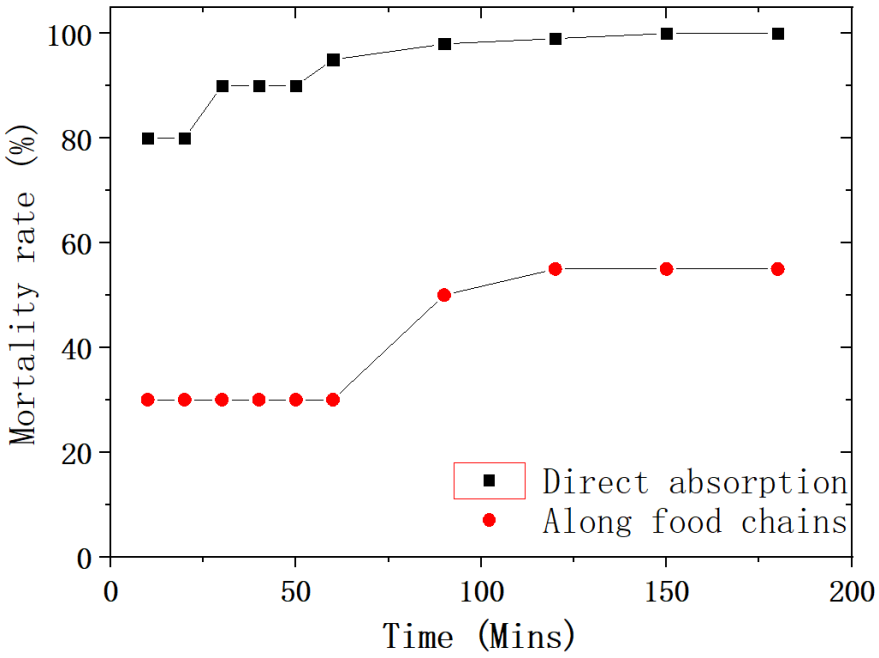

图 3-11 浸泡组与投喂组中隆线蚤死亡率比较

四、结论与展望

4.1 结论

本研究通过聚集诱导荧光探针 AIEgen 法，研究了浮游动物的代表种之一：隆线蚤对 MeHg 的富集特征，主要结论如下：

（1）聚集诱导荧光探针 AIEgen 法检测 MeHg

建立了一种聚集诱导荧光探针 AIEgen 方法，可以特异性识别溶液或生物体内的 MeHg，在通过拟合标准曲线定量检测溶液中 MeHg 的浓度的同时，也可以通过荧光示踪的方式定性检测 MeHg 在浮游动物隆线蚤体内的积累位点和富集规律。

（2）MeHg 在隆线蚤体内的富集水平

隆线蚤表现出对水体环境中 MeHg 的快速吸收现象，并且能够将

MeHg 富集在体内。以两组不同浓度的 MeHg 分别浸泡隆线蚤，在浸泡后 0-60 min 之内，2.5 μM/L 组隆线蚤体内 MeHg 的吸收量持续增加至 0.123 μM，而 5.0 μM/L 组隆线蚤体内 MeHg 的吸收量为 0.218 μM；隆线蚤对 MeHg 的释放结果表明：在 5.0 μM/L 组中，将攻毒后的隆线蚤转入纯水中 5min 后，隆线蚤向外释放了 0.061 μM 的 MeHg，而后 MeHg 的释放量变化不大。在 2.5 μM/L 组中，隆线蚤在 5 min 后释放 0.076 μM 的 MeHg，该释放量逐渐在 60 min 内稳定，随后释放的 MeHg 持续减少到 0.061 μM，直到 240 min。通过浸泡组与投喂组的比较，我们发现直接浸泡时，MeHg 的吸收量随着时间的延长而逐渐增加，直到 150 min 后 MeHg 生物积累量趋于稳定；在投喂组中，MeHg 的积累从开始计时的 10 到 30 min 持续增加，然后在 60 min 时下降，最后趋于平稳。

（3）MeHg 在隆线蚤体内的富集位点

直接将隆线蚤浸泡孵育在 MeHg 溶液中，我们发现 MeHg 主要富集在隆线蚤的复眼中，随着孵育时间的不断增加，复眼处特异性结合产物的红色荧光显现的更加明显。然而，尽管这些红色荧光靠近复眼和视神经，但在眼上细胞和大脑上并没有检测到 MeHg 的富集。通过间接摄入被 MeHg 毒化的纤细裸藻，我们发现在进食毒化藻类后，隆线蚤对 MeHg 的吸收量开始趋于平稳并随着时间的推移趋于稳定，通过共聚焦倒置荧光显微镜观察发现食入后 MeHg 富集在前肠囊和肠道处，而在复眼和视神经处未出现荧光信号。隆线蚤体内的 MeHg 大多数与机体组织相结合，难以被排泄系统通过代谢作用排出体外。通

过特异性聚集诱导荧光探针 AIEgen 对 MeHg 进行可视化研究，为观察 MeHg 在浮游动物中的分布和了解 MeHg 在水生食物网中的生物积累过程提供了一种新的工具。

4.2 展望

（1）聚集诱导荧光探针 AIEgen 法表现出对 MeHg 的特异性识别，但是用 AIEgen 法检测 MeHg 和 Hg^{2+}时，互相有较多相似之处，尤其是在荧光示踪的时候，汞离子会干扰聚集诱导荧光探针 AIEgen 对 MeHg 的荧光示踪，难以辨别两者之间的差异，需要通过试验进一步确定 AIEgen 检测 MeHg 和 Hg^{2+}的定量定性相关差异。

（2）隆线蚤这类浮游动物表现出对水体环境中 MeHg 的快速富集，无论是直接浸泡还是间接摄入，都只是水生生态系统食物链的前端，尚未研究 MeHg 在水生食物链中更高营养级（鱼类、贝类、虾等）中的富集规律和生物放大效应，需要进一步的研究补足。

项目经费支出决算表

（单位：万元）

项目名称：基于 AIEgen 的甲基汞在浮游动物体内的富集水平与分布规律

项目负责人：　　立项编号：cstc2021jcyj-msxmX0100　　单位财务部门：（公章）

经费预算			经费决算			
科目		预算数	科目		实际支出	其中市级财政支出
1	市级财政资金	5.0	一、直接费用		9.6	4.6
2	单位研发投入	5.0	1	设备费		
			2	材料费	3.64	1.15
			3	测试化验加工费		
			4	燃料动力费		
			5	出版/文献/信息传播/知识产权事务费	2.26	2.26
			6	差旅、会议、国际合作与交流费费	0.63	0.63
			7	劳务费	3.07	0.56
			8	专家咨询费		
			9	其他支出		
			二、间接费用		0.4	0.4
			1	管理费	0.4	0.4
			2	绩效支出		
合　计			合　计		10.0	5.0

注：1.经费预算：参照项目任务书中经费概算表填写；

2.经费决算根据单位财务提供实际支出明细表计算归类后填写；经费决算表后可以附带单位财务提供的实际支出明细表。

项目明细账

查询时间：[2021-01　至　2023-12]

部门:(101103)水产学院　　项目：(4312100133)基于AlEqen的甲基汞在浮游动物体内的富集水平与分布规律　　负责人:何滔

初期余额:.00　　期末余额:.00　　账套名称:

日期	凭证号	摘要	科目代码	科目名称	收入/预算	支出/借款	经办人	余额
2021-12-15	202112B 6345	何滔收重庆市科学技术局国家机关拨付专项经费	2305.2	预收账款 / 科研预收经费	50,000.00	0.00	何滔	50,000.00
2021-12-15	202112B 6345	何滔收重庆市科学技术局国家机关拨付专项经费提管理费	5001.2.99904	业务活动费用 / 科研活动费用 / 特殊经济科目 / 计提项目间接费用或管理费	0.00	4,000.00	何滔	46,000.00
2022-01-12	2022 1B 1431	何滔付学生劳务费(1170298)	5001.2.3022601	业务活动费用 / 科研活动费用 / 商品和服务支出 / 劳务费 / 科研劳务费	0.00	4,000.00	何滔	42,000.00
2022-01-20	2022 1B 4957	何滔报实验耗材(1178441)	5001.2.3021801	业务活动费用 / 科研活动费用 / 商品和服务支出 / 专用材料费 / 一般专用材料费	0.00	100.00	何滔	41,900.00
2022-03-23	2022 3B 6028	何滔报实验耗材(1206364)	5001.2.3021801	业务活动费用 / 科研活动费用 / 商品和服务支出 / 专用材料费 / 一般专用材料费	0.00	220.50	何滔	41,679.50
2022-07-28	2022 7B 7703	何滔报合肥测样差旅费(1315725)	5001.2.30211	业务活动费用 / 科研活动费用 / 商品和服务支出 / 差旅费	0.00	5,003.00	何滔	36,676.50
2022-09-01	2022 9A 247	何滔报版面费(1325573)	5001.2.3020204	业务活动费用 / 科研活动费用 / 商品和服务支出 / 印刷费 / 科研出版/文献/信息传播/知识产权事务费	0.00	3,909.83	何滔	32,766.67
2022-09-01	2022 9A 247	何滔报试剂费(1325573)	5001.2.3021801	业务活动费用 / 科研活动费用 / 商品和服务支出 / 专用材料费 / 一般专用材料费	0.00	355.41	何滔	32,411.26
2022-09-16	2022 9B 4805	何滔付学生劳务(1343949)	5001.2.3022601	业务活动费用 / 科研活动费用 / 商品和服务支出 / 劳务费 / 科研劳务费	0.00	420.00	何滔	31,991.26
2022-12-22	202212B 5892	何滔报试剂(1412411)	5001.2.3021801	业务活动费用 / 科研活动费用 / 商品和服务支出 / 专用材料费 / 一般专用材料费	0.00	9,968.00	何滔	22,023.26
2022-12-28	202212A 6837	何滔报版面费(1401506)	5001.2.3020204	业务活动费用 / 科研活动费用 / 商品和服务支出 / 印刷费 / 科研出版/文献/信息传播/知识产权事务费	0.00	18,737.71	何滔	3,285.55
2023-02-24	2023 2A 1606	刘颖报集采试剂 20230206000026(1450577)	5001.2.3021801	业务活动费用 / 科研活动费用 / 商品和服务支出 / 专用材料费 / 一般专用材料费	0.00	226.95	刘颖	3,058.60
2023-03-16	2023 3B 4481	何滔报实验耗材(1471301)	5001.2.3021801	业务活动费用 / 科研活动费用 / 商品和服务支出 / 专用材料费 / 一般专用材料费	0.00	610.00	何滔	2,448.60
2023-07-10	2023 7B 2185	何滔付学生劳务(1599103)	5001.2.3022601	业务活动费用 / 科研活动费用 / 商品和服务支出 / 劳务费 / 科研劳务费	0.00	1,200.00	何滔	1,248.60
2023-12-14	202312B 11134	何滔报江津等调研差旅费(1764995)	5001.2.30211	业务活动费用 / 科研活动费用 / 商品和服务支出 / 差旅费	0.00	1,248.60	何滔	0.00
		总计			50,000.00	50,000.00		

项目明细账

查询时间：[2022-01　至　2023-12]

部门:(105019)科学技术处（科协）　　项目：(7110100822/029)基于AIEgen的甲基汞在浮游动物体内的富集水平与分布规律　　负责人:何滔

初期余额:.00　　期末余额:.00　　账套名称:

日期	凭证号	摘要	科目代码	科目名称	收入/预算	支出/借款	经办人	余额
2022-04-08	2022 4C　15	划2021重庆市自然科学基金面上项目联合资助	9002.8.2	预算分配 / 2022年预算划转 / 预算二次划拨	50,000.00	0.00		50,000.00
2022-04-27	2022 4B　7984	何滔付学生劳务费(1233522)	5001.1.3022699	业务活动费用 / 教育活动费用 / 商品和服务支出 / 劳务费 / 其他劳务费	0.00	16,500.00	何滔	33,500.00
2022-06-02	2022 6B　802	何滔付学生劳务费(1268674)	5001.1.3022699	业务活动费用 / 教育活动费用 / 商品和服务支出 / 劳务费 / 其他劳务费	0.00	8,592.00	何滔	24,908.00
2022-09-15	2022 9B　4401	何滔报生物试剂(1341659)	5001.1.3021801	业务活动费用 / 教育活动费用 / 商品和服务支出 / 专用材料费 / 一般专用材料费	0.00	24,908.00	何滔	0.00
		总计			50,000.00	50,000.00		

重庆市自然科学基金项目结题验收表

<table>
<tr><td>项目名称</td><td colspan="3">基于 AIEgen 的甲基汞在浮游动物体内的富集水平与分布规律</td></tr>
<tr><td>立项编号</td><td>cstc2021jcyj-msxmX0100</td><td>项目负责人</td><td>何滔</td></tr>
<tr><td>二级单位名称</td><td colspan="3">西南大学水产学院</td></tr>
<tr><td>项目类别</td><td colspan="3">重庆市自然科学基金面上项目</td></tr>
<tr><td>起止时间</td><td colspan="3">2021-10-01 至 2024-1-15</td></tr>
<tr><td rowspan="2">验收时间</td><td rowspan="2">2024.01.11</td><td>单位联系人</td><td>庞旭</td></tr>
<tr><td>联系电话（手机）</td><td>13677620927</td></tr>
<tr><td>提供验收材料清单</td><td colspan="3">自评估报告、研究/技术报告、经费决算表、相关证明材料（如发表论文、授权专利、法定检测报告、用户意见、应用证明、第三方验证证明等）、重庆市自然科学基金面上项目结题备案清单。</td></tr>
<tr><td>二级单位验收情况</td><td colspan="3">验收意见：
本研究以浮游动物的代表种之一：隆线蚤（Daphnia carinata）为研究对象，建立了基于 AIEgen 的 MeHg 定量检测标准曲线：$CMeHg = 1.14*\ln(I_{585}/I_{480}) - 0.333$，并完成了浸泡组中 MeHg 在隆线蚤体内的吸收释放水平以及在体内代谢分布位点的变化检测，以及在裸藻的毒化后建立投喂组，完成了投喂组中隆线蚤对 MeHg 的吸收水平及代谢分布位点分析。
相关成果发表 SCI 论文 2 篇（均为中科院一区期刊）；参加国内学术会议一次；完成预定目标，建议结题。
验收专家签名：
二级单位盖章：
2024 年 1 月 9 日</td></tr>
<tr><td>单位受理意见</td><td colspan="3">同意验收 □
建议整改 □（理由：_____）
于_____年____月___日前完成整改。

项目管理员：　　处长：

年　月　日</td></tr>
</table>

重庆市自然科学基金项目结题验收表

<table>
<tr><td>项目名称</td><td colspan="3">基于 AIEgen 的甲基汞在浮游动物体内的富集水平与分布规律</td></tr>
<tr><td>立项编号</td><td>cstc2021jcyj-msxmX0100</td><td>项目负责人</td><td>何滔</td></tr>
<tr><td>二级单位名称</td><td colspan="3">西南大学水产学院</td></tr>
<tr><td>项目类别</td><td colspan="3">重庆市自然科学基金面上项目</td></tr>
<tr><td>起止时间</td><td colspan="3">2021-10-01 至 2024-1-15</td></tr>
<tr><td rowspan="2">验收时间</td><td rowspan="2">2024.01.11</td><td>单位联系人</td><td>庞旭</td></tr>
<tr><td>联系电话（手机）</td><td>13677620927</td></tr>
<tr><td>提供验收材料清单</td><td colspan="3">自评估报告、研究/技术报告、经费决算表、相关证明材料（如发表论文、授权专利、法定检测报告、用户意见、应用证明、第三方验证证明等）、重庆市自然科学基金面上项目结题备案清单。</td></tr>
<tr><td>二级单位验收情况</td><td colspan="3">验收意见：
聚集诱导荧光探针 AIEgen 法表现出对 MeHg 的特异性识别，但用 AIEgen 法检测 MeHg 和 Hg^{2+}时，互相有较多相似之处，尤其是在荧光示踪的时候，汞离子会干扰聚集诱导荧光探针 AIEgen 对 MeHg 的荧光示踪，难以辨别两者之间的差异，需要通过试验进一步确定 AIEgen 检测 MeHg 和 Hg^{2+}的定量定性相关差异。
隆线蚤这类浮游动物表现出对水体环境中 MeHg 的快速富集，无论是直接浸泡还是间接摄入，都只是水生生态系统食物链的前端，尚未研究 MeHg 在水生食物链中更高营养级（鱼类、贝类、虾等）中的富集规律和生物放大效应，需要进一步的研究补足。
总的来说，项目完成了预定目标，建议结题。
验收专家签名：
二级单位盖章：
2024 年 1 月 10 日</td></tr>
<tr><td rowspan="2">单位受理意见</td><td colspan="3">同意验收 □
建议整改 □（理由：_____）
于_____年____月___日前完成整改。</td></tr>
<tr><td colspan="3">项目管理员：　　处长：
年　月　日</td></tr>
</table>

重庆市自然科学基金项目结题验收表

<table>
<tr><td>项目名称</td><td colspan="3">基于 AIEgen 的甲基汞在浮游动物体内的富集水平与分布规律</td></tr>
<tr><td>立项编号</td><td>cstc2021jcyj-msxmX0100</td><td>项目负责人</td><td>何滔</td></tr>
<tr><td>二级单位名称</td><td colspan="3">西南大学水产学院</td></tr>
<tr><td>项目类别</td><td colspan="3">重庆市自然科学基金面上项目</td></tr>
<tr><td>起止时间</td><td colspan="3">2021-10-01 至 2024-1-15</td></tr>
<tr><td rowspan="2">验收时间</td><td rowspan="2">2024.01.11</td><td>单位联系人</td><td>庞旭</td></tr>
<tr><td>联系电话（手机）</td><td>13677620927</td></tr>
<tr><td>提供验收材料清单</td><td colspan="3">自评估报告、研究/技术报告、经费决算表、相关证明材料（如发表论文、授权专利、法定检测报告、用户意见、应用证明、第三方验证证明等）、重庆市自然科学基金面上项目结题备案清单。</td></tr>
<tr><td>二级单位验收情况</td><td colspan="3">验收意见：
本研究以浮游动物的代表种之一：隆线溞（Dahphia carinata）为研究对象，基于一种新型聚集诱导荧光物（AIEgen），建立定量测定甲基汞（MeHg）浓度的新方法，进而测定 MeHg 在隆线溞体内吸收及释放的变化规律；以荧光示踪的方式，检测 MeHg 在隆线溞体内的代谢位点以及分布变化；并通过浸泡和投喂两种实验手段，对比分析甲基汞在隆线溞体内的积累水平，判定 MeHg 积累的主要方式（水中吸收或是饵料摄入）。在理论上，本项目可为研究甲基汞在浮游动物体内的代谢水平及分布提供重要的理论参考，为今后研究甲基汞在水生生物群落之间的富集转移打下良好的实验基础。
本项目成果在中科院一区 top 期刊上发表论文 2 篇，完成目标，建议结题。
验收专家签名：
二级单位盖章：
2024年 1月10日</td></tr>
<tr><td>单位受理意见</td><td colspan="3">同意验收 □
建议整改 □（理由：_____）
于_____年____月___日前完成整改。

项目管理员：　　处长：

年　月　日</td></tr>
</table>

Ecotoxicology and Environmental Safety 248 (2022) 114271

Contents lists available at ScienceDirect

Ecotoxicology and Environmental Safety

journal homepage: www.elsevier.com/locate/ecoenv

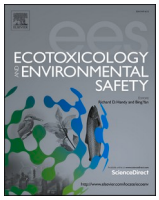

Methylmercury bioaccumulation in water flea *Daphnia carinata* by AIEgen

Tao He [a,b,1], Xiaodong Mao [a,1], Hangyu Lin [a], Md Mahbubul Hassan [c], Song Zhu [a], Qun Lu [a], Jianguang Qin [c,*], Shengqi Su [a,*]

[a] College of Fisheries, Southwest University, Chongqing 400715, China
[b] Guangdong Provincial Key Laboratory of Luminescence from Molecular Aggregates, South China University of Technology, Guangdong 510641, China
[c] College of Science and Engineering, Flinders University, South Australia 5001, Australia

ARTICLE INFO

Edited by Dr G Liu

Keywords:
MeHg
Bioaccumulation
Water flea
Aggregation-induced emission fluorogen

ABSTRACT

Mercury ion (Hg^{2+}) is a toxic heavy metal ion and Hg^{2+} is convertible to methylmercury (MeHg) by many aquatic microorganisms, leading to bioaccumulation and biomagnification in aquatic organisms, which can interfere with brain development and function in humans. This study employs a newly developed AIEgen (Aggregation-induced emission fluorogen) to quantify and visualise the process of MeHg bioaccumulation in vivo on the species of water flea *Daphnia carinata*. Two approaches to MeHg absorption were taken, either by direct incubation in a MeHg solution or by indirect consumption of algae contaminated with MeHg. We analysed the relationship between the ratio of photoluminescence (PL) intensities (I_{585}/I_{480}) and MeHg concentration (C_{MeHg}) and generated a master curve for determining MeHg concentration based on the measurement of PL intensities. Fluorescent image analysis showed the occurrence of MeHg in *D. carinata* to be mainly in the compound eyes, optic nerve and carapace. This study indicates that MeHg absorption can be quantified and visualised in the body of zooplankton, and the MeHg transfer to zooplankton is more likely through direct exposure than via indirect food intake. The accumulation of MeHg in the eye and the nervous system could be the cause of the high mortality of *D. carinata* exposed to MeHg in water.

1. Introduction

Mercury (Hg) is a toxic heavy metal and can be found in polluted water. Its wide distribution has been a worldwide concern for human health and environmental protection (Cariccio et al., 2019; Clarkson et al., 2003; Ullrich et al., 2001). Although Hg exists in aquatic ecosystems at a low concentration, it has been listed as a dangerous and ubiquitous element in water, with toxicity ranked third behind arsenic and lead as hazardous substances (Freire et al., 2020; Kidd et al., 2012). A great concern with Hg contamination is its transfer and biomagnification along the food chain in aquatic ecosystems. Hg exists in different chemical forms that can combine with other elements such as chlorine and carbon to form toxic substances (Kidd et al., 2012). The mercury ion (Hg^{2+}) can penetrate the skin and digestive tract of the human body and damage the visual and nervous systems (Campbell et al., 2005; Cariccio et al., 2019). Moreover, Hg^{2+} is convertible to organic mercury. The major form of organic mercury that has high toxicity to humans is methylmercury (MeHg, $[CH_3Hg]^+$), which is the most deadly form of mercury because it can be easily absorbed into the blood from the digestive tract (Harris et al., 2003). Moreover, Hg^{2+} is convertible to MeHg by many aquatic microorganisms, leading to bioaccumulation and magnification in aquatic organisms, which can interfere with brain development and function in humans (Watras et al., 1998).

MeHg is present in many types of seafood through bioaccumulation in aquatic food webs. The concentration of Hg in fish varies between species and age. Carnivorous and senescent fish usually contain higher Hg than herbivorous and young fish (Korbas et al., 2012). The bioaccumulation of MeHg in aquatic organisms through food chain transfer is surprisingly high. However, traditional methods for measuring MeHg absorption, accumulation and transformation provide only a static picture of organisms at a given time, life period or habitat, and the mechanism of Hg transfer between aquatic organisms is largely unknown, especially in microscopic organisms in water (Gobas et al., 2009). Moreover, existing protocols are constrained to well-established laboratories due to the requirement of expensive instrumentation, such as

* Corresponding authors.
E-mail addresses: jian.qin@flinders.edu.au (J. Qin), sushengqi@swu.edu.cn (S. Su).
[1] Equal contribution

https://doi.org/10.1016/j.ecoenv.2022.114271
Received 8 May 2022; Received in revised form 10 October 2022; Accepted 3 November 2022

inductively coupled plasma mass spectrometry (Michael et al., 1992) and synchrotron-based X-ray fluorescence (Korbas et al., 2012) and labour-costly processes for sample preparation (Kelly et al., 2007). Therefore, the development of a methodology for the detection and quantification of toxic substances is necessary to enable the understanding of the processes of MeHg bioaccumulation and transfer in aquatic organisms. Previous studies have reported MeHg transformation and respective MeHg concentrations in aquatic communities (algae and crustaceans) (Tsui and Wang, 2004b; Watras et al., 1998). However, these studies have not provided an adequate understanding of the intake and output kinetics of MeHg within organisms, yet these measures are essential to interpreting and predicting the movement of MeHg in food chains. It is unclear whether the accumulation process of MeHg in crustacean zooplankton begins directly by absorption in water or indirectly through food intake. The existing evidence suggests that MeHg in fish is obtained through food intake, but it is unclear how zooplankton obtain mercury in their body (Korbas et al., 2012; Lee and Fisher, 2017; Schartup et al., 2018; Tsui and Wang, 2004b).

Zooplanktons are an important trophic link bridging energy flux between organisms at a low and a high-food chain. As *Daphnia* have a relatively short life cycle, produce progeny through asexual reproduction and are sensitive to pollutants in water (Khangarot and Das, 2009), they are commonly chosen in the study of toxicological responses in aquatic animals (Adema, 1978; Cooman et al., 2005; Harmon et al., 2003). In recent studies, *Daphnia* species have been identified as suitable for developing an invertebrate test system for ecotoxicological assessment to improve water quality for fishery and human consumption (Korbas et al., 2012; Pereira et al., 2014; Phyu et al., 2004). For monitoring water quality, Harmon et al. (Harmon et al., 2003) suggested the need to use indigenous fauna to screen the toxicity of local biotas in order to reduce test variance due to habitant differences among species.

Aggregation-induced emission (AIE) refers to a photophysical effect whereby the light emission of a fluorogen is activated by aggregate formation, and AIE has the potential as a visual method in biological assays (Mei et al., 2015). Fluorogens with AIE effects are known as AIEgens and can luminesce more in the aggregate state than in the solution state (Mei et al., 2014). In the AIE testing process, highly concentrated solutions of fluorogens and their aggregates in an aqueous medium can trigger the fluorescence turn-on function (Ding et al., 2013). The discovery of AIE has enabled us to follow the distribution of trace substances in microscopic organisms via the detection of AIEgen florescence (Guo et al., 2015). Recently, AIEgen fluorescent probes have been used as a novel method for detecting and quantifying Hg^{2+} in solution (Chen et al., 2017), bioaccumulation in algae, and Hg^{2+} release from algae after bioaccumulation (Jiang et al., 2016). In addition, this AIEgen has been used to detect the dynamics and distribution of Hg^{2+} in aquatic invertebrates, e. g., rotifers. However, it is unclear whether organic mercury, MeHg, can be detected with AIEgens by a mechanism similar to that reported with inorganic mercury, Hg^{2+} (Chen et al., 2017).

In this study, a specially designed AIEgen was used to quantitatively evaluate the bioaccumulation of MeHg inside the waterflea *Daphnia carinata*. This animal is vital in transferring energy from primary producers to organisms at high trophic levels, such as fish. The objective of this study is to use a novel AIEgen method to visualize the kinetics and distribution of MeHg in a small aquatic invertebrate and to improve our understanding of the dynamics of MeHg transfer between aquatic organisms.

2. Materials and methods

2.1. Materials

Daphnia carinata (0.8–1.0 mm in body length, Fig. 1) were collected from an outdoor tank located in the Biological Science Building at Flinders University and fed with *Euglena gracilis* (15–20 μm long and 8–10 μm wide) and yeast. Before the experiment, the *Daphnia* were fed only yeast to reduce the effect of algal pigmentation on the reading of AIEgen fluorescence in animals. The yeast was supplied in suspension by adding 3 g yeast in 60-mL water and vertexing for 2 min *Euglena gracilis* were collected from the algal collection at Flinders University. The culture medium included a mixture of 30 g wheat grain, 25 g rice grain and 5 g skim milk powder in 1 L of water. After autoclaving at 120 °C for 5 min, the algal culture medium was preserved at 4 °C in a refrigerator. The algae were added into the culture medium at 10% (v/v) and cultivated in 250 mL vessels in a room at the constant temperature of 24 °C and illumination at 70 mmol photons m^{-2} sec^{-1}. The flask was mixed twice a day to prevent algae sinking to the bottom. The chemical reagents were purchased from Sigma-Aldrich, Australia. TPE-RNS, a kind of AIEgen synthesized by the tetraphenylethene and its acceptor, provided by AIEgen Biotechnology (Hong Kong, China) and CH_3HgCl (MeHg) were prepared at the concentration of 1.0 mM as the stock solution. The testing solutions used to determine MeHg concentration included 5 μM TPE-RNS and different concentrations of MeHg.

Fig. 1. The photo of *Daphnia carinata*.

2.2. Development of the master curve for MeHg determination

The MeHg detection mechanism for a specific AIEgen (Figs. S1, S2, S3, S4) is similar to the reaction between Hg^{2+} and AIEgen (Chen et al., 2017). Transfers of MeHg to *D. carinata* were designed using two approaches: direct MeHg incubation from the culture medium, and the food intake of MeHg-contaminated algae (Fig. 2).

The AIE characteristics of TPE-RNS were examined in water and acetonitrile (ACN) mixtures with different water fractions (f_w, vol%) from 0% to 90%, and the maximum photoluminescence (PL) intensity occurred at the 60% fraction (Fig. S5). Therefore, the fraction factor (f_w) was set at the mixture of 60/40 (water/ACN by volume) in the subsequent trials. To construct a master curve for MeHg quantification, different MeHg concentrations (0, 1, 2.5, 5, 7.5 and 10 μM) were used at the AIEgen concentration of 5 μM. As the intense emission peak of PL of the TPE-RNS and TPE-RNO, which was synthesized by the reaction of TPE-RNS and CH_3Hg^+, was displayed at 480 nm and 585 nm, respectively (Fig. S6), the PL intensity ratio was calculated at these two wavelengths (I_{585}/I_{480}). A fluorescence spectrometer (Varian, Australia) was used to determine PL intensity at the excitation wavelength of 350 nm. The data were analyzed by Excel 2016 and SPSS18.0 to develop the PL master curve, which shows the relationship between the ratio of PL intensity and the concentration of MeHg in solution.

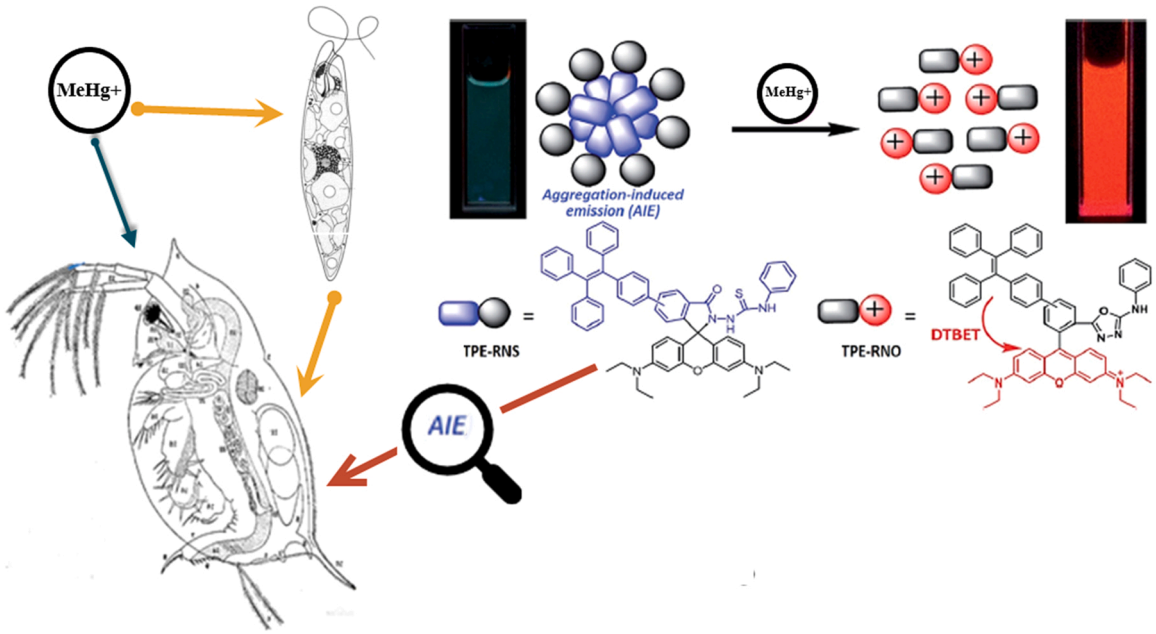

Fig. 2. Illustration of two approaches of MeHg transfer to *Daphnia,* namely, direct incubation and indirect consumption of algae containing MeHg, and the radiometric detection mechanism of MeHg using the AIEgen TPE-RNS (Chen et al., 2017).

2.3. Quantification of MeHg bioaccumulation in Daphnia

Survival was calculated based on the number of live and dead animals in each vial to determine the toxicity of MeHg to *Daphnia* at each concentration. The *D. carinata* were obtained from the tank with a 100 μm screen net and rinsed with Milli-Q water before being introduced into a solution containing different MeHg concentrations of 2.5 and 5.0 μM/L. The animal density was 25 individuals per mL. Group 1 was designed to determine the directional movement of MeHg dispersal in *Daphnia* from the environment. The supernatant (600 μL) was collected from the *Daphnia*-MeHg solution at the times of 0, 5, 10, 20, 30, 40, 50, 60, 90, 120, 150, 180, 210 and 240 min, respectively. Subsequently, each of these supernatants was mixed with 400 μL AIEgen in the ACN solution at the water-to-ACN ratio of 3–2. The PL intensity of each stained solution was determined by fluorescence spectrometer. Group 2 was set up to quantify the release of MeHg from *Daphnia* that were submerged at two concentrations of MeHg, i.e., 2.5 and 5.0 μM/L, for 10 min. The *Daphnia* were rinsed twice with Milli-Q water at the beginning of the release trial. After incubation for the same time regimes as in group one, 600 μL supernatant was collected from each *Daphnia* solution for MeHg quantification. The MeHg concentration was determined by the PL intensity read on the fluorescence spectrometer. Each treatment was set up with three replicates, and all data were analyzed by Excel 2016 and SPSS18.0 using univariate ANOVA.

2.4. Visualization of MeHg dynamics in Daphnia

Daphnia were incubated in 5.0 μM/L MeHg as described in Section 2.3 at the density of 25 individuals per mL in 80-mL vials. A total of 10–15 *Daphnia* were collected at the time intervals of 5, 10, 20, 30, 60, 90 and 120 min after submerging, then stained in the 1.0 μM/L AIEgen with the ACN to water ratio of 2–3 by volume. After rinsing with water to remove MeHg residues on the body, *Daphnia* were observed using a scanning confocal fluorescence microscope to conduct image analysis. Before the fluorescence images were taken, two light channels were set up: a blue channel with a 460–500 nm wavelength range and a red channel with a wavelength range of 570–610 nm. The blue channel was used for the image analysis of *Daphnia* submerged in AIEgen only, and the red channel fluorescence was used for the image analysis of *Daphnia* in MeHg plus AIEgen solution. The excitation wavelength of 405 nm was used.

2.5. Toxic response of Daphnia after feeding on algae containing MeHg

Euglena were counted on a haemocytometer to determine the cell density. After incubation in 5.0 μM/L MeHg for 30 min, *Euglena* were recovered using a centrifuge at 4500 rpm for 1 min as feed for *Daphnia* (25 individuals per mL). The MeHg residue in the supernatant was determined according to the PL ratio using the equation derived from the master curve. Soon after *Daphnia* were fed with *Euglena* containing MeHg, changes in appendage movement and shape of *Daphnia* were observed on an optical microscope. Images were taken every 30 min. Survival of *Daphnia* was determined by counting live and dead individuals at the end. The supernatant (600 μL) was removed from each *Daphnia* solution at 5, 10, 20, 30, 40, 50, 60, 90, 120, 150, 180, 210 and 240 min. The MeHg concentration of each sample was determined by the equation derived from the master curve. Each treatment was set up with three replicates, and all data were analyzed by Excel 2016 and SPSS18.0 using univariate ANOVA. At the end of 60 min, *Daphnia* were collected and stained with AIEgen in the working solution for 90 min to obtain fluorescence images.

3. Results

3.1. Development of the AIE method for MeHg determination

After adding 5.0 μM/L AIEgen to MeHg with different concentrations, we separately calculated the PL intensity ratio and developed the regression equation between the PL ratio (I_{585}/I_{480}) and MeHg concentration (C_{MeHg}), as shown in Fig. 3. The linear equation between C_{MeHg} and I_{585}/I_{480} was yielded as: $C_{MeHg} = 1.14 * \ln (I_{585}/I_{480}) - 0.333$.

3.2. Quantitative evaluation of MeHg bioaccumulation by D. carinata

Two groups of different concentrations, 2.5 and 5.0 μM/L, showed similar trend lines, as shown in Fig. 4. The amount of MeHg absorption increased continuously to 0.123 μM in the 2.5 μM/L group and 0.218 μM in the 5.0 μM/L group, respectively, before 60 min, with no *D. carinata*

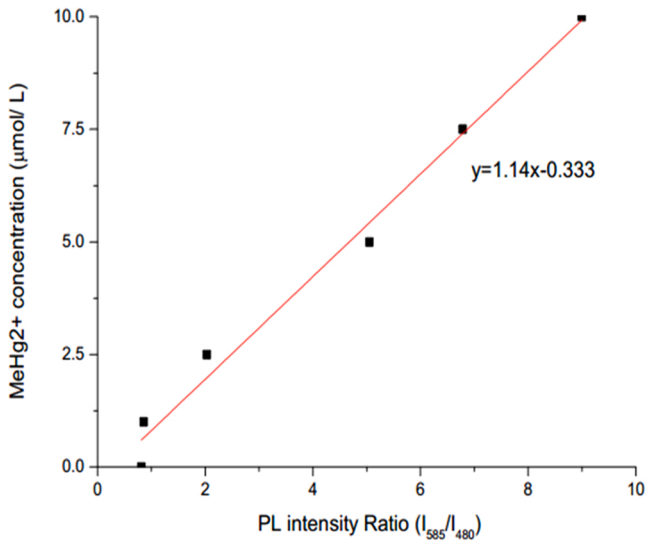

Fig. 3. The MeHg concentration is a linear function of the PL intensity ratio of I_{585}/I_{480}.

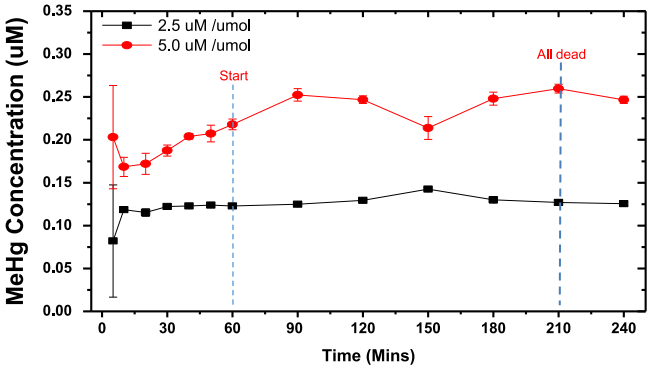

Fig. 4. MeHg absorption of *D. carinata* from the solution at different times.

mortality during that period (Fig. S7). However, mortality occurred after 60 min, and the amount of MeHg retention began to level off and plateaued until the end of the study at 240 min

Fig. 5 shows the MeHg release from *D. carinata* to water at different times. In the 5.0 μM/L group, after being transferred into Milli-Q water for 5 min, the *D. carinata* released 0.061 μM into the clean water, and the MeHg concentration in water was kept relatively stable until 60 min. Although *D. carinata* began to die after 60 min (Fig. S7), the amount of MeHg release did not change much and levelled off until the end of this experiment at 240 min. In the 2.5 μM/L group, the *D. carinata* released

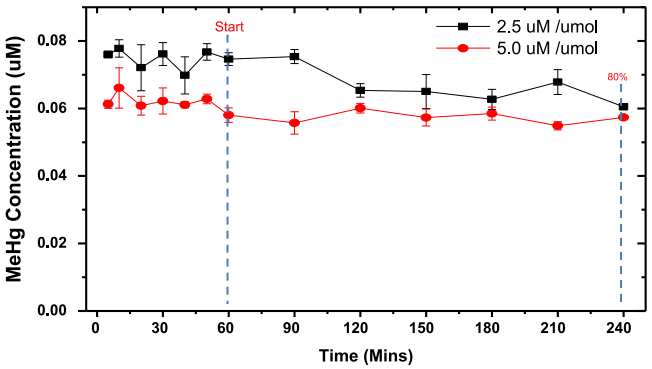

Fig. 5. MeHg release from *D. carinata* to water at different times.

0.076 μM after 5 min and kept stable until 60 min, and then the dissolved MeHg decreased continuously to 0.061 μM until 240 min

3.3. In vivo visualization of MeHg dynamics in Daphnia by AIEgen

As shown in Fig. 6(a), i.e., without MeHg and AIEgen, the *Daphnia* in the control group showed no fluorescent signals, a finding similar to that from the *Daphnia* exposed to MeHg without the addition of AIEgen, as shown in Fig. 6(b). The *Daphnia* submerged in AIEgen displayed blue fluorescence in the blue channel (Fig. 6c) and red fluorescence in the red channel after the MeHg was stained by AIEgen (Fig. 6d).

After submersion for 5 min, low emission in the red channel occurred on the compound eyes (Fig. 7(a1) and 7(a2)), demonstrating that the compound eyes were a target location for the absorption of MeHg in *Daphnia*. The red fluorescence became clearer on the surface of compound eyes (Fig. 7) and continued to move into internal tissues with the elapsed incubation time (Fig. 8). At 40 min, the red fluorescence showed weak emission at the optic nerve (Fig. 8(c)), which became more noticeable with the increased incubation time. However, there was no fluorescent signal on the ocellus and brain, despite their closeness to the compound eyes and optic nerve (Fig. 8(c1) and 8(c2)).

3.4. Toxic response of Daphnia after eating algae containing MeHg

The *Daphnia* fed *Euglena gracilis* containing MeHg demonstrated responses unlike those suffering direct submersion in the MeHg solution, as shown in Fig. 9. In the direct absorption group, the amount of MeHg absorption became increasingly higher with the lapse of incubation time until 150 min. In the other group where *Daphnia* were indirectly supplied with MeHg via food intake, the MeHg accumulation continued to increase from 10 to 30 min and then decreased at 60 min. After the *Daphnia* had fed on contaminated algae for 60 min, the amount of absorption began to level off and plateaued over time.

After feeding on algae, *Daphnia* showed red fluorescence at the foregut sac and intestine after ingestion. However, no signals appeared at the compound eyes and optic nerve, as shown in Fig. 10(b1) and 10 (b2), a result which is remarkably different from *Daphnia* directly incubated in MeHg solution, as shown in Fig. 10(a1) and 10(a2).

4. Discussion

4.1. Quantitative evaluation of MeHg bioaccumulation by D. carinata

On increasing the concentration of MeHg, the emission intensity of AIEgen at 480 nm dropped, and a new peak at 585 nm enhanced gradually (Fig. S6), while 480 nm and 595 nm in Hg^{2+} respectively (Chen et al., 2017). Cheng et al. suggested using PL intensity ratio (I_{595}/I_{480}) and Hg^{2+} concentrations as the ratio can better reflect the change of Hg^{2+} concentrations than the absolute value from a single wavelength. Jiang et al. (2016) established the function between PL intensity ratio (I_{595}/I_{480}) and Hg^{2+} concentration, which was used to quantitative evaluate the bioaccumulation of Hg^{2+} by the rotifer.

In the present study, we further developed a linear regression between MeHg concentration and AIEgen fluorescence ratio (I_{585}/I_{480}) to quantify MeHg in a solution. The dynamic of MeHg change was possibly associated with the reduction of the *Daphnia* population and MeHg efflux through faecal production, shell replacement and reproduction (Tsui and Wang, 2004a, 2004b). In a previous study, MeHg concentrations were strongly correlated to zooplankton (Copepoda, Cladocera and Rotifera) community and biomass composition, and the biomasses of *Daphnia hyalina* were negatively correlated with MeHg accumulation, while *Bosmina longirostris, Thermocyclops brevifurcatus,* and *Asplanchna priodonta* had a positive association (Long et al., 2018). In addition, nutrients could mediate the effects of temperature on methylmercury concentrations in freshwater zooplankton. High temperature treatments increased *Daphnia* methylmercury relative to controls, but with

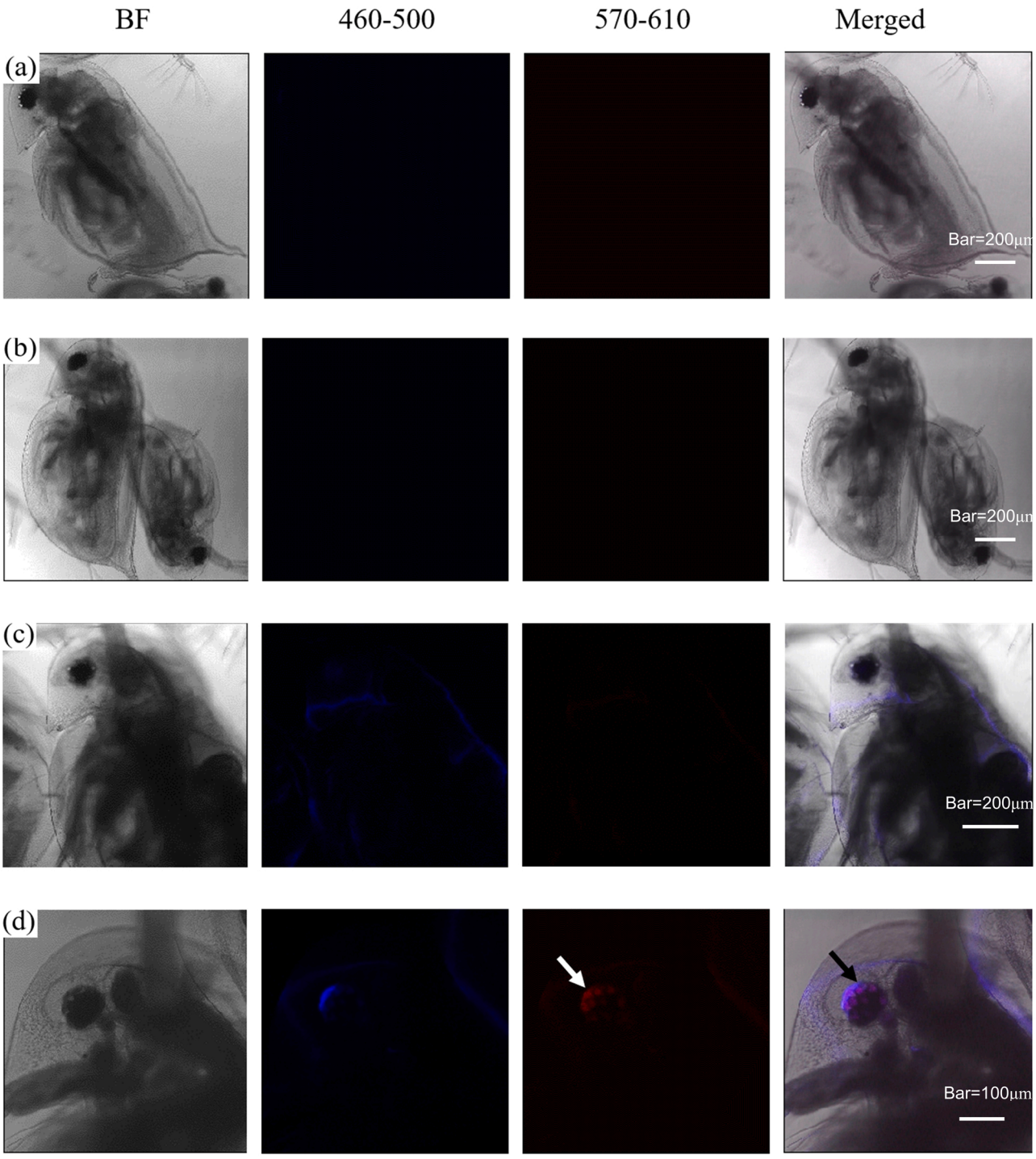

Fig. 6. Images of *Daphnia* on a confocal microscope using 5.0 μM MeHg. (a) the control, i.e., presence of AIEgens but absence of MeHg; (b) exposure to MeHg but in the absence of AIEgens; (c) exposure to 1.0 μM AIEgens in the absence of MeHg, emitting blue fluorescence; (d) exposure to 5.0 μM MeHg stained in the 1.0 μM AIEgens solution, emitting red fluorescence (arrow). BF: bright field.

warming, nutrients reduced zooplankton methylmercury compared to no nutrients (Jordan et al., 2019). Other factors, such as terrestrial organic matter, could also increase methylmercury accumulation in zooplankton (Poste et al., 2019). Poste et al. found that increases in terrestrial organic matter transport from catchments to brown water can affect methylmercury accumulation in aquatic biota both directly by increasing concentrations of aqueous MeHg, and indirectly through effects on MeHg bioavailability.

In reality, researchers have done lots of work on the MeHg accumulation in recent years (Huffman et al., 2020; Wu et al., 2020; Yao et al., 2020). However, the MeHg release from the zooplankton has not been studied closely. In this study, we tested the MeHg release from *D. carinata* to water at different times. The result showed that the amount of MeHg released from *D. carinata* was extremely small, and it seemed that MeHg was locked inside the body of *D. carinata*, similar to the result of Hg^{2+} release from the *D. carinata* (He et al., 2019). Interestingly, Hg^{2+} could not be deposited in the rotifer, possibly dissipating from the rotifer body via the processes of defecation and excretion (Jiang et al., 2017).

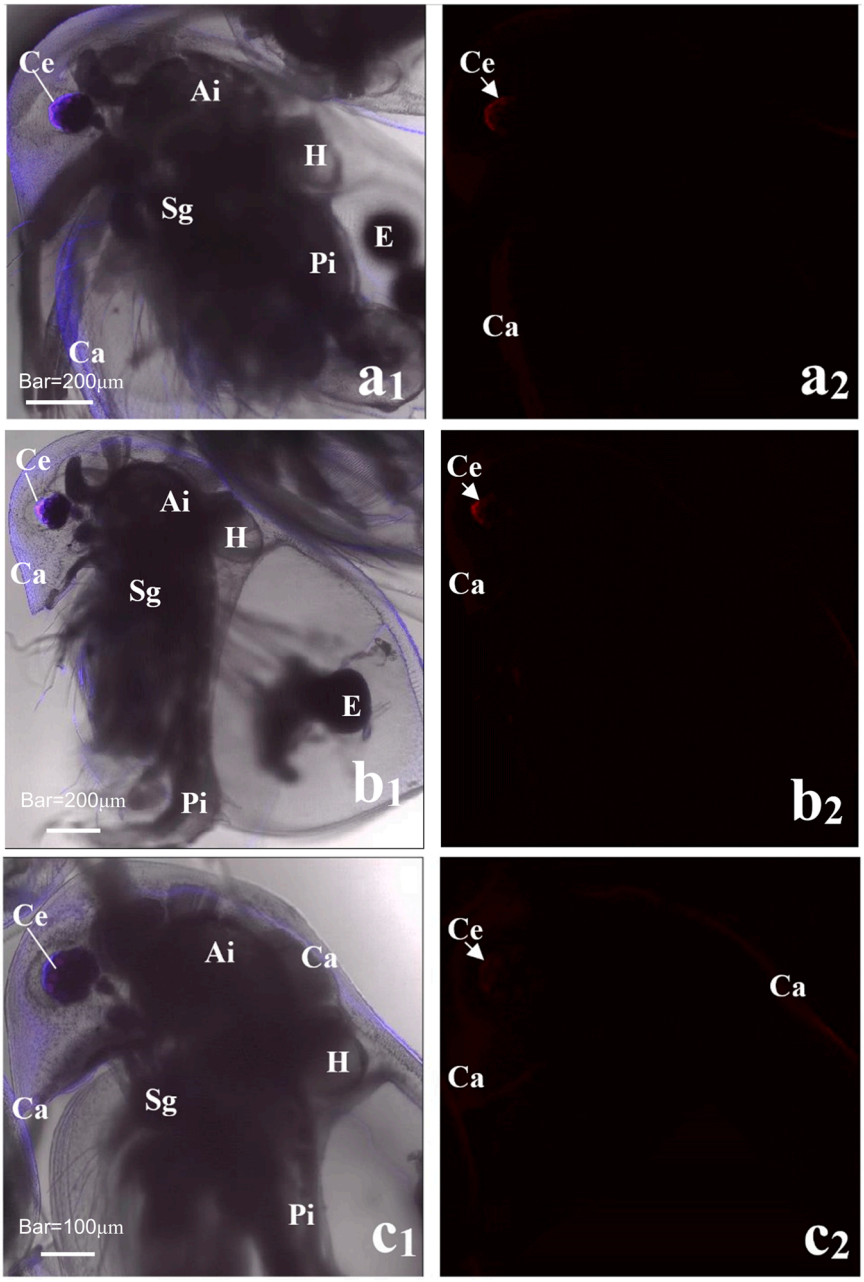

Fig. 7. Confocal fluorescent images of *Daphnia* in MeHg solution after incubation for (a) 5 min; (b) 20 min; (c) 60 min. Ai: anterior intestine; B: brain; Ca: carapace; Ce: compound eye; E: embryo; H: heart; Pi: posterior intestine; Sg: shell gland. (a_1, b_1, c_1: white background) and (a_2, b_2, c_2: black background).

4.2. Visualization of MeHg dynamics in Daphnia

Conventional fluorescent probes suffer from the notorious effect of aggregation-caused quenching that limits their labelling efficiency or concentration to achieve the desired sensitivity. The recently emerged fluorogens with aggregation-induced emission (AIE) feature offer a timely remedy to tackle the challenge (Liang et al., 2015). TPE-RNS based AIEgens have been used for Hg^{2+} detection in zooplankton, rotifer and *Daphnia* (He et al., 2019; Jiang et al., 2017). The potential MeHg detection for TPE-RNS in the solution provided a hint for us to investigate the application in the MeHg image in *Daphnia*. In our previous study, Hg^{2+} was observed in the compound eyes of *D. carinata*, but Hg^{2+} could not move through the eyes and reach the optic nerve. Similarly, the heavier and broader red signals on the body carapace corresponded to the elapsed incubation time. A previous study reported that the carapace of *Daphnia* was comprised of chitin (Anderson, 1933). Since the binding of mercury to chitin is strong and irreversible (Barriada et al., 2008), *Daphnia*'s carapace is a target location for MeHg deposition, as indicated through the fluorescence signals of the AIEgen. Although the reaction between MeHg and chitin occurred on the carapace, the carapace shape remained intact (Fig. S8) as observed by optic microscopy. In contrast, the carapace of *D. carinata* became deformed and even fragmented after direct incubation with Hg^{2+}, indicating that the reaction between $Hg^{2+}$and chitin was stronger than that of MeHg with chitin.

Ingested Hg in fish can be found in muscle, kidney, gonad, liver, and gut (Kasper et al., 2009). Korbas et al. (2012) found that the maximum MeHg deposition was in zebrafish's eye lens and skin. Wang (2021) tested the toxicity of Hg at the subcellular level using embryonic zebrafish fibroblast cell line by AIEgen as a model, and lysosomal pH could be used as a potential biomarker to assess the cellular toxicity of Hg in vitro (Yuan et al., 2021).

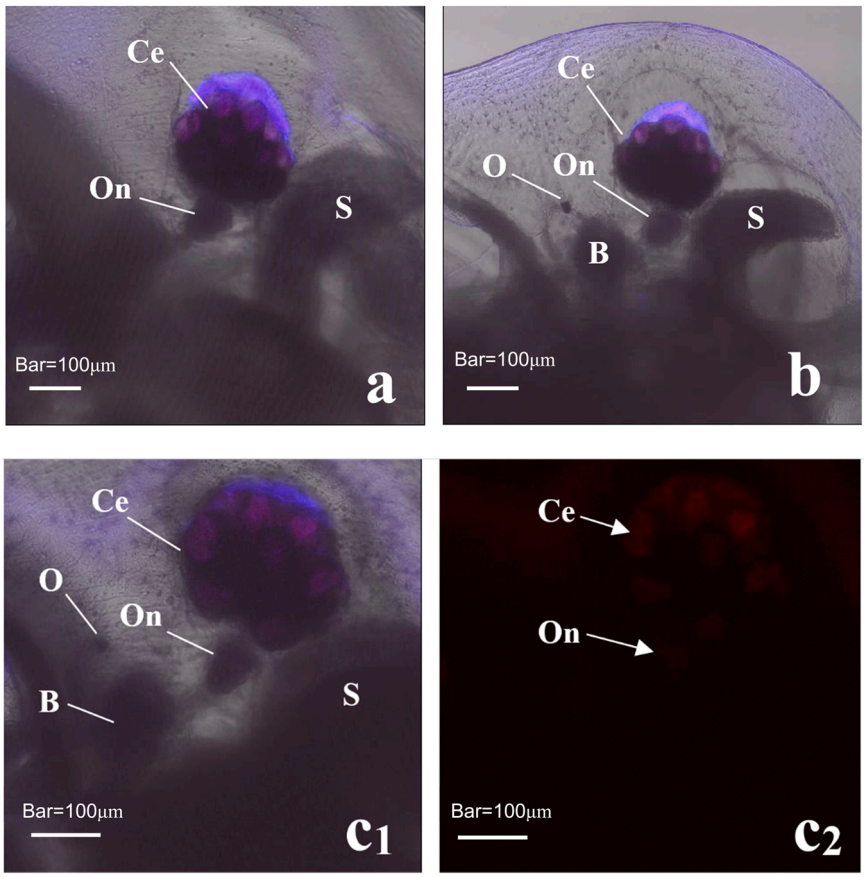

Fig. 8. Fluorescent images of the head of *Daphnia* after (a) 5 min; (b) 20 min; (c) 40 min. B: brain; Ce: compound eye; O: ocellus; On: Optic nerve; Sac: S. (c_1: white background) & (c_2: black background).

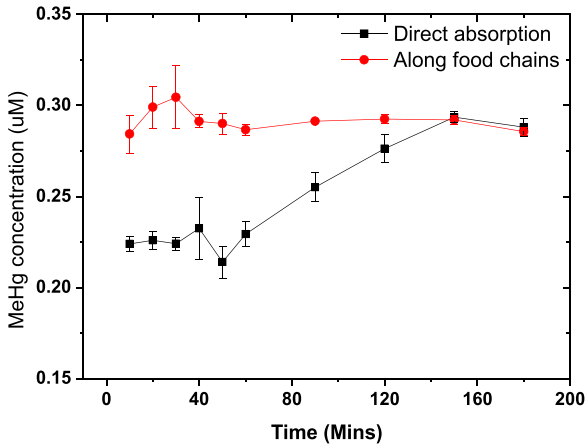

Fig. 9. Comparative MeHg concentration in *Daphnia* between direct absorption and indirect food intake through contaminated algae.

In addition, The Hg accumulation in golden grey mullet *Chelon aurata* was observed at the brain and eyes (Pereira et al., 2014), and in river prawn *Macrobrachium nipponense* was at the gonads and fertilized egg (Sun et al., 2021). Nevertheless, the location for MeHg deposition in planktonic crustaceans is unclear due to their small size. The AIEgen fluorescence was used for the first time to visualize MeHg distribution in *Daphnia* after MeHg was absorbed from the water. Interestingly, the visual (compound eyes and optic nerve) and protective (carapace) organs were the major targets for MeHg distribution in *D. carinata*, but the nerve (brain), digestive (intestine), excretory (shell gland), and circulatory systems were less engaged in MeHg absorption.

Methylmercury is greatly bioconcentrated and biomagnified in aquatic ecosystems by plankton, and these communities form the basis of food webs (Ullrich et al., 2001). Some particular zooplankton, such as *Daphnia* could be important in transferring Hg to higher trophic levels in aquatic food webs (Pickhardt et al., 2005). Long et al. (2018) demonstrated that MeHg concentration was strongly correlated to zooplankton community and biomass composition, and MeHg concentration increased significantly as body size increased. Other researchers also suggested that MeHg biomagnification is more prominent in large zooplankton, and the trophic magnification ratio to food assimilation efficiency increases with increasing body size while the excretion rates decrease (Wu et al., 2020). The biomagnification of methylmercury was mainly considered by the quantitative evaluation (Kidd et al., 2012; Yao et al., 2020). However, the visualization MeHg test, especially in vivo, has not been reported in the food web. In this paper, the toxic response of *Daphnia* after eating algae containing MeHg was visualized by AIEgen. *Daphnia* may take longer to release MeHg from algae due to the slow digestive process of algal cells in the digestive tract. After digestion, MeHg could be released from algae and then show the signal of red fluorescence after AIEgen staining. Moreover, *Daphnia* showed higher mortality in submersion with MeHg than those fed on the algae containing methylmercury (Fig. S9). Most *Daphnia* died in 150 min after direct incubation in MeHg, but 50% of those fed algae were still alive at 180 min (Fig. S7). The reason for this low mortality was possibly the differential diffusion of MeHg through direct incubation and indirect food intake through contaminated algae. It is inferred that the deposition of MeHg into the visual organs is the likely reason for the high mortality of *D. carinata*.

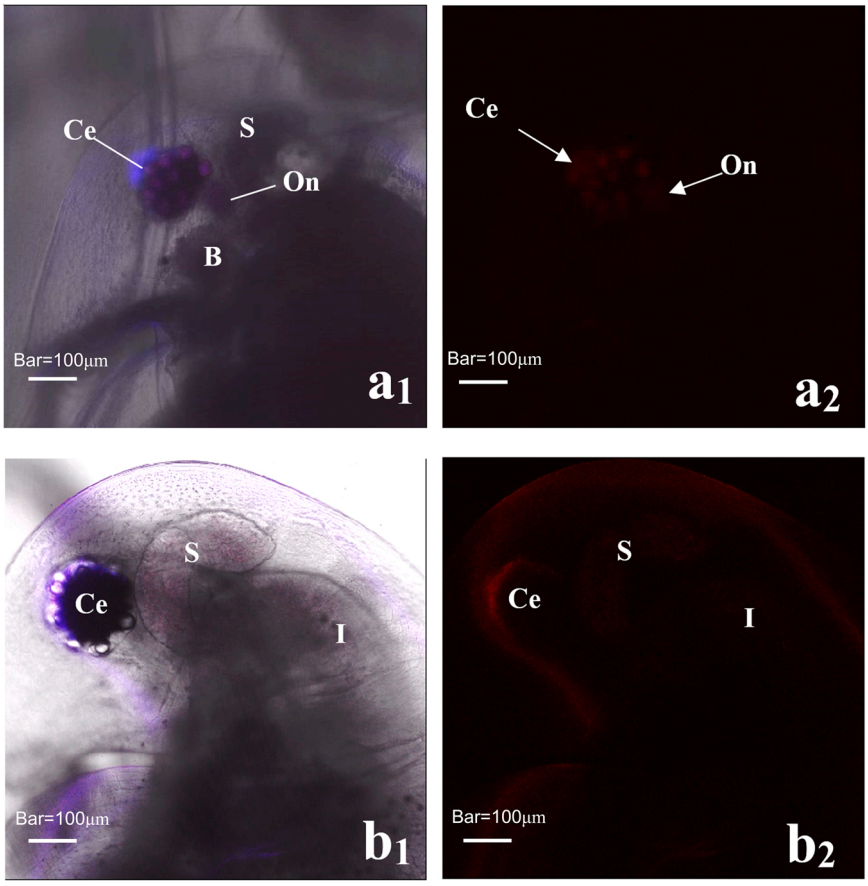

Fig. 10. Comparative confocal fluorescent images of *Daphnia* submerged in MeHg (a) and fed with algae containing MeHg (b). B: brain; Ce: compound eye; Intestine: I; On: Optic nerve; Sac: S. (a_1, b_1: white background) and (a_2, b_2: black background).

5. Conclusion

The specially designed AIEgen is a simple and easy procedure for evaluating the bioaccumulation of MeHg in *Daphnia*. The AIEgen method could visualize the MeHg dynamic and distribution in *Daphna* for the first time with fluorescent image analysis. The visual (compound eyes and optic nerve) and protective (carapace) organs were the major targets for MeHg distribution in *D. carinata*. *Daphnia carinata* suffered higher mortality by directly incubating MeHg in a solution than by indirectly ingesting algae contaminated by MeHg. The reception of MeHg by visual organs may trigger the death of *D. carinata*. The visualization of MeHg through AIEgen provides a novel tool for observing the distribution of MeHg in microscopic organisms and understanding the bioaccumulation process of MeHg in aquatic food webs.

Funding

This research was sponsored by the Natural Science Foundation of Chongqing, China (No. cstc2021jcyj-msxmX0100), the Open Fund of Guangdong Provincial Key Laboratory of Luminescence from Molecular Aggregates (South China University of Technology) (No. 2020-kllma-12), and National Key Research and Development Program of China (Technological Innovation of Blue Granary: No. 2019YFD0900305-03).

CRediT authorship contribution statement

Tao He: Conceptualization, Writing – original draft, Xiaodong Mao: Investigation, Formal analysis, Hangyu Lin: Investigation, Data curation, Md Mahbubul Hassan: Resources, Investigation, Song Zhu: Data curation, Qun Lu: Formal analysis, Jianguang Qin: Methodology, Writing – review & editing, Shengqi Su: Conceptualization, Validation, Funding acquisition.

Declaration of Competing Interest

The authors declare that they have no known competing financial interests or personal relationships that could have appeared to influence the work reported in this paper.

Data Availability

Data will be made available on request.

Acknowledgements

This work was carried out at the College of Science and Engineering, Flinders University. The authors thank Prof. Y.S. Jiang for his technical support.

Appendix A. Supporting information

Supplementary data associated with this article can be found in the online version at doi:10.1016/j.ecoenv.2022.114271.

References

Adema, D.M.M., 1978. *Daphnia magna* as a test animal in acute and chronic toxicity tests. Hydrobiologia 59, 125–134.

Anderson, B.G., 1933. Regeneration in the Carapace of *Daphnia magna*. I. The relation between the amount of regeneration and the area of the wound during single adult instars. Biol. Bull. 64, 70–85.

Barriada, J.L., Herrero, R., Prada-Rodríguez, D., Sastre de Vicente, M.E., 2008. Interaction of mercury with chitin: A physicochemical study of metal binding by a natural biopolymer. React. Funct. Polym. 68, 1609–1618.
Campbell, L.M., Norstrom, R.J., Hobson, K.A., Muir, D.C., Backus, S., Fisk, A.T., 2005. Mercury and other trace elements in a pelagic Arctic marine food web (Northwater Polynya, Baffin Bay). Sci. Total. Environ. 351–352, 247–263.
Cariccio, V.L., Samà, A., Bramanti, P., Mazzon, E., 2019. Mercury involvement in neuronal damage and in neurodegenerative diseases. Biol. Trace Elem. Res. 187, 341–356.
Chen, Y., Zhang, W., Cai, Y., Kwok, R.T.K., Hu, Y., Lam, J.W.Y., Gu, X., He, Z., Zhao, Z., Zheng, X., Chen, B., Gui, C., Tang, B.Z., 2017. AIEgens for dark through-bond energy transfer: design, synthesis, theoretical study and application in ratiometric $Hg^{(2+)}$ sensing. Chem. Sci. 8, 2047–2055.
Clarkson, T.W., Magos, L., Myers, G.J., 2003. The toxicology of mercury - current exposures and clinical manifestations. New. Engl. J. Med. 349, 1731–1737.
Cooman, K., Debels, P., Gajardo, M., Urrutia, R., Barra, R., 2005. Use of Daphnia spp. for the ecotoxicological assessment of water quality in an agricultural watershed in South- Central Chile. Arch. Environ. Contam. Toxicol. 48, 191–200.
Ding, D., Li, K., Liu, B., Tang, B.Z., 2013. Bioprobes based on AIE fluorogens. Acc. Chem. Res. 46, 2441–2453.
Freire, M.A., Lima, R.R., Nascimento, P.C., Gomes-Leal, W., Pereira, A., 2020. Effects of methylmercury on the pattern of NADPH diaphorase expression and astrocytic activation in the rat. Ecotoxicol. Environ. Safe 201, 110799–110805.
Gobas, F.A., Wolf, W., Burkhard, L.P., Verbruggen, E., Plotzke, K., 2009. Revisiting bioaccumulation criteria for POPs and PBT assessments. Integr. Environ. Asses. 5, 624–637.
Guo, F., Gai, W.P., Hong, Y., Tang, B.Z., Qin, J., Tang, Y., 2015. Aggregation-induced emission fluorogens as biomarkers to assess the viability of microalgae in aquatic ecosystems. Chem. Commun. 51, 17257–17260.
Harmon, S.M., Specht, W.L., Chandler, G.T., 2003. A comparison of the daphnids *Ceriodaphnia dubia* and *Daphnia ambigua* for their utilization in routine toxicity testing in the Southeastern United States. Arch. Environ. Contam. Toxicol. 45, 79–85.
Harris, H.H., Pickering, I.J., George, G.N., 2003. The chemical form of mercury in fish. Science 301, 1203.
He, T., Ou, W.X., Tang, B.Z., Qin, J.G., Tang, Y.H., 2019. In vivo visualization of the process of Hg^{2+} bioaccumulation in water flea *Daphnia carinata* by a novel aggregation-induced emission fluorogen. Chem. Asian J. 14, 796–801.
Huffman, W.W., Dam, H.G., Mason, R.P., Baumann, Z., 2020. Formalin-preserved zooplankton are not reliable for historical reconstructions of methylmercury bioaccumulation. Sci. Total. Environ. 738, 139803–139809.
Jiang, Y., Chen, Y., Alrashdi, M., Luo, W., Tang, B.Z., Zhang, J., Qin, J., Tang, Y., 2016. Monitoring and quantification of the complex bioaccumulation process of mercury ion in algae by a novel aggregation-induced emission fluorogen. RSC. Adv. 6, 100318–100325.
Jiang, Y.S., He, T., Chen, Y.C., Ruan, Y.L., Zhou, Y.B., Tang, B.Z., Qin, J.G., Tang, Y.H., 2017. Quantitative evaluation and in vivo visualization of mercury ion bioaccumulation in rotifers by novel aggregation-induced emission fluorogen nanoparticles. Environ. Sci. Nano 4, 2186–2192.
Jordan, M.P., Stewart, A.R., Eagles-Smith, C.A., Strecker, A.L., 2019. Nutrients mediate the effects of temperature on methylmercury concentrations in freshwater zooplankton. Sci. Total. Environ. 667, 601–612.
Kasper, D., Dias, A.C.M.I., Leitão, R.P., Palermo, E.F.A., Ferreira, G.L., Branco, C.W.C., Malm, O., 2009. Mercury distribution in different tissues and trophic levels of fish from a tropical reservoir, Brazil. Neotrop. Ichthyol. 7, 751–758.
Kelly, B.C., Ikonomou, M.G., Blair, J.D., Morin, A.E., Gobas, F.A., 2007. Food web–specific biomagnification of persistent organic pollutants. Science 317, 236–239.
Khangarot, B.S., Das, S., 2009. Toxicity of mercury on in vitro development of parthenogenetic eggs of a freshwater cladoceran *Daphnia carinata*. J. Hazard. Mater. 161, 68–73.
Kidd, K.A., Muir, D.C., Evans, M.S., Wang, X., Whittle, M., Swanson, H.K., Johnston, T., Guildford, S., 2012. Biomagnification of mercury through lake trout (*Salvelinus namaycush*) food webs of lakes with different physical, chemical and biological characteristics. Sci. Total. Environ. 438, 135–143.
Korbas, M., Macdonald, T.C., Pickering, I.J., George, G.N., Krone, P.H., 2012. Chemical form matters: differential accumulation of mercury following inorganic and organic mercury exposures in zebrafish larvae. ACS Chem. Biol. 7, 411–420.
Lee, C.S., Fisher, N.S., 2017. Bioaccumulation of methylmercury in a marine copepod. Environ. Toxicol. Chem. 36, 1287–1293.
Liang, J., Tang, B.Z., Liu, B., 2015. Specific light-up bioprobes based on AIEgen conjugates. Chem. Soc. Rev. 44, 2798–2811.
Long, S.X., Hamilton, P.B., Yang, Y., Wang, S., Huang, W., Chen, C., Tao, R., 2018. Differential bioaccumulation of mercury by zooplankton taxa in a mercury-contaminated reservoir Guizhou China. Environ. Pollut. 239, 147–160.
Mei, J., Hong, Y., Lam, J.W., Qin, A., Tang, Y., Tang, B.Z., 2014. Aggregation-induced emission: the whole is more brilliant than the parts. Adv. Mater. 26, 5429–5479.
Mei, J., Leung, N.L., Kwok, R.T., Lam, J.W., Tang, B.Z., 2015. Aggregation-Induced Emission: Together We Shine, United We Soar! Chem. Rev. 115, 11718–11940.
Michael, J., Campbell, Gerda, V., Dams, R., 1992. Influence of chemical species on the determination of mercury in a biological matrix (cod muscle) using inductively coupled plasma mass spectrometry. J. Anal. At. Spectrom. 7, 617–621.
Pereira, P., Raimundo, J., Araujo, O., Canario, J., Almeida, A., Pacheco, M., 2014. Fish eyes and brain as primary targets for mercury accumulation - a new insight on environmental risk assessment. Sci. Total. Environ. 494–495, 290–298.
Phyu, Y.L., Warne, M.S.J., Lim, R.P., 2004. Toxicity of atrazine and molinate to the cladoceran *Daphnia carinata* and the effect of river water and bottom sediment on their bioavailability. Arch. Environ. Contam. Toxicol. 46, 308–315.
Pickhardt, P.C., Folt, C.L., Chen, C.Y., Klaue, B., Blum, J.D., 2005. Impacts of zooplankton composition and algal enrichment on the accumulation of mercury in an experimental freshwater food web. Sci. Total. Environ. 339, 89–101.
Poste, A.E., Hoel, C.S., Andersen, T., Arts, M.T., Færøvig, P.J., Borgå, K., 2019. Terrestrial organic matter increases zooplankton methylmercury accumulation in a brown-water boreal lake. Sci. Total. Environ. 674, 9–18.
Schartup, A.T., Qureshi, A., Dassuncao, C., Thackray, C.P., Harding, G., Sunderland, E. M., 2018. A model for methylmercury uptake and trophic transfer by marine plankton. Environ. Sci. Technol. 52, 654–662.
Sun, S.M., Wang, N., Shi, X.T., 2021. In vivo visualization assay to evaluate the effects of maternal exposure to mercury on offspring bioaccumulation in the oriental river prawn (*Macrobrachium nipponense*). Chemosphere 270, 129440–129448.
Tsui, M.T., Wang, W.X., 2004a. Temperature influences on the accumulation and elimination of mercury in a freshwater cladoceran, *Daphnia magna*. Aquat. Toxicol. 70, 245–256.
Tsui, M.T.K., Wang, W.-X., 2004b. Uptake and elimination routes of inorganic mercury and methylmercury in *Daphnia magna*. Environ. Sci. Technol. 38, 808–816.
Ullrich, S.M., Tanton, T.W., Abdrashitova, S.A., 2001. Mercury in the aquatic environment: a review of factors affecting methylation. Crit. Rev. Environ. Sci. Tec. 31, 241–293.
Wang, W.X., 2021. Bioimaging of metals in environmental toxicological studies: linking localization and functionality. Crit. Rev. Environ. Sci. Tec. 52, 3384–3414.
Watras, C.J., Back, R.C., Halvorsen, S., Hudson, R.J.M., Morrison, K.A., Wente, S.P., 1998. Bioaccumulation of mercury in pelagic freshwater food webs. Sci. Total. Environ. 219, 183–208.
Wu, P.P., Zakem, E.J., Dutkiewicz, S., Zhang, Y.X., 2020. Biomagnification of methylmercury in a marine plankton ecosystem. Environ. Sci. Technol. 54 (9), 5446–5455.
Yao, C., He, T.R., Xu, Y.Y., Ran, S., Qian, X.L., Long, S.X., 2020. Mercury bioaccumulation in zooplankton and its relationship with eutrophication in the waters in the karst region of Guizhou Province, Southwest China. Environ. Sci. Pollut. Res. 27, 8596–8610.
Yuan, L.L., Shi, X.J., Tang, B.Z., Wang, W.X., 2021. Real-time in vitro monitoring of the subcellular toxicity of inorganic Hg and methylmercury in zebrafish cells. Aquat. Toxicol. 236, 105859–105870.

Methylmercury bioaccumulation in water flea *Daphnia carinata* by AIEgen

By

He, T (He, Tao) [1], [2] ; Mao, XD (Mao, Xiaodong) [1] ; Lin, HY (Lin, Hangyu) [1] ; Hassan, MM (Hassan, Md Mahbubul) [3] ; Zhu, S (Zhu, Song) [1] ; Lu, Q (Lu, Qun) [1] ; Qin, JG (Qin, Jianguang) [3] ; Su, SQ (Su, Shengqi) [1]

View Web of Science ResearcherID and ORCID (provided by Clarivate)

Source

ECOTOXICOLOGY AND ENVIRONMENTAL SAFETY

Volume: 248

DOI: 10.1016/j.ecoenv.2022.114271

Article Number

114271

Published

DEC 15 2022

Early Access

NOV 2022

Indexed

2023-02-21

Document Type

Article

Abstract

Mercury ion (Hg2+) is a toxic heavy metal ion and Hg2+ is convertible to methylmercury (MeHg) by many aquatic microorganisms, leading to bioaccumulation and biomagnification in aquatic organisms, which can interfere with brain development and function in humans. This study employs a newly developed AIEgen (Ag-gregation-induced emission fluorogen) to quantify and visualise the process of MeHg bioaccumulation in vivo on the species of water flea Daphnia carinata. Two approaches to MeHg absorption were taken, either by direct incubation in a MeHg solution or by indirect consumption of algae contaminated with MeHg. We analysed the relationship between the ratio of photoluminescence (PL) intensities (I585/I480) and MeHg concentration (CMeHg) and generated a master curve for determining MeHg concentration based on the measurement of PL intensities. Fluorescent image analysis showed the occurrence of MeHg in D. carinata to be mainly in the compound eyes, optic nerve and carapace. This study indicates that MeHg absorption can be quantified and visualised in the body of zooplankton, and the MeHg transfer to zooplankton is more likely through direct exposure than via indirect food intake. The accumulation of MeHg in the eye and the nervous system could be the cause of the high mortality of D. carinata exposed to MeHg in water.

Keywords

Author Keywords: MeHg; Bioaccumulation; Water flea; Aggregation -induced emission fluorogen

Keywords Plus: AGGREGATION-INDUCED EMISSION; IN-VIVO VISUALIZATION; MERCURY; TOXICITY; BIOMAGNIFICATION; ACCUMULATION; CLADOCERAN; ELIMINATION; RESERVOIR; MAGNA

Author Information

Corresponding Address: Su, Shengqi (corresponding author)

Southwest Univ, Coll Fisheries, Chongqing 400715, Peoples R China

Corresponding Address: Qin, Jianguang (corresponding author)

Flinders Univ S Australia, Coll Sci & Engn, Adelaide, SA 5001, Australia

Addresses :

1 Southwest Univ, Coll Fisheries, Chongqing 400715, Peoples R China

2 South China Univ Technol, Guangdong Prov Key Lab Luminescence Mol Aggregates, Guangzhou 510641, Guangdong, Peoples R China

3 Flinders Univ S Australia, Coll Sci & Engn, Adelaide, SA 5001, Australia

E-mail Addresses :

jian.qin@flinders.edu.au; sushengqi@swu.edu.cn

Categories/ Classification

Research Areas:

Environmental Sciences & Ecology; Toxicology

Citation Topics: 3 Agriculture, Environment & Ecology › 3.91 Contamination & Phytoremediation › 3.91.644 Mercury

Web of Science Categories

Environmental Sciences; Toxicology

MeSH Terms *From MEDLINE®* Search terms found

Chemical *From MEDLINE®* Search terms found

Funding

Funding agency	Grant number	Show All Details
Natural Science Foundation of Chongqing	2019YFD0900305-03	Show details
Open Fund of Guangdong Provincial Key Laboratory of Luminescence from Molecular Aggregates (South China University of Technology)		
National Key Research and Development Program of China		
	cstc2021jcyj-msxmX0100	

View funding text

+ See more data fields

Journal information

ECOTOXICOLOGY AND ENVIRONMENTAL SAFETY

ISSN
0147-6513

eISSN
1090-2414

Current Publisher
ACADEMIC PRESS INC ELSEVIER SCIENCE, 525 B ST, STE 1900, SAN DIEGO, CA 92101-4495

Journal Impact Factor
Journal Citation Reports ™

Research Areas
Environmental Sciences & Ecology; Toxicology

Web of Science Categories
Environmental Sciences; Toxicology

23

6.8

Journal Impact Factor ™ (2022)

1.5

Journal Citation Indicator ™ (2022)

Citation Network

In All Databases

2 Citations

Create citation alert

2 Times Cited in All Databases

+ See more times cited

44 Cited References

View Related Records →

Citing items by classification New

Breakdown of how this article has been mentioned, based on available citation context data and snippets from 1 citing item(s).

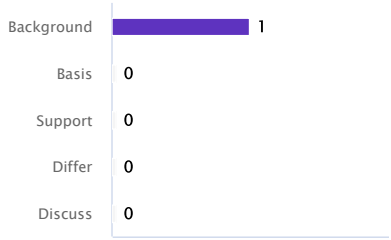

Most Recently Cited by

Jeong, H; Byeon, E; Lee, JS; et al.
Heavy metals and metalloid in aquatic invertebrates: A review of single/ mixed forms, combination with other pollutants, and environmental factors
MARINE POLLUTION BULLETIN

Liu, DL; Shi, QH; Zeng, X; et al.
Effects of Endocrine-Disrupting Heavy Metals on Human Health
TOXICS

Use in Web of Science

5
Last 180 Days

12
Since 2013

Learn more →

This record is from:

Web of Science Core Collection

- Science Citation Index Expanded (SCI-EXPANDED)

View record in other databases:

- View biological data (in BIOSIS Previews)
- View medical data (in MEDLINE®)

Suggest a correction

If you would like to improve the quality of the data in this record, please **Suggest a correction**

44 Cited References

→ View as set of results

Showing 30 of 44 *(from All Databases)*

Science of the Total Environment 905 (2023) 167063

Contents lists available at ScienceDirect

Science of the Total Environment

journal homepage: www.elsevier.com/locate/scitotenv

Metabolic pathways of methylmercury in rotifer *Brachionus plicatilis*

Hangyu Lin [a,b,1], Xiaodong Mao [a,b,1], Yanlin Wei [a,b], Songzhang Li [a,b], Jianguang Qin [c], Song Zhu [a,b], Shengqi Su [a,b,*], Tao He [a,b,*]

[a] College of Fisheries, Southwest University, Chongqing 400715, China
[b] Key Laboratory of Freshwater Fish Reproduction and Development (Ministry of Education), Key Laboratory of Aquatic Science of Chongqing, 400715, China
[c] College of Science and Engineering, Flinders University, South Australia 5001, Australia

HIGHLIGHTS

- We explored the dynamic accumulation and metabolic regulation of MeHg in *B. plicatilis*.
- MeHg accumulated mainly in the ciliary corona, various digestive organs of *B. plicatilis*.
- Changes in some metabolic pathways in *B. plicatilis* may be related to MeHg exposure in the intestine.
- MeHg accumulated in *B. plicatilis* was difficult to metabolize outside the body.
- MeHg induced significant enrichment of arginine biosynthesis and metabolism pathway in *B. plicatilis*.

GRAPHICAL ABSTRACT

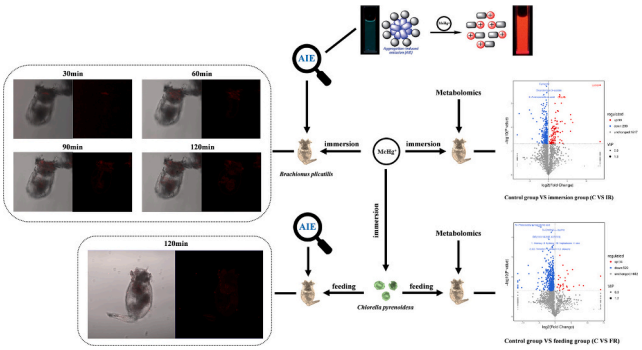

ARTICLE INFO

Editor: Christopher Rensing

Keywords:
Methylmercury
Aggregation-induced emission fluorogen
Metabolomics
Brachionus plicatilis

ABSTRACT

Methylmercury (MeHg) readily accumulates in aquatic organisms while transferring and amplifying in the aquatic food chains. This study firstly explores the in vivo accumulation sites and metabolic regulation of MeHg in the rotifer *Brachionus plicatilis* by aggregation-induced emission fluorogen (AIEgen) and metabolomics. Fluorescent image analysis by AIEgen showed that MeHg in *B. plicatilis* mainly occured in the ciliary corona, esophagus, mastax, stomach and intestine in the direct absorption group. In the other group, where *B. plicatilis* were indirectly supplied with MeHg via food intake, the accumulation of MeHg in the rotifer occurred in the ciliary corona, various digestive organs, and the pedal gland. However, the MeHg accumulated in the rotifer is difficult to metabolize outside the body. Metabolomics analysis showed that the significant enrichment of ABC transporters was induced by the direct exposure of rotifers to dissolved MeHg. In contrast, exposure of rotifers to MeHg via food intake appeared to influence carbon, galactose, alanine, aspartate and glutamate metabolisms. Besides, the disturbed biological pathways such as histidine metabolism, beta-alanine metabolism and pantothenate and CoA biosynthesis in rotifers may be associated with L-aspartic acid upregulation in the feeding group. The significant enrichment of ABC transporters and carbon metabolism in rotifers may be related to the accumulation of MeHg in the intestine of rotifers. In both pathways of MeHg exposure, the arginine biosynthesis and metabolism of rotifers were disturbed, which may support the hypothesis that rotifers produce more energy

* Corresponding authors at: College of Fisheries, Southwest University, Chongqing 400715, China.
E-mail addresses: sushengqi@swu.edu.cn (S. Su), hh1985@swu.edu.cn (T. He).
[1] Equal contribution.

https://doi.org/10.1016/j.scitotenv.2023.167063
Received 15 July 2023; Received in revised form 7 September 2023; Accepted 11 September 2023
Available online 13 September 2023

to resist MeHg toxicity. This study provides new insight into the accumulation and toxicity mechanisms of MeHg on marine invertebrates from the macro and micro perspectives.

1. Introduction

The heavy metals in aquatic ecosystems are a widespread concern because they tend to accumulate in aquatic organisms (Kakade et al., 2023). Mercury (Hg), a heavy metal element known to be one of the top environmental pollutants in water (Muñoz et al., 2023), has been recognized as a priority hazardous substance that enters aquatic ecosystems through natural processes and anthropogenic activities (Moltedo et al., 2019). Human exposure to Hg is primarily associated with its organic form, methylmercury (MeHg), through the uptake of polluted seafood (Nogueira et al., 2019). MeHg is the most toxic form of all mercury compounds, and it is formed when inorganic mercury in the aquatic environment is methylated by microorganisms (Lin et al., 2021).

MeHg pollution risks human health via fish intake due to bioaccumulation and magnification of MeHg in aquatic food chains (Kucharzyk et al., 2015). Phytoplankton can concentrate MeHg from the surroundings, which is the first step of MeHg entry into the aquatic food webs (Li et al., 2022). MeHg concentrations in zooplankton can increase with a rise in body size and biomass (Todorova et al., 2015). Research has shown that MeHg reaches up to 80–100 % of the total Hg (THg) measured in fish muscle (Bloom, 1992; Bravo et al., 2014; Lamborg et al., 2014). The biomagnification of mercury was observed through the food web, and the top predator tigerfish, *Hydrocynus vittatus*, has the highest mercury concentration (van Rooyen et al., 2023). There is ample evidence that mercury accumulates in fish at concentrations of concern for human consumption (Pickhardt et al., 2005). Thus, studying the distribution and metabolic level of MeHg in aquatic food chains is of great practical significance. However, there is limited information on MeHg accumulation in invertebrates, such as rotifers and copepods (Lee et al., 2017), which play an important role in energy transfer in aquatic ecosystems (Kim et al., 2017).

In aquatic food chains, zooplankton is a crucial link between primary producers and higher trophic-level consumers (Petrik et al., 2022) and plays a vital role in global biogeochemical cycles (Ratnarajah et al., 2023). Rotifers are a primary class of zooplankton widely distributed in aquatic environments (Mao et al., 2022), as they consume microalgae and organic detritus and also serve as food for fish, shrimp and crabs (Daewel et al., 2014). The species of *Brachionus plicatilis* has been used as live food for fish and crustacean larvae in aquaculture (Rahman et al., 2018). In addition, *B. plicatilis* has been used as a model species on the influence and toxicity measurements in marine ecosystems due to its suitable size, short life cycle, fast population growth and ease of cultivation (Li et al., 2020). Yang et al. explored the effects on the ingestion and digestive performance of rotifer *B. plicatilis* after treatment with 2,2′,4,4′-tetrabromodiphenyl ether (BDE-47) (Yang et al., 2021). Han et al. studied the deleterious effects on reproductive features of temperate *B. plicatilis* after exposure to iron (Fe) (Han et al., 2022). Furthermore, Cao et al. explored the reproductive toxicity of triphenyltin (TPT) to *B. plicatilis* (Cao et al., 2022).

In 2001, Professor Ben Zhong Tang and co-workers raised the concept of aggregation-induced emission (AIE) (Luo et al., 2001). Over the last two decades, massive attention has focused on AIE in materials science, analytical chemistry, and life sciences (Mei et al., 2015). The fluorogens with AIE attributes have been referred to as AIEgens, which have appeared as an appealing tool for bioimaging due to their flexible steerability, ignorable toxicity and superior photostability (Wang et al., 2019). So far, AIEgens for detecting heavy metal ions (including mercury, arsenic, cadmium, copper, zinc, chromium, and lead) have been developed (Huang et al., 2021). AIEgen (m-TPE-RNS) is an Hg^{2+} sensor with high selectivity and high sensitivity to Hg^{2+} in water (Chen et al., 2017) and has been used to in vivo visualize Hg^{2+} kinetics in rotifers (Jiang et al., 2017). In previous research, we found that the MeHg detection mechanism for m-TPE-RNS resembles the reaction between Hg^{2+} and m-TPE-RNS, and visualized the process of MeHg bioaccumulation in vivo on water flea *Daphnia carinata* by m-TPE-RNS (He et al., 2022). However, information about potential mechanisms of MeHg toxicity in zooplankton is limited.

Metabolomics is to profile metabolites in biofluids, cells and tissues in response to environmental stressors and exposure to toxicants or pathogens (Lankadurai et al., 2013). Metabolomics provides a snapshot of the phenotype of biological systems, which is conducive to understanding organisms' functional states and critical metabolic processes (Lin et al., 2006). Metabolomics has been widely applied in aquatic ecotoxicology (Hu et al., 2023) and become an important tool in exposure studies (Bedia, 2022). According to the metabolomic analysis in zebrafish, exposure to norethindrone (NET) can disrupt the antioxidant defense system of zebrafish by inhibiting the Nrf2-ARE and NF-kB pathways in the synthesis of superoxide dismutase and glutathione (Wang et al., 2021). In the metabolomic analysis of *B. plicatilis* under tributyl phosphate (TnBP) stress, high concentrations of TnBP can interfere with the basic metabolic pathways in rotifers, causing disturbances in purine metabolism and lipid metabolism, thus adversely affecting rotifer reproduction and population growth (Zhang et al., 2021). A previous study exploring the mechanisms of nanoplastics (NPs) in *B. plicatilis*, indicates that disruptions in purine-pyrimidine metabolism, TCA cycle, and protein synthesis might be collectively responsible for the changes at individual and population levels (Li et al., 2023). Recently, metabolomics research has helped explore the biological effects at the molecular level exerted by xenobiotics.

In this study, we specially designed an AIEgen to visualize the bioaccumulation of MeHg inside *B. plicatilis* and aimed to understand how MeHg is transferred from primary producers to higher trophic level consumers. Furthermore, the impact of MeHg on the metabolite composition of rotifers was analyzed to clarify the potential mechanisms of MeHg toxicity. This study sheds new light on the bioaccumulation and toxic effects of MeHg on an invertebrate that is an essential player in the aquatic food web.

2. Materials and methods

2.1. Materials

Unless otherwise specified, all reagents were gained from Aladdin (Shanghai, China). The AIEgen (m-TPE-RNS) was produced by AIEgen Biotechnology (Hong Kong, China) and dissolved in acetonitrile (ACN). Stock solutions of AIEgen and CH_3HgCl (MeHg) at a concentration of 2.5 μM were prepared. The maximum photoluminescence (PL) intensity of AIEgen appeared with the ACN to water ratio of 2–3 by volume (He et al., 2022). Therefore, the water volume fractions (fw, vol%) were fixed at 60 % in water/ACN mixtures in the subsequent fluorescence staining experiments.

Rotifers *Brachionus plicatilis* were initially collected from Ningbo, China, and hatched from the resting eggs stocked in the College of Fisheries, Southwest University (Chongqing, China). The rotifers were cultured in artificial seawater (20–35 ‰ salinity) under the photoperiod of 16 h light and 8 h dark at 3000 lx of illumination and 26 °C. The artificial seawater comprised NaCl 21.1 g/L, Na_2SO_4 3.55 g/L, KCl 5.99 g/L, $NaHCO_3$ 2.94 g/L, KBr 86.0 mg/L, H_3BO_3 23.0 mg/L, NaF 3.00 mg/L, $MgCl_2{\cdot}6H_2O$ 9.96 g/L, $CaCl_2$ 10.1 g/L, $SrCl_2{\cdot}6H_2O$ 22.0 mg/L. *Chlorella pyrenoidesa* were used to feed the rotifers. The algae were cultured in f/2 medium under photoperiods of 12 h (LD 12:12) at 5000 lx in an illumination incubator at 28 °C.

2.2. Visualization of MeHg accumulation in B. plicatilis by AIEgen

This study examined MeHg accumulation in *B. plicatilis* by directly incubating in a MeHg solution and indirectly consuming *Chlorella pyrenoidesa* that had accumulated MeHg. In group one, rotifers were harvested from an aquarium tank with a 50-μm mesh net and added to a solution containing 1.0 μM MeHg with a density of 400 rotifers mL^{-1}. Rotifers (10–15 ind.) were collected at 5, 30, 60 and 120 min intervals after submerging, then stained in the m-TPE-RNS solution of 1.0 μM with the ACN to water ratio of 2:3 by volume. After rinsing twice, rotifers were subjected to a scanning confocal fluorescence microscope for imaging. In group two, rotifers were harvested by the method above and adjusted to a density of 400 ind mL^{-1} in artificial seawater. After incubation with MeHg-poisoned algae for 120 min, the rotifers were collected and stained in the m-TPE-RNS solution described above to obtain fluorescence images.

For fluorescence imaging, the wavelength range of blue channels was set at 460–500 nm for the image analysis of *B. plicatilis* submerged in AIEgen. The red channel fluorescence was set at 570–610 nm for the image analysis of *B. plicatilis* exposed to MeHg and stained in AIEgen solution. Furthermore, the excitation wavelength was set at 405 nm. The algae contaminated with MeHg were obtained as follows: after incubation in 1.0 μM MeHg for 60 min with the algae density of 3.6×10^6 ind mL^{-1}, algae were collected by centrifugation at 4500 rpm for 1 min as feed for *B. plicatilis*.

2.3. Metabolomics analysis of rotifers exposed to MeHg

The newly-born rotifers (<6 h, 1000 ind mL^{-1}) were exposed to MeHg for metabolomics profiling. Rotifers of the control group (C) were fed with non-toxic *C. pyrenoidesa* (3.6×10^6 ind mL^{-1}) only. Based on the control group, the immersion group (IR) rotifers were exposed to MeHg at a concentration of 1.0 μM. Furthermore, rotifers of the feeding group (FR) were fed with 3.6×10^6 ind mL^{-1} MeHg-poisoned *C. pyrenoidesa*, and the algae contaminated with MeHg were obtained as described in Section 2.2. Each group had three replicates. After 60 min of exposure, the rotifers were rinsed and introduced into the medium without MeHg. The rotifers were collected in 50-mL centrifuge tubes after incubation for 24 h. Absolute ethyl alcohol was added to reach a concentration of 10 % (*v*/v), mixed the samples and stood for 5 min, and centrifuged (2000*g*, room temperature) for 10 min. After centrifugation, the supernatant was discarded, the rotifers were resuspended, introduced into the 300 kDa microsep, and centrifuged (13,000*g*, 4 °C) for 2 min. The resulting samples were drained and stored in liquid nitrogen for subsequent testing. Metabolomics detection of rotifers entrusted Biomarker Technologies (Beijing, China) to complete.

2.4. Statistical analysis

The principal component analysis (PCA) and orthogonal partial least squares discriminant analysis (OPLS-DA) of multivariate statistical analysis methods were used for data analysis. We employed the PCA to determine the differences in metabolites of rotifers between the treatment groups and the control group. The R software (www.r-project.org/) was used for hierarchical cluster analysis (HCA) on the accumulation patterns of metabolites between different samples. For initially screening for metabolites with differences, a multivariate analysis of variable importance in the project (VIP) in the OPLS-DA model was used based on the results of the OPLS-DA. At the same time, by combining the *P*-values in the univariate analysis, differential metabolites could be further screened. The differential metabolites were ultimately confirmed and annotated using the KEGG database (Kanehisa and Goto, 2000). Enrichment analysis of KEGG annotation results using R package clusterProfiler (Yu et al., 2012).

3. Result

3.1. In vivo visualization of MeHg accumulation in B. plicatilis by AIEgen

The rotifers in control without MeHg and AIEgen showed no fluorescent signals (Fig. 1A), which was similar to the fluorescence imaging from rotifers exposed to MeHg without AIEgen (Fig. 1B). Blue fluorescence at 460–500 nm was observed inside rotifers after they were directly submerged in AIEgen (Fig. 1C). Red fluorescence at 570–610 nm was observed within rotifers after the rotifers incubated with MeHg and stained by AIEgen (Fig. 1D).

After submersion in MeHg for 5 min, emission in the red channel occurred in the ciliary corona of the rotifers (Fig. 2A). After submersion for 30 min, red fluorescence signals appeared in the ciliary corona and mastax. A small amount of fluorescence existed on the lorica of the rotifers (Fig. 2B). At 60 min, red fluorescence appeared in the ciliary corona, mastax, stomach and lorica of rotifers (Fig. 2C). As shown in Fig. 2(D), the red fluorescence became more noticeable after submersion for 120 min. In addition to the above sites, red fluorescence also appeared in the intestine of rotifers, and the fluorescence intensity in vivo rotifers was significantly stronger than that on the lorica. There were no fluorescent signals in the kidneys of the rotifer in the process of MeHg accumulation in the rotifer within 120 min.

After feeding on algae containing MeHg, rotifers showed no fluorescent signals in the blue channel due to the reaction between MeHg and AIEgen (Fig. 3). Contrary to the blue channel, the red fluorescence became more noticeable because of the combination of MeHg and AIEgen. Our results demonstrated that red fluorescence appeared in the ciliary corona, mastax, stomach, intestine and pedal gland, and a small amount of fluorescence on the lorica of the rotifers. MeHg-containing algae delivered the MeHg and accumulated in the digestive system through rotifer digestion. Besides, the MeHg also accumulated in the pedal gland of the rotifers.

3.2. Metabolomic alterations of rotifers induced by MeHg

Principal component analysis (PCA) showed the control group (C) separated from the immersion group (IR) and feeding group (FR), respectively, indicating that metabolic profiles in the rotifers were significantly affected by exposure to MeHg via immersion and feeding (Fig. 4).

The HCA could assess discrepancies in the characteristics of MeHg treatment that resulted in metabolite accumulation, including intra-treatment homogeneity and inter-treatment variability. As shown in Fig. 5, compared with the feeding group, the location of the immersion group was farther away from the control group, indicating that the immersion group had a greater influence on the metabolite expression of rotifers. Metabolites with a VIP of >1 and a *P*-value of <0.05 were selected. The metabolites screened under the above conditions had significant differences. Compared to the control group, the rotifers of the immersion group significantly up-regulated 99 metabolites and down-regulated 299 metabolites, while the rotifers in the feeding group significantly up-regulated 34 metabolites and down-regulated 529 metabolites (Fig. 6; Table S1-S2).

Compared to the control group, the functional annotation of differential metabolites in the immersion and feeding groups was performed according to the pathway type in the KEGG database (http://www.genome.jp/kegg/) (Tables S3–S4). The differential metabolites were mostly organic acids, alkaloids, aldehydes and phenols. Table S5 shows the results of the enrichment analysis of differential metabolites in the immersion and feeding groups compared with the control group. In the immersion group compared to the control group, a total of four KEGG pathways show significant enrichment of differential metabolites, including arginine biosynthesis (ko00220), arginine and proline metabolism (ko00330), ABC transporters (ko02010), central carbon metabolism in cancer (ko05230). Among them above, arginine biosynthesis,

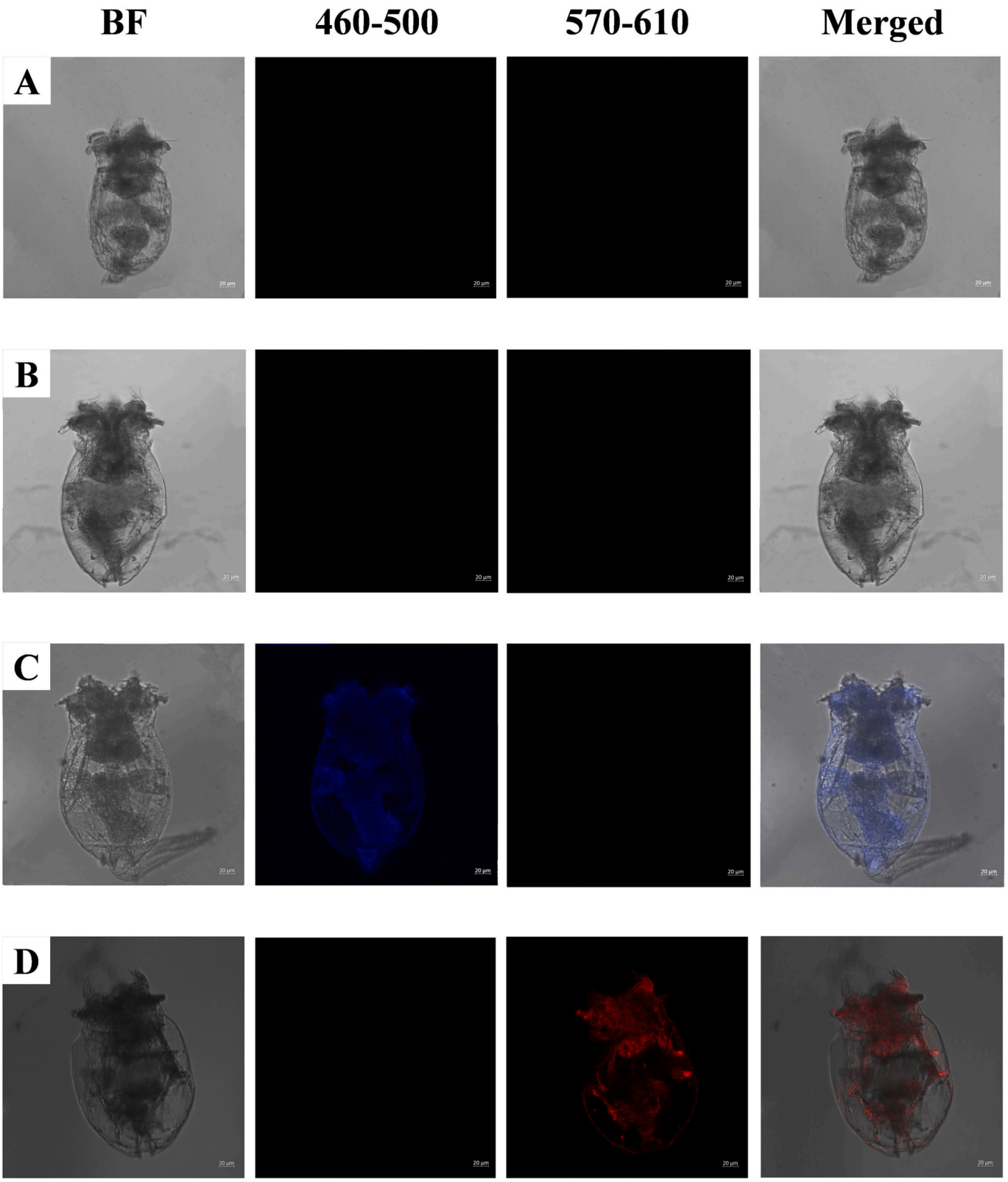

Fig. 1. Images of *B. plicatilis* on a confocal microscope using 1.0 μM MeHg. (A) the control without MeHg in rotifers and AIEgen staining; (B) exposure to MeHg but in the absence of AIEgen; (C) exposure to 1.0 μM AIEgen in the absence of MeHg, emitting blue fluorescence; (D) exposure to 1.0 μM MeHg stained in the 1.0 μM AIEgen solution, emitting red fluorescence; BF: bright field.

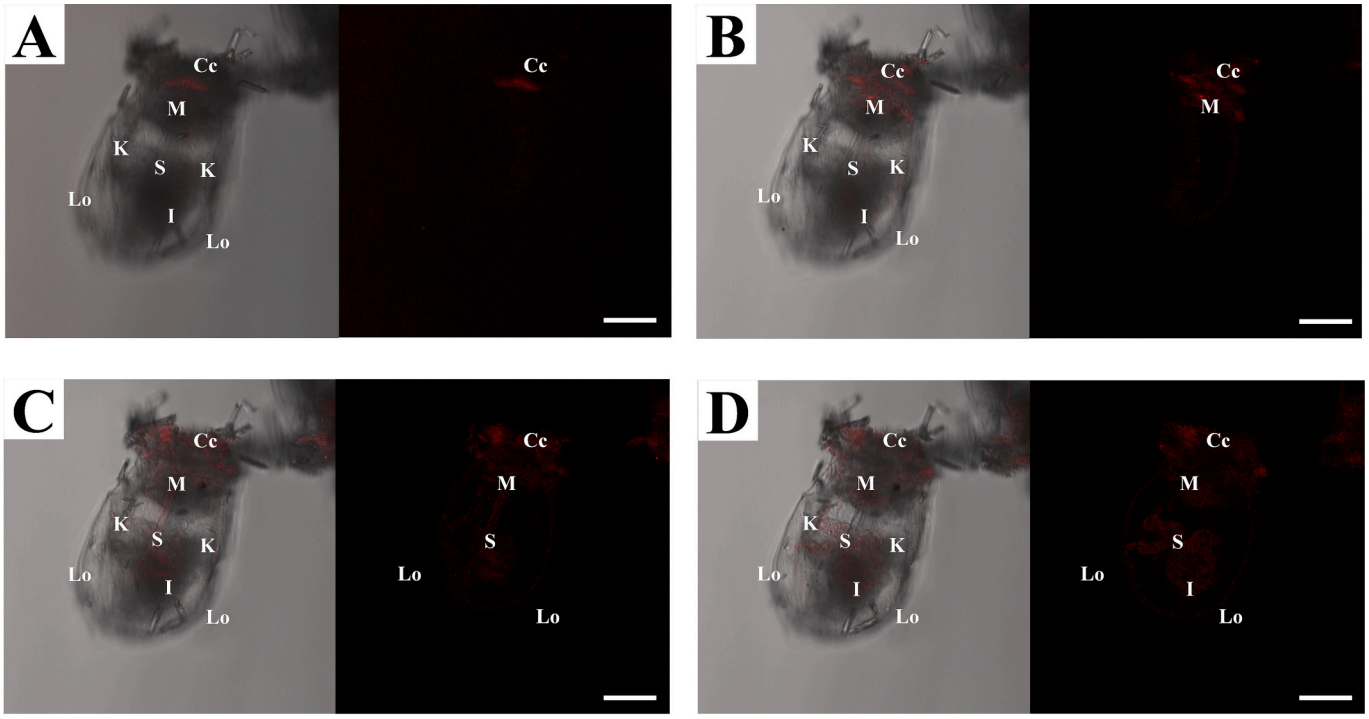

Fig. 2. Confocal fluorescent images of *B. plicatilis* in MeHg solution after incubation for (A) 5 min; (B) 30 min; (C) 60 min; (D) 120 min. Cc: ciliary corona; M: mastax; Lo: lorica; S: stomach; I: intestine; K: kidneys; Bar = 30 um.

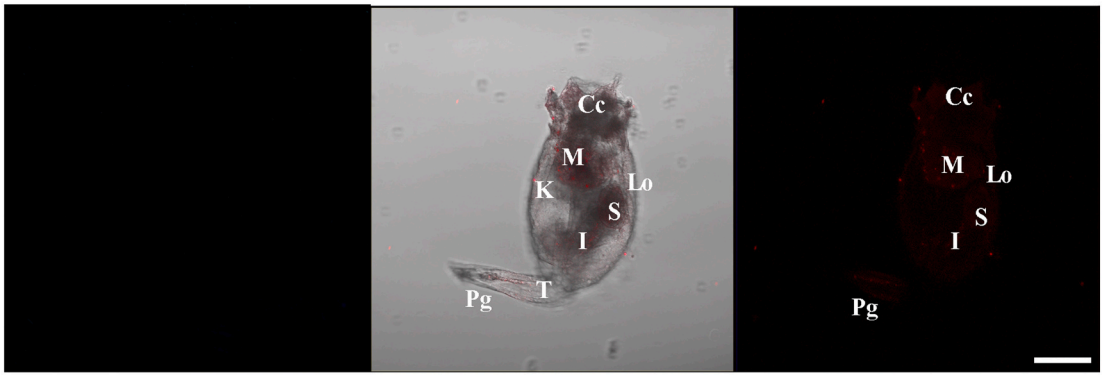

Fig. 3. Confocal fluorescent images of *B. plicatilis* incubated with MeHg-containing algae for 120 min. Cc: ciliary corona; M: mastax; Lo: lorica; S: stomach; I: intestine; K: kidneys; T: tail; Pg: pedal gland; Bar = 30 μm.

arginine and proline metabolism and ABC transporters showed extremely significant enrichment. In the feeding group compared to the control group, a total of ten KEGG pathways show significant enrichment of differential metabolites, including galactose metabolism (ko00052), arginine biosynthesis (ko00220), alanine, aspartate and glutamate metabolism (ko00250), arginine and proline metabolism (ko00330), histidine metabolism (ko00340), beta-Alanine metabolism (ko00410), pantothenate and CoA biosynthesis (ko00770), carbon metabolism (ko01200), biosynthesis of amino acids (ko01230), estrogen signaling pathway (ko04915). Among them, arginine biosynthesis, beta-Alanine metabolism, pantothenate and CoA biosynthesis showed extremely significant enrichment.

4. Discussion

4.1. Visualization of MeHg accumulation in B. plicatilis by AIEgen

The uptake of MeHg by phytoplankton primarily via passive diffusion of neutral complexes across a cell membrane, thus permeating into cellular cytoplasm and bioconcentrated in phytoplankton (Gosnell and Mason, 2015). Prior research suggests that MeHg accumulates mainly in the compound eyes, optic nerve and carapace of *D. carinata* (He et al., 2022). In addition, ingested MeHg in fish can be found in muscles, kidneys, gonads, liver and gut (Kasper et al., 2009). However, the accumulation mode of MeHg in rotifers has not been reported yet. In this study of MeHg fluorescence tracing by AIEgen, we found that the MeHg accumulation sites in rotifers could be observed by superimposing the bright field of a light microscope and the fluorescence field of a scanning confocal fluorescence microscope. The target organs or sites of MeHg accumulation in rotifers were outlined in the fluorescence field by AIEgen, and the specific organs or tissues of MeHg accumulation in rotifers could be identified by combining the images of bright fields.

In this study, the fluorescence imaging from rotifers directly exposed to MeHg showed that MeHg entered the rotifers through the digestive tract and accumulated in the ciliary corona and various digestive organs. In addition, a small number of fluorescent signals were observed on the

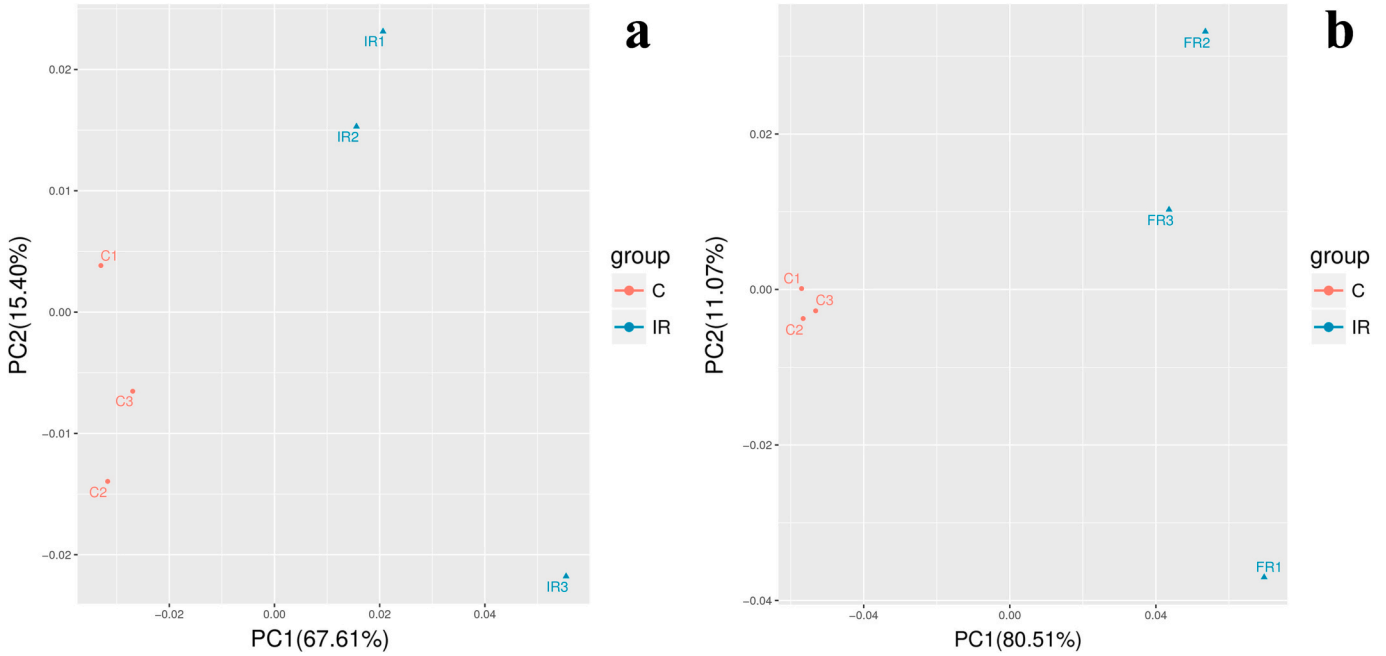

Fig. 4. Principal component analysis (PCA) score map: (**a**) control group (C) and immersion group (IR), (**b**) control group (C) and feeding group (FR).

lorica of rotifers, and there were no fluorescent signals in the kidneys of rotifers during the study period. However, the fluorescence imaging from rotifers directly exposed to dissolved Hg^{2+} showed that the Hg^{2+} accumulated in various digestive organs, visualized around the lorica of rotifers, and observed in the excretory system such as the kidneys (Jiang et al., 2017). MeHg is somewhat lipophilic and binds readily to proteins (Chattopadhyay, 2005). For example, once MeHg passes through the cell membrane, it strongly binds with the protein sulfhydryl groups (Li et al., 2022). It is reasonable to infer that MeHg can be absorbed by the rotifer by binding to proteins in the body integument, resulting in low fluorescence intensity on the lorica, while Hg^{2+} cannot permeate into the rotifer by diffusion through the body integument (Jiang et al., 2017). In addition, unlike Hg^{2+}, the fluorescence signal of MeHg was not found in the excretory system of the rotifers. The transformation from the hydrophilic of inorganic mercury to the lipophilic state of organic mercury makes mercury more apt to biomagnification in aquatic food chains (Hansen and Danscher, 1997). Most of the MeHg may not be metabolized by the excretory system of rotifers but instead remained in the rotifers by combining with protein sulfhydryl groups. Moreover, MeHg could be formed when exposed to inorganic mercury by gut microbiota from aquatic organisms like fish, and mammals like rats and even human beings (Li et al., 2019).

Significant fluorescence was observed in the ciliary corona, mastax, stomach and intestine of rotifers fed on MeHg-poisoned algae, indicating that the accumulation of MeHg in various digestive organs of rotifers was caused by the process of MeHg-exposed algae passing through the digestive tract of rotifers. The biomagnification of MeHg through aquatic food webs can adversely affect the health of organisms. The elevated dietary MeHg exposure reduced spawning success, altered reproductive behaviors, and suppressed the sex hormones of fish (Drevnick and Sandheinrich, 2003; Sandheinrich and Miller, 2006). Moreover, embryos of *Pimephales promelas* exposed to high-diet MeHg delayed hatching and lowered livability (Bridges et al., 2016). The pedal glands of rotifers can secrete an adhesive for temporary attachment to surfaces, and the ducts of pedal glands exit near the toes (Wallace, 2015). In the present study, the fluorescence results showed that the MeHg also accumulated in the pedal glands of the secretory system of rotifers via food take, which may affect the adhesion behavior of rotifers. This study firstly visualized MeHg distribution in the rotifer by AIEgen, which enhanced the understanding of the MeHg bioaccumulation process in aquatic food webs.

4.2. *Metabolomics analysis of rotifers exposed to MeHg*

In rotifers *B. plicatilis*, some studies have used biomarkers such as glutathione S-transferase (GSTs), acetylcholinesterase (ACHE), adenosine triphosphatase (ATPase) and cytochrome P450 (CYP) to determine the response of *B. plicatilis* to microplastics, harmful algae, organic pollutants and pesticides (Han et al., 2019; Kang et al., 2021; Xiaodong et al., 2020; Yang et al., 2021). In this research, we investigated the toxic effects of MeHg on rotifers by the functional annotation and enrichment analysis of differential metabolites according to the KEGG database.

Compared to the feeding group, the differential metabolites of rotifers in the immersion group showed up in ABC transporters. The ABC transporters constitute a large, ubiquitous and diverse superfamily of integral membrane proteins (Rees et al., 2009) that are responsible for the transportation of a variety of substrates, including inorganic ions, amino acids, nucleotide, polysaccharides, polypeptides and proteins (Neumann et al., 2017). ABC transporters constitute an integral part of cell detoxification, which can pull a variety of endogenous and exogenous substances out of the cell through ATP binding and hydrolysis, thus limiting the accumulation and potential toxicity of endogenous and exogenous substances (Szakács et al., 2008). In the various biological functions of ABC transporters, the ABC transporters mediated by multixenobiotic resistance are considered the first line of defense for aquatic organisms to cope with environmental pollutants (Jeong et al., 2017). Investigators believed that, in aquatic organisms, ABC efflux transporters should be expressed in organs involved in secretion, absorption or as a barrier function, like the liver and intestine (Ferreira et al., 2014). Previous studies have shown that ABC transporter family genes in aquatic invertebrates had several roles, such as cellular lipid transport, formation of a waterproof barrier and efflux pump for metals (Jeong et al., 2017). In several aquatic invertebrates, such as *B. plicatilis*, *Daphnia magna* and *Mytilus galloprovincialis*, the protective effect of the ABC transporters has been demonstrated when the aquatic invertebrates responded to various environmental contaminants (Della Torre et al., 2014; Jeong et al., 2017). Futhermore, numerous studies have confirmed the expression and function of ABC transporters in fish

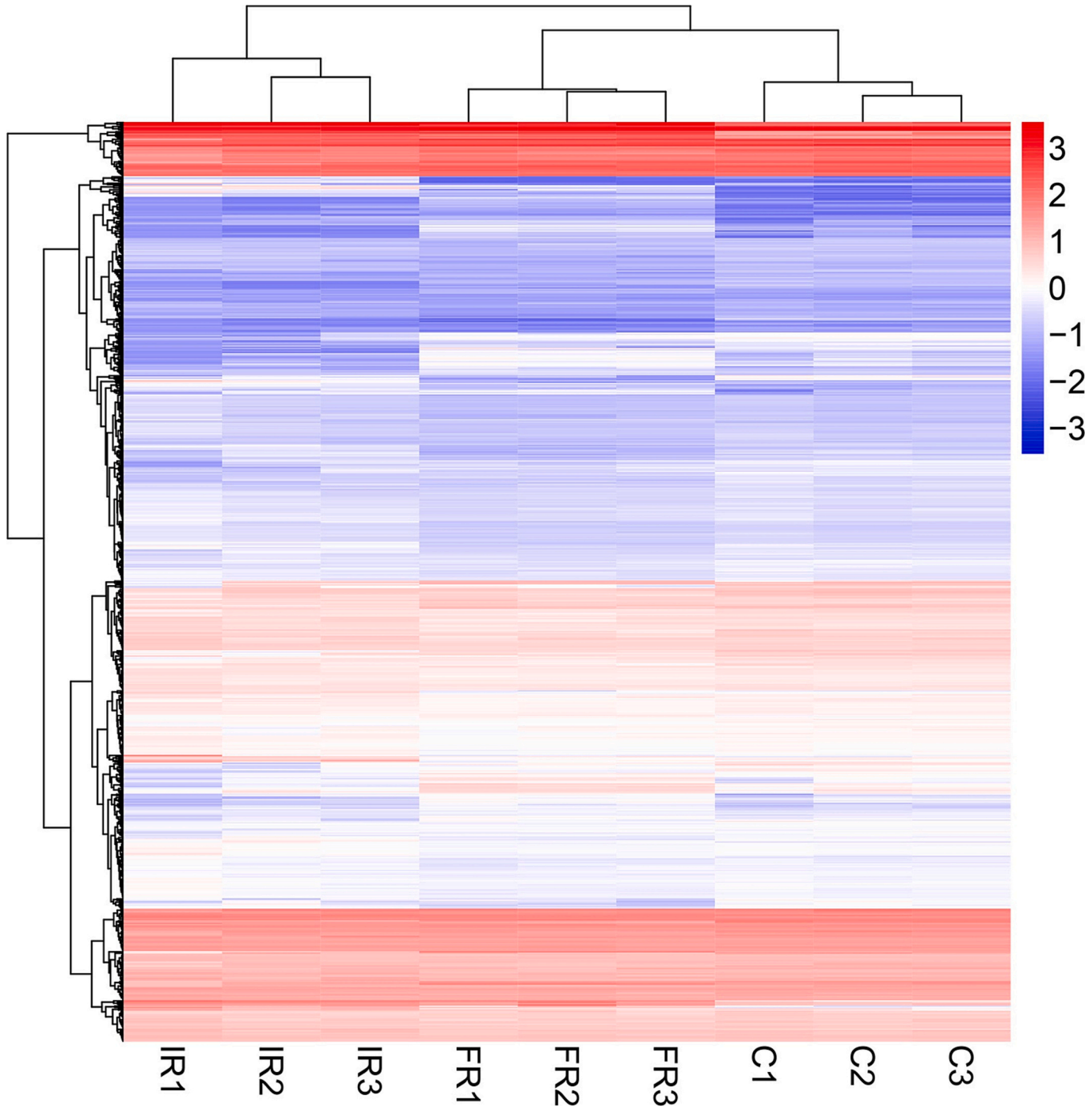

Fig. 5. Heat maps of differentially expressed metabolites in rotifers in the immersion groups (IR), feeding groups (FR), and control groups (C). Red color stands for the upregulation, and blue for the downregulation of metabolites.

intestines (Bieczynski et al., 2021). Long et al. discovered that Hg and Pb significantly induced ABCC2 expression in the intestine of zebrafish (Long et al., 2011). Zhang et al. reported the upregulation of ABCG2B induced by Hg in the intestine of zebrafish (Zhang et al., 2020). The results suggest that the MeHg directly exposed to the rotifers is accumulated in various digestive organs such as the intestine and is induced the significant enrichment of ABC transporters pathway. Presumably, MeHg accumulated in the intestine induced the expression and efflux of ABC transporters in the intestine of rotifers.

In addition, compared to the immersion group, the significant enrichment pathways of differential metabolites of rotifers in the feeding group were mainly found in carbon metabolism, galactose metabolism and alanine, aspartate and glutamate metabolism. Carbon metabolism is the most basic aspect of life and is the basic pathway in vertebrates and invertebrates of energy generation (Dubois-Deruy et al., 2020). Galactose belongs to carbohydrates, and galactose metabolism is one of the carbon metabolism pathways. Carbohydrate is a nutrient that first degrades when the organisms are subjected to external pressure (Jyothi and Narayan, 2000). The change in carbohydrate metabolism readily produces harmful effects on the survival of animals. In humans, the metabolites involved in carbohydrate metabolism were used as indicators to evaluate cancer and other diseases (Beger, 2013). Previous studies proved that the process of carbohydrate metabolism in fish and shellfish was affected by toxic stress (Verma et al., 1983). In this

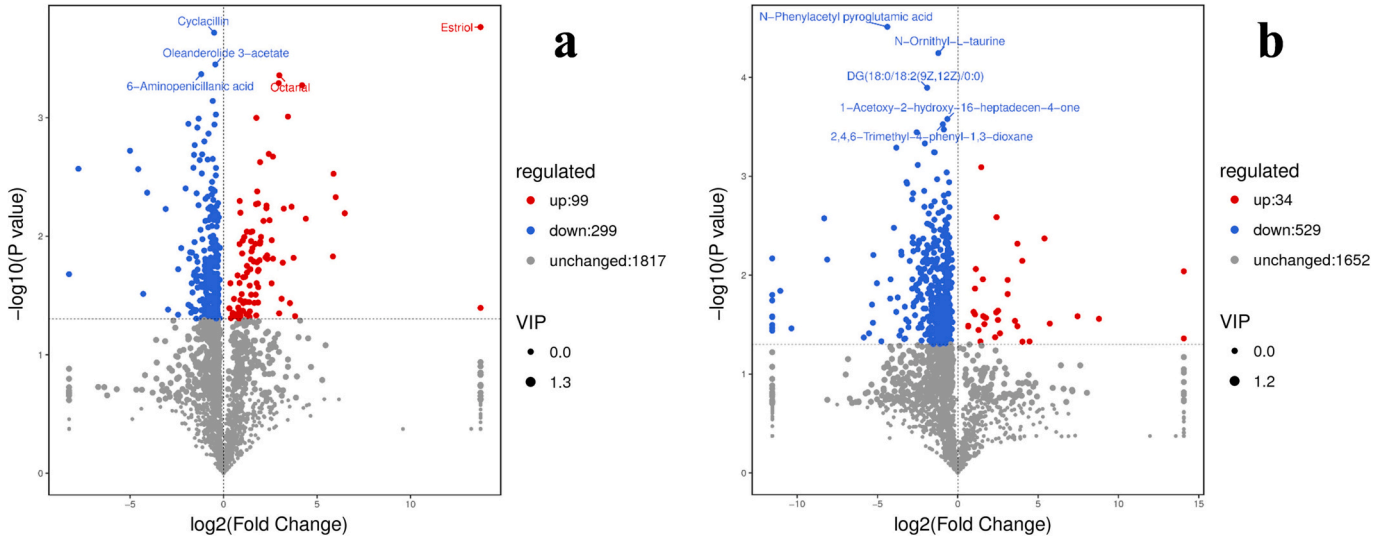

Fig. 6. Volcano plot of metabolites in rotifers exposed to MeHg: (**a**) immersion group vs control group, (**b**) feeding group vs control group.

research, the rotifers exposed to MeHg through directing feeding showed significant enrichment of the carbon metabolism pathway, L-Glutamate and L-Malic acid metabolites were downregulated, and L-Aspartic acids were upregulated, thus affecting energy production in rotifers. The down-regulation of amino acid metabolism is always accompanied by impaired protein synthesis and causes abnormalities in functional proteins such as neurotransmitters, hormones and enzymes (Li et al., 2023). Unfortunately, information about the carbohydrate metabolism of rotifers induced by toxic stress is quite limited. In addition, glutamate is a major excitatory neurotransmitter for signaling and is connected with alanine, aspartate and glutamate metabolism (Duman et al., 2019). Furthermore, the glutamatergic neurotransmitter system is a major target mediating MeHg-induced neurotoxicity (Farina et al., 2017). MeHg exposure disturbs neurotransmitter metabolites, thus increasing sensitivity to neurological responses. Wang et al. reported the regulatory role of the gut microbiota of rats in MeHg-disturbed neurotransmitter metabolic pathways (Wang et al., 2023). The intestine of rotifers is involved in the absorption of nutrients, and the results showed that the MeHg exposed to rotifers via food intake accumulated in the intestine of rotifers. Thus, we speculated that the MeHg accumulated in the intestine of rotifers via food intake may affect the absorption of nutrients, further influencing the degradation of carbohydrates and the process of carbon metabolism in rotifers. Also, the significant enrichment metabolic pathways such as histidine metabolism, beta-alanine metabolism and pantothenate and CoA biosynthesis in rotifers were disturbed, given that L-aspartic acid was upregulated while other metabolites were downregulated in the pathways.

The results showed that the arginine biosynthesis and metabolism significantly enriched rotifers in both exposure pathways to MeHg. Arginine plays a vital role in the metabolism of organisms and is involved in the synthesis of proteins in animal cells (Wu and Morris, 1998). It has been proved that arginine can promote the growth of various fish species (Alam et al., 2002). Chen et al. found that arginine also promoted the expression of genes associated with fish growth at the transcriptional level (Chen et al., 2012). The metabolism of arginine is initiated by arginase, resulting in the production of ornithine and urea (Berge et al., 2002). In invertebrates, the phosphoarginine is dephosphorylated by arginine kinas to produce arginase and a lot of ATP, which can provide energy for energy-consuming processes such as cell division and movement (Tanaka et al., 2007). The existing reports have proved that arginine kinase (AK) is an important indicator of stress response in various species (Kim et al., 2022). Previous studies have shown that the *Daphnia magna* stressed with microcystins will produce more energy to resist the toxin of the microcystins and improve its tolerance through the catalytic action of arginine kinase in *D. magna* (Lyu et al., 2015). Our results demonstrate that the MeHg exposed to rotifers by immersion and feeding induced the significant enrichment of arginine biosynthesis and metabolism pathways in rotifers. These results support the hypothesis that the rotifer produces more energy to counteract the toxicity of MeHg.

5. Conclusion

This study indicated that the accumulation of MeHg in the rotifer by ingestion of contaminated algae was via the mouth surrounded by the ciliary corona to the digestive tract. In addition, the MeHg accumulated in the rotifer is arduous to metabolize out of the body, thus, remaining in the rotifers and biomagnifying through aquatic food webs. The mercury can be absorbed and methylated/demethylated in the gut and cause intestinal microbial disorders (Tian et al., 2023). The investigation of the effects of mercury exposure on intestinal microbes could reveal the mechanism of mercury toxicity, especially the neurotoxicity of MeHg (Li et al., 2019). Our results suggest that changes in some metabolic pathways in rotifers may be related to MeHg exposure in the intestine. However, the effects of MeHg exposure on the intestinal microbes of rotifers are unclear and require further studies. Taken together, our study revealed the distribution of MeHg in zooplankton *B. plicatilis* and promoted the understanding of the bioaccumulation process of MeHg in aquatic food webs. Meanwhile, the present study provided an essential theoretical basis for understanding the toxicity mechanisms of MeHg in zooplankton.

CRediT authorship contribution statement

Hangyu Lin: Conceptualization, Writing – original draft. **Xiaodong Mao:** Investigation, Formal analysis. **Yanlin Wei:** Visualization, Data curation. **Songzhang Li:** Investigation, Data curation. **Jianguang Qin:** Methodology, Writing – review & editing. **Song Zhu:** Project administration, Software. **Shengqi Su:** Resources, Supervision. **Tao He:** Conceptualization, Validation, Funding acquisition.

Declaration of competing interest

The authors declare that they have no known competing financial interests or personal relationships that could have appeared to influence the work reported in this paper.

Data availability

I have shared the link to my data at the Attach File step.

Acknowledgements

The authors thank Ms. Hong Duan (College of Agronomy and Biotechnology, Southwest University, China) for technical support in confocal fluorescence imaging and Biomarker Technologies (Beijing, China) for technical support in metabolomics.

Funding

This research was sponsored by the Natural Science Foundation of Chongqing, China (No. cstc2021jcyj-msxmX0100).

Appendix A. Supplementary data

Supplementary data to this article can be found online at https://doi.org/10.1016/j.scitotenv.2023.167063.

References

Alam, M.S., Teshima, S.-i., Koshio, S., Ishikawa, M., 2002. Arginine requirement of juvenile Japanese flounder *Paralichthys olivaceus* estimated by growth and biochemical parameters. Aquaculture 205, 127–140.
Bedia, C., 2022. Metabolomics in environmental toxicology: applications and challenges. Trends Environ. Anal. Chem. 34, e00161.
Beger, R.D., 2013. A review of applications of metabolomics in cancer. Metabolites 3, 552–574.
Berge, G., Sveier, H., Lied, E., 2002. Effects of feeding Atlantic salmon (*Salmo salar* L.) imbalanced levels of lysine and arginine. Aquac. Nutr. 8, 239–248.
Bieczynski, F., Painefilú, J.C., Venturino, A., Luquet, C.M., 2021. Expression and Function of ABC Proteins in Fish Intestine, 12.
Bloom, N.S., 1992. On the Chemical Form of Mercury in Edible Fish and Marine Invertebrate Tissue, 49, pp. 1010–1017.
Bravo, A.G., Cosio, C., Amouroux, D., Zopfi, J., Chevalley, P.-A., Spangenberg, J.E., et al., 2014. Extremely elevated methyl mercury levels in water, sediment and organisms in a Romanian reservoir affected by release of mercury from a chlor-alkali plant. Water Res. 49, 391–405.
Bridges, K.N., Soulen, B.K., Overturf, C.L., Drevnick, P.E., Roberts, A.P., 2016. Embryotoxicity of maternally transferred methylmercury to fathead minnows (Pimephales promelas). Environ. Toxicol. Chem. 35, 1436–1441.
Cao, Z., Li, P., Cao, X., Wang, X., Liu, B., He, S., et al., 2022. Reproductive toxicity of environmental levels of triphenyltin to the marine rotifer, *Brachionus plicatilis*. Comp. Biochem. Physiol. C: Toxicol. Pharmacol. 254, 109272.
Chattopadhyay, S., 2005. Grain incidents and other mercury tragedies: forms, fate, and effects. In: Encyclopedia of Toxicology, pp. 464–469.
Chen, N., Jin, L., Zhou, H., Qiu, X., 2012. Effects of dietary arginine levels and carbohydrate-to-lipid ratios on mRNA expression of growth-related hormones in largemouth bass, Micropterus salmoides. Gen. Comp. Endocrinol. 179, 121–127.
Chen, Y., Zhang, W., Cai, Y., Kwok, R.T.K., Hu, Y., Lam, J.W.Y., et al., 2017. AIEgens for dark through-bond energy transfer: design, synthesis, theoretical study and application in ratiometric Hg^{2+} sensing. Chem. Sci. 8, 2047–2055.
Daewel, U., Hjøllo, S.S., Huret, M., Ji, R., Maar, M., Niiranen, S., et al., 2014. Predation control of zooplankton dynamics: a review of observations and models. ICES J. Mar. Sci. 71, 254–271.
Della Torre, C., Bocci, E., Focardi, S.E., Corsi, I., 2014. Differential ABCB and ABCC gene expression and efflux activities in gills and hemocytes of Mytilus galloprovincialis and their involvement in cadmium response. Mar. Environ. Res. 93, 56–63.
Drevnick, P.E., Sandheinrich, M.B., 2003. Effects of dietary methylmercury on reproductive endocrinology of fathead minnows. Environ. Sci. Technol. 37, 4390–4396.
Dubois-Deruy, E., Peugnet, V., Turkieh, A., Pinet, F., 2020. Oxidative stress in cardiovascular diseases. Antioxidants (Basel) 9.
Duman, R.S., Sanacora, G., Krystal, J.H., 2019. Altered connectivity in depression: GABA and glutamate neurotransmitter deficits and reversal by novel treatments. Neuron 102, 75–90.
Farina, M., Aschner, M., da Rocha, J.B.T., 2017. The catecholaminergic neurotransmitter system in methylmercury-induced neurotoxicity. Adv. Neurotoxicol. 1, 47–81.
Ferreira, M., Costa, J., Reis-Henriques, M.A., 2014. ABC transporters in fish species: a review. Front. Physiol. 5, 266.
Gosnell, K.J., Mason, R.P., 2015. Mercury and methylmercury incidence and bioaccumulation in plankton from the central Pacific Ocean. Mar. Chem. 177, 772–780.
Han, C., Kim, H.-J., Lee, J.-S., Sakakura, Y., Hagiwara, A., 2022. Iron reproductive toxicity of marine rotifer sibling species: adaptation to temperate and tropical habitats. Aquat. Toxicol. 246, 106135.
Han, J., Park, J.C., Choi, B.-S., Kim, M.-S., Kim, H.-S., Hagiwara, A., et al., 2019. The genome of the marine monogonont rotifer Brachionus plicatilis: genome-wide expression profiles of 28 cytochrome P450 genes in response to chlorpyrifos and 2-ethyl-phenanthrene. Aquat. Toxicol. 214, 105230.
Hansen, Jens Carl, Danscher, Gorm, 1997. Organic Mercury—An Environmental Threat to the Health of Exposed Societies?, 12, pp. 107–116.
He, T., Mao, X., Lin, H., Hassan, M.M., Zhu, S., Lu, Q., et al., 2022. Methylmercury bioaccumulation in water flea *Daphnia carinata* by AIEgen. Ecotoxicol. Environ. Saf. 248, 114271.
Hu, G., Wang, H., Zhu, J., Zhou, L., Li, X., Wang, Q., et al., 2023. Combined toxicity of acetamiprid and cadmium to larval zebrafish (Danio rerio) based on metabolomic analysis. Sci. Total Environ. 867, 161539.
Huang, X., Feng, B., Gao, T., Bi, A., Huang, L., Song, R., et al., 2021. AIE-Based Fluorescent Nanosensors for Detection of Heavy Metal Ions, pp. 53–96.
Jeong, C.-B., Kim, H.-S., Kang, H.-M., Lee, J.-S., 2017. ATP-binding cassette (ABC) proteins in aquatic invertebrates: evolutionary significance and application in marine ecotoxicology. Aquat. Toxicol. 185, 29–39.
Jiang, Y., He, T., Chen, Y., Ruan, Y., Zhou, Y., Tang, B., et al., 2017. Quantitative evaluation and: in vivo visualization of mercury ion bioaccumulation in rotifers by novel aggregation-induced emission fluorogen nanoparticles. Environ. Sci. Nano 4.
Jyothi, B., Narayan, G., 2000. Pesticide induced alterations of non-protein nitrogenous constituents in the serum of a fresh water cat fish, Clarias batrachus (Linn.). Indian J. Exp. Biol. 38, 1058–1061.
Kakade, A., Sharma, M., Salama, E.-S., Zhang, P., Zhang, L., Xing, X., et al., 2023. Heavy metals (HMs) pollution in the aquatic environment: role of probiotics and gut microbiota in HMs remediation. Environ. Res. 223, 115186.
Kanehisa, M., Goto, S., 2000. KEGG: Kyoto encyclopedia of genes and genomes. Nucleic Acids Res. 28, 27–30.
Kang, H.-M., Byeon, E., Jeong, H., Lee, Y., Hwang, U.-K., Jeong, C.-B., et al., 2021. Arsenic exposure combined with nano- or microplastic induces different effects in the marine rotifer Brachionus plicatilis. Aquat. Toxicol. 233, 105772.
Kasper, D., Palermo, E., Dias, A., Ferreira, G., Pereira Leitão, R., Branco, C., et al., 2009. Mercury distribution in different tissues and trophic levels of fish from a tropical reservoir, Brazil. Neotrop. Ichthyol. 7, 751–758.
Kim, D.S., Jang, K., Kim, W.S., Ryu, M., Park, J.H., Kim, Y.J., 2022. Crystal structure of H227A mutant of arginine kinase in *Daphnia magna* suggests the importance of its stability. Molecules 27.
Kim, H., Kim, J.-S., Lee, Y.-M., 2017. Changes in activity and transcription of antioxidant enzymes and heat shock protein 90 in the water flea, Daphnia magna - exposed to mercury. Toxicol. Environ. Heal. Sci. 9, 300–308.
Kucharzyk, K.H., Deshusses, M.A., Porter, K.A., Hsu-Kim, H., 2015. Relative contributions of mercury bioavailability and microbial growth rate on net methylmercury production by anaerobic mixed cultures. Environ Sci Process Impacts 17, 1568–1577.
Lamborg, C.H., Hammerschmidt, C.R., Bowman, K.L., Swarr, G.J., Munson, K.M., Ohnemus, D.C., et al., 2014. A global ocean inventory of anthropogenic mercury based on water column measurements. Nature 512, 65–68.
Lankadurai, B.P., Nagato, E.G., Simpson, M.J., 2013. Environmental metabolomics: an emerging approach to study organism responses to environmental stressors. Environ. Rev. 21, 180–205.
Lee, Y.H., Kang, H.-M., Kim, D.-H., Wang, M., Jeong, C.-B., Lee, J.-S., 2017. Adverse effects of methylmercury (MeHg) on life parameters, antioxidant systems, and MAPK signaling pathways in the copepod Tigriopus japonicus. Aquat. Toxicol. 184, 133–141.
Li, H., Lin, X., Zhao, J., Cui, L., Wang, L., Gao, Y., et al., 2019. Intestinal methylation and demethylation of mercury. Bull. Environ. Contam. Toxicol. 102, 597–604.
Li, X., Lu, L., Ru, S., Eom, J., Wang, D., Samreen, et al., 2023. Nanoplastics induce more severe multigenerational life-history trait changes and metabolic responses in marine rotifer *Brachionus plicatilis*: Comparison with microplastics. J. Hazard. Mater. 449, 131070.
Li, X.D., Wang, X.Y., Xu, M.E., Jiang, Y., Yan, T., Wang, X.C., 2020. Progress on the usage of the rotifer Brachionus plicatilis in marine ecotoxicology: a review. Aquat. Toxicol. 229, 105678.
Li, Z., Chi, J., Shao, B., Wu, Z., He, W., Liu, Y., et al., 2022. Inhibition of methylmercury uptake by freshwater phytoplankton in presence of algae-derived organic matter. Environ. Pollut. 313, 120111.
Lin, C., Viant, M., Tjeerdema, R., 2006. Metabolomics: methodologies and applications in the environmental sciences. J. Pestic. Sci. 31, 245–251.
Lin, H., Ascher, D.B., Myung, Y., Lamborg, C.H., Hallam, S.J., Gionfriddo, C.M., et al., 2021. Mercury methylation by metabolically versatile and cosmopolitan marine bacteria. ISME J. 15, 1810–1825.
Long, Y., Li, Q., Zhong, S., Wang, Y., Cui, Z., 2011. Molecular characterization and functions of zebrafish ABCC2 in cellular efflux of heavy metals. Comp. Biochem. Physiol. C Toxicol. Pharmacol. 153, 381–391.
Luo, J., Xie, Z., Lam, J.W., Cheng, L., Chen, H., Qiu, C., et al., 2001. Aggregation-induced emission of 1-methyl-1,2,3,4,5-pentaphenylsilole. Chem. Commun. (Camb.) 1740–1741.
Lyu, K., Zhang, L., Zhu, X., Cui, G., Wilson, A.E., Yang, Z., 2015. Arginine kinase in the cladoceran *Daphnia magna*: cDNA sequencing and expression is associated with resistance to toxic Microcystis. Aquat. Toxicol. 160, 13–21.
Mao, T., Lu, Y., Ma, H., Pan, Z., Zhang, R., Zhu, T., et al., 2022. Variations in the life-cycle parameters and population growth of rotifer *Brachionus plicatilis* under the stress of microplastics and 17β-estradiol. Sci. Total Environ. 835, 155390.
Mei, J., Leung, N.L., Kwok, R.T., Lam, J.W., Tang, B.Z., 2015. Aggregation-induced emission: together we shine, united we soar! Chem. Rev. 115, 11718–11940.

Moltedo, G., Martuccio, G., Catalano, B., Gastaldi, L., Maggi, C., Virno-Lamberti, C., et al., 2019. Biological responses of the polychaete *Hediste diversicolor* (O.F.Müller, 1776) to inorganic mercury exposure: a multimarker approach. Chemosphere 219, 989–996.

Muñoz, N.C., González-Álvarez, D., Jaramillo, A.C., Soto-Ospina, A., Ruiz, Á.A., 2023. Toxicological risk in individuals exposed to methylmercury and total mercury through daily-consumed foodstuffs in one of the mining regions of Bajo Cauca, Antioquia, Colombia. Emerging Contam. 9, 100226.

Neumann, J., Rose-Sperling, D., Hellmich, U.A., 2017. Diverse relations between ABC transporters and lipids: an overview. Biochim. Biophys. Acta Biomembr. 1859, 605–618.

Nogueira, L.S., Vasconcelos, C.P., Mitre, G.P., da Silva Kataoka, M.S., Lima, M.O., de Oliveira, E.H.C., et al., 2019. Oxidative damage in human periodontal ligament fibroblast (hPLF) after methylmercury exposure. Oxidative Med. Cell. Longev. 2019, 8470857.

Petrik, C.M., Luo, J.Y., Heneghan, R.F., Everett, J.D., Harrison, C.S., Richardson, A.J., 2022. Assessment and constraint of mesozooplankton in CMIP6 Earth system models. Glob. Biogeochem. Cycles 36 (n/a–n/a).

Pickhardt, P.C., Folt, C.L., Chen, C.Y., Klaue, B., Blum, J.D., 2005. Impacts of zooplankton composition and algal enrichment on the accumulation of mercury in an experimental freshwater food web. Sci. Total Environ. 339, 89–101.

Rahman, A.R.A., Cob, Z.C., Jamari, Z., Mohamed, A.M., Toda, T., Ross, O.H., 2018. The effects of microalgae as live food for Brachionus plicatilis (rotifer) in intensive culture system. Trop Life Sci Res 29, 127–138.

Ratnarajah, L., Abu-Alhaija, R., Atkinson, A., Batten, S., Bax, N.J., Bernard, K.S., et al., 2023. Monitoring and modelling marine zooplankton in a changing climate. Nat. Commun. 14, 564.

Rees, D., Johnson, E., Lewinson, O., 2009. ABC transporters: the power to change. Nature reviews. Mol. Cell. Biol. 10, 218–227.

van Rooyen, D., Erasmus, J.H., Gerber, R., Nachev, M., Sures, B., Wepener, V., et al., 2023. Bioaccumulation and trophic transfer of total mercury through the aquatic food webs of an African sub-tropical wetland system. Sci. Total Environ. 889, 164210.

Sandheinrich, M.B., Miller, K.M., 2006. Effects of dietary methylmercury on reproductive behavior of fathead minnows (*Pimephales promelas*). Environ. Toxicol. Chem. 25, 3053–3057.

Szakács, G., Váradi, A., Özvegy-Laczka, C., Sarkadi, B., 2008. The role of ABC transporters in drug absorption, distribution, metabolism, excretion and toxicity (ADME–Tox). Drug Discov. Today 13, 379–393.

Tanaka, K., Ichinari, S., Iwanami, K., Yoshimatsu, S., Suzuki, T., 2007. Arginine kinase from the beetle Cissites cephalotes (Olivier). Molecular cloning, phylogenetic analysis and enzymatic properties. Insect Biochem. Mol. Biol. 37, 338–345.

Tian, X., Lin, X., Zhao, J., Cui, L., Gao, Y., Yu, Y.-L., et al., 2023. Gut as the target tissue of mercury and the extraintestinal effects. Toxicology 484, 153396.

Todorova, S., Driscoll, C.T., Matthews, D.A., Effler, S.W., 2015. Zooplankton community changes confound the biodilution theory of methylmercury accumulation in a recovering mercury-contaminated lake. Environ. Sci. Technol. 49, 4066–4071.

Verma, S.R., Rani, S., Tonk, I.P., Dalela, R.C., 1983. Pesticide-induced dysfunction in carbohydrate metabolism in three freshwater fishes. Environ. Res. 32, 127–133.

Wallace, R.L., 2015. Chapter 13 – Phylum Rotifera.

Wang, W., Chen, F., Zhang, L., Wen, F., Yu, Q., Li, P., et al., 2023. Neurotransmitter disturbances caused by methylmercury exposure: microbiota-gut-brain interaction. Sci. Total Environ. 873, 162358.

Wang, X., Tan, Z., Chen, S., Gui, L., Li, X., Ke, D., et al., 2021. Norethindrone causes cellular and hepatic injury in zebrafish by compromising the metabolic processes associated with antioxidant defence: insights from metabolomics. Chemosphere 275, 130049.

Wang, Y., Zhang, Y., Wang, J., Liang, X.J., 2019. Aggregation-induced emission (AIE) fluorophores as imaging tools to trace the biological fate of nano-based drug delivery systems. Adv. Drug Deliv. Rev. 143, 161–176.

Wu, G., Morris Jr., S.M., 1998. Arginine metabolism: nitric oxide and beyond. Biochem. J. 336 (Pt 1), 1–17.

Xiaodong, L., Yan, T., Zhang, Q., Yu, R., Zhou, M.-J., 2020. Inhibition to crucial enzymes in the lethal effects of the dinoflagellate Karenia mikimotoi on the rotifer Brachionus plicatilis. Mar. Environ. Res. 157, 104866.

Yang, Y., Jian, X., Tang, X., Ma, W., Sun, Z., Zhang, X., et al., 2021. Feeding behavior toxicity in the marine rotifer Brachionus plicatilis caused by 2,2′,4,4′-tetrabromodiphenyl ether (BDE-47): characteristics and mechanisms. Chemosphere 271, 129512.

Yu, G., Wang, L.G., Han, Y., He, Q.Y., 2012. clusterProfiler: an R package for comparing biological themes among gene clusters. Omics 16, 284–287.

Zhang, Q.L., Dong, Z.X., Luo, Z.W., Zhang, M., Deng, X.Y., Guo, J., et al., 2020. The impact of mercury on the genome-wide transcription profile of zebrafish intestine. J. Hazard. Mater. 389, 121842.

Zhang, X., Tang, X., Yang, Y., Sun, Z., Ma, W., Tong, X., et al., 2021. Responses of the reproduction, population growth and metabolome of the marine rotifer Brachionus plicatilis to tributyl phosphate (TnBP). Environ. Pollut. 273, 116462.

Metabolic pathways of methylmercury in rotifer Brachionus plicatilis.

By

Lin, Hangyu; Mao, Xiaodong; Wei, Yanlin; Li, Songzhang; Qin, Jianguang; Zhu, Song; Su, Shengqi; He, Tao

Source

The Science of the total environment

Volume: 905 Page: 167063

DOI: 10.1016/j.scitotenv.2023.167063

Published

2023-Sep-13

Indexed

2023-09-21

Document Type

Journal Article

Abstract

Methylmercury (MeHg) readily accumulates in aquatic organisms while transferring and amplifying in the aquatic food chains. This study firstly explores the in vivo accumulation sites and metabolic regulation of MeHg in the rotifer Brachionus plicatilis by aggregation-induced emission fluorogen (AIEgen) and metabolomics. Fluorescent image analysis by AIEgen showed that MeHg in B. plicatilis mainly occured in the ciliary corona, esophagus, mastax, stomach and intestine in the direct absorption group. In the other group, where B. plicatilis were indirectly supplied with MeHg via food intake, the accumulation of MeHg in the rotifer occurred in the ciliary corona, various digestive organs, and the pedal gland. However, the MeHg accumulated in the rotifer is difficult to

carbon metabolism in rotifers may be related to the accumulation of MeHg in the intestine of rotifers. In both pathways of MeHg exposure, the arginine biosynthesis and metabolism of rotifers were disturbed, which may support the hypothesis that rotifers produce more energy to resist MeHg toxicity. This study provides new insight into the accumulation and toxicity mechanisms of MeHg on marine invertebrates from the macro and micro perspectives.

Conflict of interest statement

Declaration of competing interest The authors declare that they have no known competing financial interests or personal relationships that could have appeared to influence the work reported in this paper.

Keywords

Keyword List: Aggregation-induced emission fluorogen; Brachionus plicatilis; Metabolomics; Methylmercury

Author Information

Addresses :

College of Fisheries, Southwest University, Chongqing 400715, China; Key Laboratory of Freshwater Fish Reproduction and Development (Ministry of Education), Key Laboratory of Aquatic Science of Chongqing, 400715, China.

College of Science and Engineering, Flinders University, South Australia 5001, Australia.

College of Fisheries, Southwest University, Chongqing 400715, China; Key Laboratory of Freshwater Fish Reproduction and Development (Ministry of Education), Key Laboratory of Aquatic Science of Chongqing, 400715, China. Electronic address: sushengqi@swu.edu.cn.

College of Fisheries, Southwest University, Chongqing 400715, China; Key Laboratory of Freshwater Fish Reproduction and Development (Ministry of Education), Key Laboratory of Aquatic Science of Chongqing, 400715, China. Electronic address: hh1985@swu.edu.cn.

Language
English

Medium
Internet

Accession Number
MEDLINE:37709075

PubMed ID
37709075

eISSN
1879-1026

Published Electronically
2023-09-13

NLM Unique ID
0330500

Country/Region
Netherlands

Date Revised
2023-09-18

Record Owner
NLM

Citation Subset
Index Medicus

Status
Publisher

– See fewer data fields

Journal information

The Science of the total environment

eISSN
1879-1026

Current Publisher
ELSEVIER, RADARWEG 29, 1043 NX AMSTERDAM, NETHERLANDS

9.8
Journal Impact Factor ™ (2022)

1.67
Journal Citation Indicator ™ (2022)

Citation Network

In All Databases

0 Citations

Create citation alert

0 Cited References

View PubMed related articles →

Use in Web of Science

1
Last 180 Days

1
Since 2013

Learn more →

This record is from:

MEDLINE®

Suggest a correction
If you would like to improve the quality of the data in this record, please **Suggest a correction**

2023年中国水产学会青年学术年会

2023年9月26-27日 中国·武汉

主办单位：中国水产学会

承办单位：中国水产学会青年工作委员会、华中农业大学

协办单位：湖北省水产学会、农业农村部淡水生物繁育重点实验室
教育部长江经济带大宗水生生物产业绿色发展工程研究中心

葛楚天

张 韦

2023年中国水产学会青年学术年会

代表证

2023年9月26-27日

中国·武汉

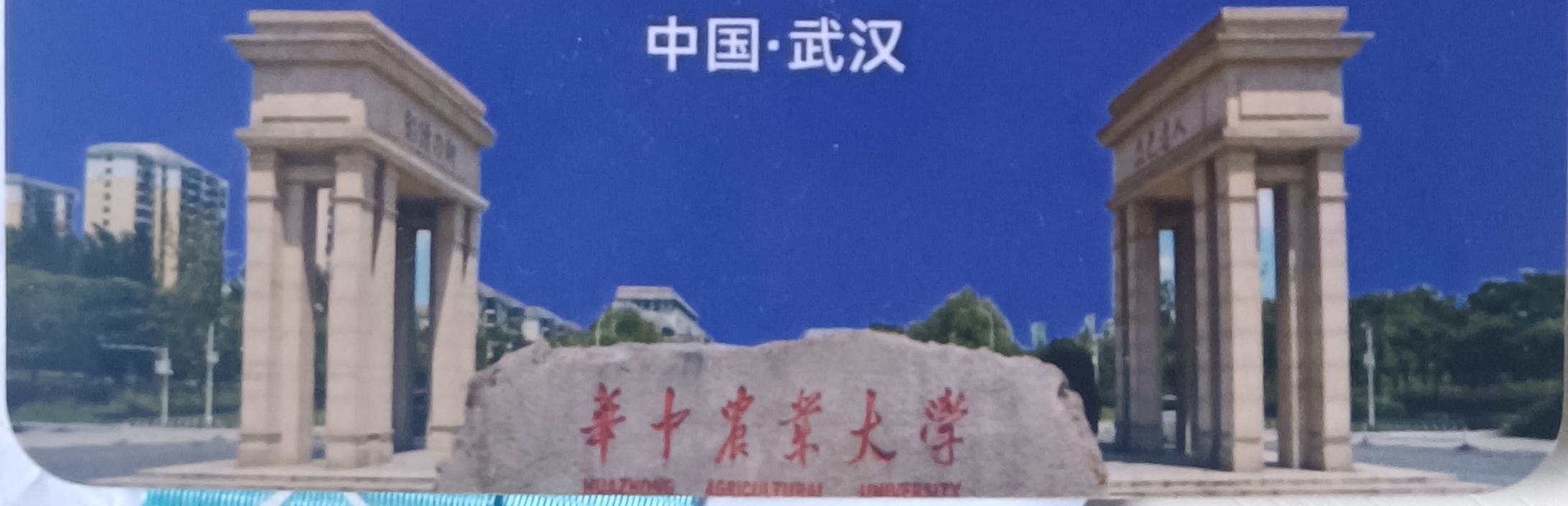


2023年中国水产学会青年学术年会
2023.9.26

2023年中国水产学会青年学术年会

2023年9月26-27日 中国·武汉

渔业创新 青年担当